Robust Corrective Topology Control for System Reliability and Renewable Integration

by

Akshay Shashikumar Korad

A Dissertation Presented in Partial Fulfillment
of the Requirements for the Degree
Doctor of Philosophy

Approved March 2015 by the
Graduate Supervisory Committee:

Kory W. Hedman, Chair
Raja Ayyanar
Vijay Vittal
Muhong Zhang

ARIZONA STATE UNIVERSITY

May 2015

ABSTRACT

Corrective transmission topology control schemes are an essential part of grid operations and are used to improve the reliability of the grid as well as the operational efficiency. However, topology control schemes are frequently established based on the operator's past knowledge of the system as well as other ad-hoc methods. This research presents robust corrective topology control, which is a transmission switching methodology used for system reliability as well as to facilitate renewable integration.

This research presents three topology control (corrective transmission switching) methodologies along with the detailed formulation of robust corrective switching. The robust model can be solved off-line to suggest switching actions that can be used in a dynamic security assessment tool in real-time. The proposed robust topology control algorithm can also generate multiple corrective switching actions for a particular contingency. The solution obtained from the robust topology control algorithm is guaranteed to be feasible for the entire uncertainty set, i.e., a range of system operating states.

Furthermore, this research extends the benefits of robust corrective topology control to renewable resource integration. In recent years, the penetration of renewable resources in electrical power systems has increased. These renewable resources add more complexities to power system operations, due to their intermittent nature. This research presents robust corrective topology control as a congestion management tool to manage power flows and the associated renewable uncertainty. The proposed day-ahead method determines the maximum uncertainty in renewable resources in terms of do-not-exceed limits combined with corrective topology control. The results obtained from the topology control algorithm are tested for system stability and AC feasibility.

The scalability of do-not-exceed limits problem, from a smaller test case to a realistic test case, is also addressed in this research. The do-not-exceed limit problem is simplified by proposing a zonal do-not-exceed limit formulation over a detailed nodal do-not-exceed

limit formulation. The simulation results show that the zonal approach is capable of addressing scalability of the do-not-exceed limit problem for a realistic test case.

DEDICATION

To Aai, Baba, Neha and Uttara

ACKNOWLEDGMENTS

I am very grateful for the cooperation and support of my advisor Dr. Kory W. Hedman, who has shown a great deal of patience and confidence in my work. Besides my advisor, I would like to thank the rest of my thesis committee: Dr. Raja Ayyanar, Dr. Vijay Vittal, and Dr. Muhong Zhang.

There are several other faculty members who have widened my horizons considerably through their courses and guidance. To my friends and classmates, I thank you for helping and motivating me along the way. I would also like to thank my parents; they have always been a strong support for my academic endeavors.

This thesis work is sponsored by the Power Systems Engineering Research Center (PSERC) under project S-51.

TABLE OF CONTENTS

CHAPTER Page

CHAPTER Page

CHAPTER Page

CHAPTER Page

LIST OF TABLES

LIST OF FIGURES

Figure Page

NOMENCLATURE

Indices

$\delta(n)^+$	Set of Lines With n as the "to" Node/Zone.
$\delta(n)^-$	Set of Lines With n as the "from" Node/Zone.
g	Generator.
$g(n)$	Set of Generators at Node/Zone n.
k	Transmission Asset (Line or Transformer).
N	Number of Buses.
$n(g)$	Node Location of Generator g.
$n,\ m$	Nodes/Zones.
w	Set of Wind Injection Locations.
$w(n)$	Set of Wind Generators at Node/Zone n.

Parameters

δ	Penalty for Constraint Violation. Set to 1.
θ^{max}	Maximum Voltage Angle Difference.
θ^{min}	Minimum Voltage Angle Difference.
B_k	Electrical Susceptance of Transmission Line k.
c_g	Operation Cost ($\$/MWh$) of Generator g.
c_g^{NL}	No Load Cost ($\$/MWh$) of Generator g.

c_g^{SD}	Shut Down Cost ($\$/MWh$) of Generator g.
c_g^{SU}	Start-Up Cost ($\$/MWh$) of Generator g.
DT_g	Minimum Down Time for Generator g.
$f_k,\ P_k^{max}$	Maximum MVA Capacity of Transmission Line k.
G_k	Series Conductance of Transmission Line k.
M_k	Big M Value for Transmission Line k.
M_n	Big M Value for Load Connected at Bus/Zone n.
$N1_g$	Binary Parameter That is 0 When g^{th} Generator Contingency Occurred and 1 Otherwise.
$N1_k$	Binary Parameter that is 0 When k^{th} Transmission Contingency Occurred and 1 Otherwise.
NSP_t	Minimum Non-Spinning Reserve Required for Time t.
P_g^{max}	Maximum Capacity of Generator g.
P_g^{min}	Minimum Capacity of Generator g.
$P_g^{uc},\ P_g^*$	Real Power Supplied by Generator g (Solution Obtained From the Unit Commitment Problem).
P_k^{min}	Minimum MVA Capacity of Transmission Line k.
$P_w^{fix},\ P_w^*$	Real Power Supplied by Wind Generators Connected at Bus/Zone $w(n)$ (Solution Obtained From the Unit Commitment Problem).
$Pd_n,\ d_n^{fix}$	Forecasted Real Part of System Demand at Bus/Zone n.

$PTDF^{R}_{k,i}$	Power Transfer Distribution Factor Over Line k for an Injection at Bus i Sent to the Reference Bus R.
Q_g^{max}	Maximum Reactive Power Supplied by Generator g.
Q_g^{min}	Minimum Reactive Power Supplied by Generator g.
Qd_n	Reactive Part of System Demand at Bus n.
R_g^{+c}	Maximum 10 Minute Ramp Up Rate for Generator g.
R_g^{+}	Maximum Hourly Ramp Up Rate for Generator g.
R_g^{-c}	Maximum 10 Minute Ramp Down Rate for Generator g.
R_g^{-}	Maximum Hourly Ramp Down Rate for Generator g.
R_g^{nsp}	Maximum Non-Spinning Reserve Supplied by Generator g.
R_g^{SD}	Maximum Shut Down Ramp Down Rate for Generator g.
R_g^{sp}	Maximum Spinning Reserve Supplied by Generator g.
R_g^{SU}	Maximum Start-Up Ramp Up Rate for Generator g.
SP_t	Minimum Spinning Reserve Required for Time t.
u_g	Unit Commitment Status of Generator g.
UT_g	Minimum Up Time for Generator g.
V^{max}	Maximum Bus Voltage.
V^{min}	Minimum Bus Voltage.

$\overline{Z_k}$	Binary Parameter for Transmission Element k; 0 if Line is Open/Not In Service; 1 if Line is Closed/In Service.

Variables

γ_k^+, γ_k^-	Violation in the Line Flow Limits of Line k.
λ_{Pn}	Real Power LMP at Node n.
λ_{Qn}	Reactive Power LMP at Node n.
θ_n	Voltage Angle at Node n.
$\theta_n, \theta_n^{ub}, \theta_n^{lb}$	Voltage Angle at Node/Zone n.
θ_{mn}	Voltage Angle Difference: $\theta_n - \theta_m$.
d_n	System Demand at Bus n.
d_{Pn}	Real Power Demand at Bus n.
d_{Qn}	Reactive Power Demand at Bus n.
L_n^+, L_n^-	Violation in the Node Balance Constraint at Zone n.
P_g, P_g^{ub}, P_g^{lb}	Real Power Supplied by Generator g.
P_k, P_k^{ub}, P_k^{lb}	Real Power From Node m to n for Line k.
P_w, P_w^{ub}, P_w^{lb}	Real Power Supplied by Wind Generator w.
P_w^{UP}, P_w^{LP}	Max and Min Wind Injection Deviation at Zone n, From its Forecasted Level.
P_{gt}	Real Power Supplied by Generator g in Time t.

P_{kn}	Real Power Flow Along Line k at Node n.
Q_g	Reactive Power Supplied by Generator g.
Q_k	Reactive Power From Node m to n for Line k.
Q_{kn}	Reactive Power Flow Along Line k at Node n.
r_{gt}^{nsp}	Non-Spinning Reserve Supplied by Generator g in Time t.
r_{gt}^{sp}	Spinning Reserve Supplied by Generator g in Time t.
S_{kn}	Complex Power Flow Along Line k.
u_{gt}	Unit Commitment Status of Generator g in Time t; 0 if Generator is Not In Service; 1 if Generator is In Service.
V_n	Voltage at Node n.
v_{gt}	Start-Up Status of Generator g in Time t; 0 if Generator is Not Turned On in Time t; 1 if Generator is Tuned On in Time t
w_{gt}	Shut Down Status of Generator g in Time t; 0 if Generator is Not Turned Off in Time t; 1 if Generator is Tuned Off in Time t
Z_k	Binary Variable for Transmission Element k; 0 if Line is Open/Not in Service; 1 if Line is Closed/In Service.

Chapter 1

INTRODUCTION

1.1 Motivation

Robust optimization has existing in literature since the 1950s; however, it has not been studied in connection with electrical power systems until recently. The key feature of robust optimization, to utilize uncertainty sets to capture uncertain system parameters, is useful to analyze many power systems operational related studies. The increasing level of intermittent renewable resources in electrical power systems is adding more complexities to power system operations. The standard power system operational tools, present today, are not capable of analyzing these uncertainties to its full extent. As a result, existing power systems optimization packages are either inefficient by overcommitting generation in an ad-hoc fashion in order to handle the uncertainties or the solutions may jeopardize reliability by not accounting for such uncertainties. This research focuses on developing robust optimization based tools and algorithms, which can be used to analyze system uncertainties in power system operations.

High-voltage electric power grids include thousands of miles of transmission lines with hundreds to thousands of large generators that frequently span multiple countries. Operational models of the bulk power grid include complex constraints: branch (transmission line) flows, stability limits, voltage restrictions at buses (nodes), security constraints, integer restrictions on the generation, and the fact that electricity is instantaneously generated, transported, and then consumed. These characteristics makes electrical power systems one of the most complex network flow models that exist today. This is further complicated by the fact that there is minimal control over the path that the current takes. The electric

grid is built to be a redundant network in order to ensure mandatory reliability standards. The current travels over many branches and can potentially travel over all paths to reach its final destination. The flow of current is governed by Kirchhoff's laws and is subject to the impedance of the transmission lines as well as other factors. With the advent of high levels of intermittent resources (wind and solar), it is becoming even more difficult to ensure safe, reliable, and cost effective delivery of electric power. A variety of solutions exist to deal with this issue. While it is also possible to invest in additional transmission capability by building additional transmission lines, the primary barriers to such a solution include expensive capital costs to invest in such infrastructure followed by the frequent societal objection of having to acquire additional land (rights of way) to build new lines. There are also frequent fights over who should pay for such an infrastructure. This research investigates an alternative solution: robust corrective topology control.

The proposed robust corrective topology control methodology utilizes existing assets, circuit breakers or electrical switches, to temporarily take high-voltage transmission lines out of service. Typically, taking an available transmission path out of service reduces the transfer capability of electric power across the grid and may degrade system reliability. However, it is also possible that temporarily removing a line can improve the transfer capability and reliability of the system. Since the flow of electric power on one particular transmission path is dependent on the impedances of alternative paths, it is possible to increase the transfer capability on other paths that are left in service by taking out other transmission lines. If the path that has its transfer capability increased is a critical path, e.g., there is excess wind in that region, then taking the line out of service may improve operations and reliability.

In most of the system studies today, the modeling of the transmission network is simplified and limited attention is given to the flexibility in the network topology. To overcome this issue, there is a national push to model the grid by a more sophisticated, smarter way

as well as to introduce advanced technologies and control mechanisms into grid operation. One aspect of smart grid aims at making better use of the current infrastructure as well as additions to the grid that will enable more sophisticated use of the network. This research examines smart grid applications of harnessing the full control of transmission assets by incorporating their discrete state into the network optimization problem and it analyzes the benefits of this concept for system reliability and renewable resources integration.

1.2 Topology Control: As a Concept

The following 3-node network flow model in Fig. 1.1 illustrates the concept of topology control. All of the generators in this example have different operating costs and have no limit on their capacity. The objective is to determine the optimal economic dispatch to meet the demand at node C. All of the transmission lines are assumed to have equal impedances. However, the thermal capacities of the lines are assumed to be different.

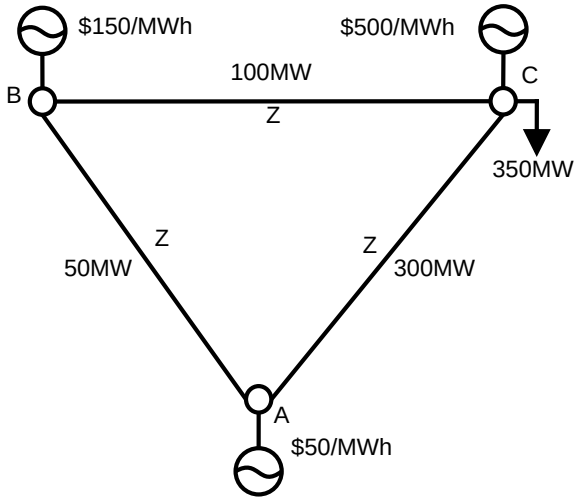

Figure 1.1: Topology Control Example.

Fig. 1.2 represents the different feasible sets of solutions for two different network topology configurations. When all lines are in service, the solution space, for generator

A's and generator B's production, is defined by the vertices $\{0, 1, 2, 3\}$. However, when line A-B is opened (taken out of service), the solution space changes and it is defined by the vertices $\{0, 4, 6, 8\}$. Therefore, when topology control is simultaneously considered while solving for the optimal economic dispatch, the union of these two solutions spaces define the set of feasible solutions, which is $\{0, 1, 5, 6, 8\}$. Thus, it is obvious that the flexibility gained by topology control creates a superset of feasible solutions, meaning that the resulting solution will never be worse than if topology control is not considered. Furthermore, the optimal dispatch with all lines in service would be defined by G_a=200 MW, G_b=50 MW and G_c=100 MW at a cost of $\$67,500$; with transmission topology control, the optimal dispatch solution is G_a=300 MW,G_b=50 MW and G_c= 0 MW at a cost of $\$22,500$.

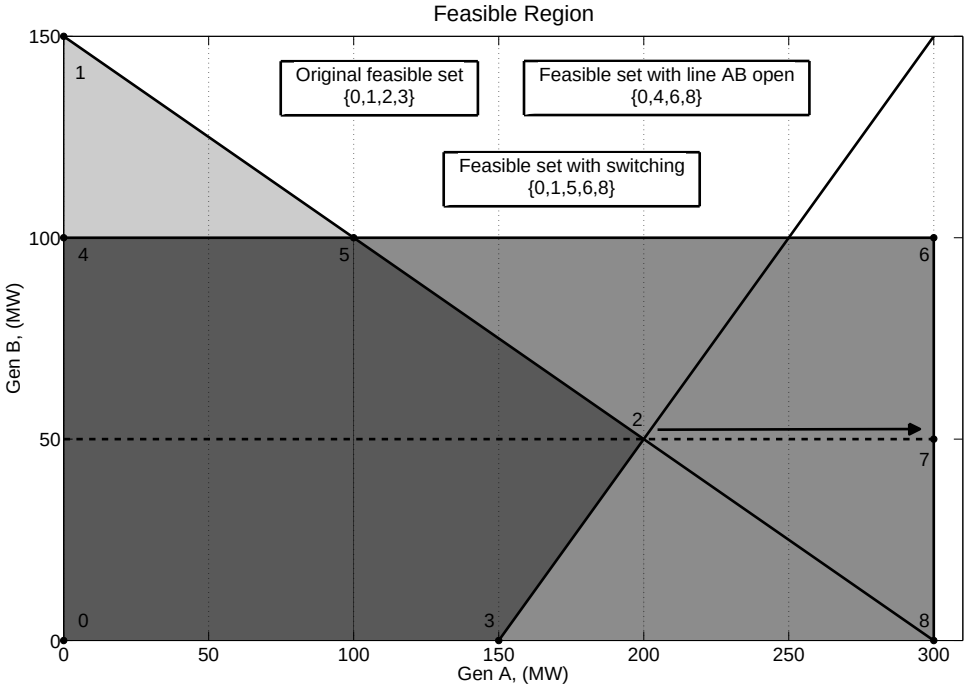

Figure 1.2: Feasible Region for the Topology Control Example.

1.3 Example: Topology Control in Real Life Application

Past research to identify and show the benefits of topology control for power system operation is presented in Section 2.3. In this section, a real life example of topology control action to mitigate post-contingency situation is presented; in this example, the topology control action is used to overcome the overvoltage situation caused by post-contingency flows.

Fig. 1.3 shows the voltage contour plots for the pre-contingency, contingency, and post-contingency states for a subsection of the Tennessee Valley Authority (TVA) system. In pre-contingency state, all bus voltages are within the acceptable operating range, i.e., between 0.9-1.1 pu; however, in the post-contingency state, a subsection of transmission network experiences the overvoltage situation. To overcome this overvoltage situation, a topology control action is proposed, which alters the post-contingency flows and helps to reduce voltages on buses experiencing overvoltage. This particular pre-contingency state corresponds to a lightly loaded period, in which most of the high voltage transmission lines in presented area are lightly loaded compared with its peak-load condition. In the contingency state, the reactive power available within the affected area is more than the requirement, which results in overvoltage in this area. Implementation of topology control inherently reduces the excessive flow of reactive power into the affected area and helps to reduce the bus voltages to safe operating limits.

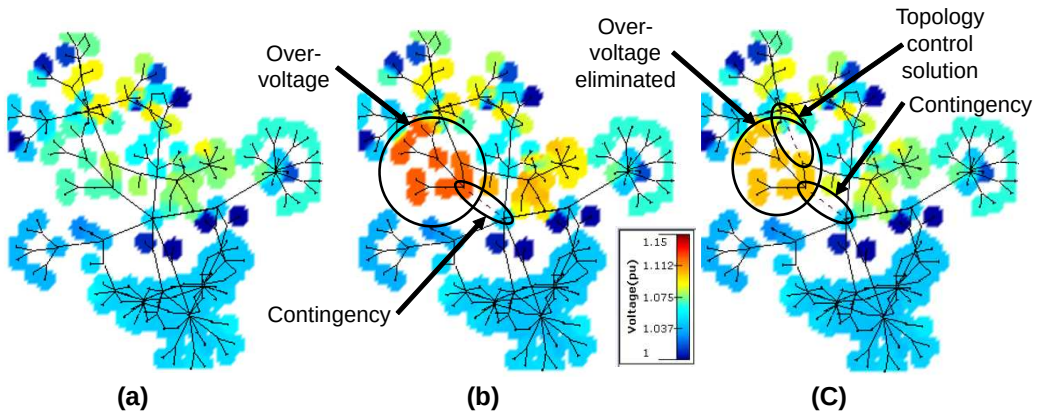

Figure 1.3: Example for Corrective Topology Control.

Note that in this example, the generator dispatch in pre-contingency and the post-contingency is same and no re-dispatch request is sent to generators. Furthermore, Fig. 1.3 represents the part of network above 500kV.

1.4 Summary of Chapters

Chapter 2 gives a literature review, which provides the basic understanding of transmission switching proposed in literature for various reasons, such as corrective switching, congestion management, and the various techniques adopted are listed. It also covers present industrial practices involving topology control as a corrective mechanism to overcome power systems operational issues.

Chapter 3 presents an overview of electric energy dispatch problems. In particular, it discusses the formulation for the alternating current optimal power flow (ACOPF) problem as well as a common approximation of the ACOPF and the direct current optimal power flow (DCOPF) problem. Finally, a discussion of the unit commitment problem, used in this research, as well as its formulations is presented.

Chapter 4 provides background information regarding robust optimization. The derivation for the robust topology control algorithm is presented, which converts a complex three

stage optimization problem into a two stage problem. The comparison of robust optimization and stochastic optimization is also given.

Chapter 5 provides a brief introduction to stability studies and information about the dynamic models used in this thesis. The short description of different types of stability studies are also presented.

Chapter 6 presents the effect of demand uncertainties on system reliability. In this chapter, three topology control (corrective transmission switching) methodologies are presented along with the detailed formulation of robust corrective switching algorithm. The results for N-1 reliability analysis with robust corrective switching algorithm are also presented. These studies were conducted on the IEEE 118-bus test case.

Chapter 7 presents the effect of renewable uncertainties on renewable resources integration and system reliability. In this chapter, a robust methodology to determine the do-not-exceed limits for renewable resources is presented, along with a detailed analysis of the robust corrective switching algorithm under renewable uncertainties. The simulation results for do-not exceed limits with robust corrective switching algorithm are also presented. These studies were conducted on the IEEE 118-bus test case and a realistic test system of Tennessee Valley Authority (TVA).

Chapter 8 presents the zonal DNE limit methodology to address the scalability of the DNE limit problem. The proposed zonal DNE limit method is tested on the IEEE 118-bus test case and a realistic test system of TVA.

Chapter 9 addresses the practical limitations of the topology control algorithm. The issues associated with the scalability and large computational time of topology control algorithm are discussed in this chapter.

Chapter 10 concludes this dissertation and discusses potential future research that is connected with the main theme of this dissertation, developing a more flexible electric grid.

1.5 List of Abbreviations

The list of abbreviations used in this thesis are listed below.

ACOPF	Alternating Current Optimal Power Flow
DCOPF	Direct Current Optimal Power Flow
DDP	Desired Dispatch Point
FACTS	Flexible Alternating Current Transmission Systems
FERC	Federal Energy Regulatory Commission
LP	Linear Programming
LMP	Locational Marginal Price
MIP	Mixed Integer Programming
NERC	North American Electric Reliability Corporation
OMC	Out-of-market Correction
OPF	Optimal Power Flow
PF	Power Flow
PTDF	Power Transfer Distribution Factor
RTC	Robust Corrective Topology Control
SCUC	Security Constraint Unit Committment
SCED	Security Constraint Economic Dispatch
TC	Topology Control
UC	Unit Committment

Chapter 2

LITERATURE REVIEW

2.1 Introduction

The objective of this research is to study the impact of topology control on system reliability and renewable integration. Past research has identified topology control as a valuable asset that can be used to mitigate various power system operational concerns. This chapter presents a thorough literature review on the motivation for this research, past related research on topology control, and an overview of present industrial operational procedures where transmission control is employed.

2.2 National Directives

The demand of electrical power has increased considerably during the past few years. This increase in system demand causes a great amount of stress on transmission infrastructure; to overcome this issue, there is a national push to create a smarter, more flexible, electrical grid. A smarter grid not only improves the efficiency of the electric transmission systems, but it also ensures secure and reliable power system operations. This research is in line with several national directives addressing this need for a smarter and more flexible power grid.

The United States Energy Policy ACT (EPACT) of 2005 calls for advanced transmission technologies, which includes a directive for federal agencies to "encourage ... deployment of advanced transmission technologies," including "optimized transmission line configuration." This research also follows the Federal Energy Regulatory Commission (FERC) order

890, which encourages the improvements in economic operations of transmission grid. It also addresses the Energy Independence and Security Act of 2007: (1) "increased use of...controls technology to improve reliability, stability, and efficiency of the grid" and (2) "dynamic optimization of grid operations and resources." The intention of this research is to harness the control of transmission assets by the dynamic optimization of the transmission grid, and the co-optimization of transmission with generation, using robust optimization techniques, thereby encouraging a smarter, flexible, and more efficient electric network.

2.3 Literature Review: Topology Control

Topology control has been in literature since 1980s and, till today, it has been used to overcome power systems related operational issues, such as voltage violations, line overloads [2, 3, 4, 5], line losses and cost reduction [6, 7, 8], system security [9], or a combination of these [10, 11]. In this section, the brief overview of past research related to topology control are presented.

2.3.1 Topology Control as a Congestion Management Tool

Topology control actions are used to manage congestion within the electrical network; [2] proposes topology control actions as a tool to manage congestion in the electrical grid. It discuss ways to solve this problem by genetic algorithms along with deterministic approaches. This approach attempt to minimize the amount of overloads in the network since they are not co-optimizing the generation with the topology. Thus, this is a disconnected approach where generation is first dispatched optimally and then this method is employed to reduce network congestion. Once again, the optimal transmission switching concept goes further than this concept since it co-optimizes the generation with the network topology in order to maximize the market surplus. In [12], the topology control actions are proposed to mitigate transmission network congestion due to high renewable penetration.

In general, it has been assumed that taking transmission elements/lines out of service increases the congestion in the system. This misconception has been proven wrong in [13]. Network topology optimization allows for a system re-dispatch, which makes it impossible to state the impact on congestion.

2.3.2 Topology Control as a Corrective Mechanism

Past research has shown topology control as a control method for a variety of power system operational problems. The primary focus of past research has been on proposing transmission switching as a corrective mechanism when there are voltage violations, line overloads [2, 3, 4, 5], line losses and cost reduction [6, 7, 8], system security [9], or a combination of these [10, 11]. While this past research acknowledges certain benefits of harnessing the control of transmission network for short term benefits, they do not use the flexibility of the transmission grid to co-optimize the generation along with the network topology during steady-state operations. In [14], the unit commitment problem with topology control actions are co-optimized, with N-1 reliability, which has shown that co-optimization of topology control actions with unit commitment can provide substantial economic savings, even while maintaining N-1 reliability standards. Furthermore, the use of transmission switching as a corrective mechanism to respond to a contingency has been acknowledged in some past research to have an impact on the cost of generation rescheduling due to the contingency. However, it has not been acknowledged that such flexibility should be accounted for while solving for the steady-state optimal dispatch, probably due to computational difficulties and extended solution time.

In [15], topology control is used as a corrective mechanism in response to a contingency. It also presents the formulation of such a problem and provides an overview of search techniques to solve the problem. This idea is further extended to alleviate line overloading due to a contingency by [3] using topology control heuristics. The limitation of

this method is that it is based on topology control heuristics, which does not consider all corrective topology control actions and does not co-optimize topology control with the generation. In [16], topology control actions are used as a corrective mechanism, with linearized approximate optimal power flow formulation and solved using branch and bound method. The corrective topology control using AC power flow is studied in [10]; however, in this study, it is assumed that the generator dispatch is fixed thereby not acknowledging the benefit of co-optimizing the network topology with generation.

The corrective topology control actions provide optimal results when topology control actions are co-optimized with generation. In [9, 8], a corrective topology control is used to mitigate contingencies, where, a corrective switching algorithm is used to mitigate contingencies, while considering the ability to re-dispatch generation. However, due to the computational complexity of this problem, this method does not search for the actual optimal topology but rather considers limited switching actions. The review of past research on topology control is provided in [17]. In [11, 4] the topology control actions are used to relieve line overloads and voltage violations.

The optimal transmission switching for contingencies using DC optimal power flow is presented in [18], which shows that in power system operations, using topology control actions, considerable cost benefits can be achieved. Furthermore, reference [18] also shows that co-optimizing topology control with generation can give operational flexibility to system operators' to respond to emergency situations. Furthermore, in [19] this idea is further extended to determine topology control actions for contingency mitigation in real-time. In this study, the fast DCOPF based heuristic is used to determine candidate topology control actions.

2.3.3 Optimal Topology Control

The bulk electric transmission network is built with redundant paths to ensure mandatory reliability standards, such as NERC requirements for N-1 and these standards require protection against possible worst-case scenarios. However, it is well known that the redundancies in these networks can cause dispatch inefficiency, due to line congestion, or voltage violations. Furthermore, a network branch that is required to be built in order to meet reliability standards during specific operational periods may not be required to be in service during other periods. Consequently, due to the interdependencies between network branches (transmission lines and transformers), it is possible to temporarily take a branch out of service during certain operating conditions and improve the efficiency of the network while maintaining reliability standards. This corrective switching action is the basis for the optimal topology control.

Optimal transmission switching includes the control of transmission assets into the optimal power flow (OPF) formulation in order to co-optimize the network topology simultaneously with the generation. This added level of control to the traditional OPF problem creates a superior optimization problem compared with the traditional OPF formulation. Furthermore, by harnessing the control of transmission and co-optimizing the electrical grid topology with the generation, the optimal transmission switching problem guarantees a solution that is as good as the one obtained by the traditional dispatch formulation.

The concept of a dispatchable network was first introduced in [20], which led to the research work related to optimal transmission switching in [21, 18, 14, 22, 23, 24, 13, 19]. This past research has also shown that substantial economic savings can be obtained even for models that explicitly incorporate N-1. For example, in [18, 14] it is observed that savings on the order of $4 - 15\%$ can be achieved even while maintaining N-1. Note that, this past research has been based on the DCOPF formulation, a linear approximation to the

ACOPF problem, which is a lossless model and reactive power flow are ignored.

2.3.4 Topology Control and Minimize Losses

In [6], the topology control actions are used to minimize system losses, which shows that, contrary to general belief, it is possible to reduce electrical losses in the network by opening a transmission line for a short timeframe. Furthermore, in [7], the author proposed a mixed integer linear programming approach to determine the optimal transmission topology, with the objective to minimize electrical transmission losses. Unlike past research, this model searches for an optimal topology, but does not consider the generator re-dispatch. The ideal way to use topology control for loss minimization is to consider the topology control along with generator re-dispatch, which will determine the optimal transmission topology and generator dispatch.

2.3.5 Topology Control for Maintenance Scheduling

Past research focused on the effect of topology control on system reliability. However, topology control actions not only affect the system reliability, but also help to reduce the operational cost of the electric grid. Nowadays, system operators consider topology control as a controlling tool in maintenance scheduling of electrical bulk power system. For example, in 2008, the Independent System Operator of New England (ISONE) saved more than $\$50$ million by considering the impact of transmission line maintenance scheduling on the overall operational costs [25]. However, the study done by ISONE is based on estimating cost instead of employing mathematical optimization tools, which determine the total system cost considering transmission network reliability. Furthermore, the benefit of this research is that it underlines the need of developing more practical mathematical models to solve the maintenance scheduling problem.

2.3.6 Topology Control for Transmission Expansion Planning

The bulk power transmission network is built with redundancies to improve system reliability and/or to improve operational efficiency. Therefore, it is often assumed that topology control actions will reduce operating costs only for poorly planned transmission networks. However, this assumption is not true. Optimal transmission switching and transmission planning are two different optimization problems with different objectives: transmission planning is a long-term problem, which determines the line(s) to build over a long time horizon; on the other hand, optimal transmission switching is a short-term problem, which determines the optimal network for short term benefits, such as reduction in operating cost. The ideal method to obtain better benefits over a long timescale is to consider the optimal transmission expansion plan. Note that, the optimal plan does not guarantee benefits to the system during each individual operating period. As a result, a network can be perfectly planned, but still benefit from short-term network reconfiguration, using optimal topology control actions.

Transmission expansion planning is a complicated multi-period optimization problem. In traditional literature, topology control actions are not considered in the planning process. However, in [26], the methodology for transmission expansion studies with topology control action are presented. The DCOPF based formulation is used in this analysis, considering higher wind penetration. A more detailed analysis for transmission planning with topology control is presented in [27].

2.3.7 Topology Control for System Reliability

The electrical transmission network is designed to handle various contingencies and demand levels. However, such deviations do not exist at the same time with the same intensity. Therefore, a particular line that is required to be in service to meet reliability standards for a

specific operating point may not be required to be in service for other operating conditions. Hence, corrective topology control can be used to meet N-1 standards. The NERC policy dictates that after the occurrence of a contingency, the system must be reconfigured and re-dispatched to handle another contingency within 30 minutes. However, in real-time the analysis of N-1 reliability is a complex problem. The real-time dynamic assessment tools used today in power system operation monitor some of these critical contingencies, as it is not possible to monitor all the N-1 contingencies in real-time.

Furthermore, it is possible to improve system reliability by temporarily taking a line out of service. System reliability not only depends on the network topology, it also depends on the generation dispatch solution, e.g., available generation capacity and ramping capabilities of the generators. Since modifying the topology changes the feasible set of dispatch solutions, it is possible to obtain a different generation dispatch solution that was infeasible with the original topology, but is feasible with the modified topology. Even though there may be a line(s) temporarily out of service, this new generation dispatch solution may make the system more reliable if it has more available capacity with faster generators. In [19], N-1 and N-2 contingency analysis for IEEE test cases is presented, which shows that, with topology control actions, $12 - 63\%$ more load can be served during N-1 contingencies and $5 - 50\%$ more load can be served with N-2 contingencies.

2.3.8 Special Protection Schemes (SPSs)

Corrective switching is one example of topology control that is implemented today [28]. These methods are based on operators' prior knowledge, as specified in [28] on page 107; such actions may also be based on historical information. Ideally, corrective switching algorithms should be solved in real-time. Once the disturbance occurs, the switching algorithm is executed to suggest switching actions to alleviate any constraint violations. This approach is beneficial since the current operating status is known, which ensures the

accuracy of the solution. However, the challenge with real-time mechanisms is that they must be extremely fast while also ensuring AC feasibility, voltage stability, and transient stability. Topology control models could be solved offline by estimating the operating state of the system. However, deterministic offline mechanisms also have limitations since the operating state must be predicted prior to the disturbance. Thus, the proposed offline corrective action is, susceptible to problematic reliance on perfect foresight.

Special protection schemes (SPSs), also known as remedial action schemes (RASs) or system integrity protection schemes (SIPSs), are an important part of grid operations. SPSs are used to improve the reliability of the grid and improve the operational efficiency. SPSs are primarily identified and developed based on ad-hoc procedures. The development of such corrective mechanisms like SPSs reflects a change, a push, by the industry to switch from preventive approaches, to the use of corrective approaches. The use of transmission switching as a corrective mechanism can be a powerful tool. For instance, PJM has a number of SPSs that involve post-contingency transmission switching actions [29]. For example, the following action is listed in [29] on page 221: "The 138 kV tieline L28201 from Zion to Lakeview (WEC) can be opened to relieve contingency overloads for the loss of either of the following two lines: Zion Station 22 to Pleasant Prairie (WEC) 345 kV Red (L2221), Zion Station 22 to Arcadian (WEC) 345 kV Blue (L2222)."

In practice, topology control actions are employed during blackouts caused by rare weather conditions [30]. In 2012, due to Superstorm Sandy, PJM lost about 82 bulk electric facilities, which caused extremely high voltages on the system during low load levels. To overcome this high voltage situation, a corrective switching plan was employed, several 500kV lines were switched out to mitigate over voltage concerns during these low load level periods. Note that, the corrective switching methodology employed in this particular case is unknown.

Such operational protocols, like SPSs, are often viewed as a necessary protocols to

maintain system reliability. While these transmission switching SPSs do help maintain system reliability, there are alternatives that the operator can employ instead. Possible alternatives may include: re-dispatching the system after the contingency occurs; choosing a different steady-state (no-contingency) dispatch prior to the contingency occurring to ensure there is no overloading; or upgrading the equipment so that it is able to handle these contingency flows. Re-dispatching the system is likely to increase the operating costs. Choosing a different dispatch solution for steady-state operations would increase the operating cost, otherwise, that dispatch solution would have been initially chosen. Investing in new equipment increases the capital cost of the system.

2.3.9 Seasonal Transmission Switching

Topology control actions are used for short term benefits as well as seasonal benefits. For instance, in the state of California, the load requirements are lower in the winter and the probability of an outage is higher due to winter storms. The summer is the exact opposite; during the summer, the load is the highest in the year, but the probability of outages is lower since there are fewer and less severe storms. As a result, some utilities have determined that it is beneficial to leave certain transmission lines in service during the winter when there is a greater chance of winter storms for reliability purposes, but yet these lines are taken out of service during summer periods since the threat of an outage is lower.

These lines are primarily redundant transmission lines in the lower voltage network. Such redundancies are less important during summer periods when the probability of an outage is lower. Furthermore, these redundant lines can cause overloading concerns during summer periods since the load conditions during the summer are higher. For instance, there can be two parallel lines with different thermal capacity ratings. The lower capacity line, generally a part of the lower voltage network, may reach its capacity first and, therefore, inhibit the higher voltage network from transferring as much power as desired. Due to the

higher loading conditions, it is, therefore, preferred to take the redundant, lower capacity line out of service, as long as the line is not necessary to maintain system reliability. Since the outage rates are lower during the summer periods, the operators are able to take the line out of service without jeopardizing system reliability. In contrast, having these redundancies in service during the winter is integral to maintaining system reliability since the probability of an outage is greater. In addition, the redundancies do not cause overloading concerns during the winter since the winter loading levels are lower.

While this operation is acknowledged by utilities today, the tradeoff between protecting against potential contingencies versus the potential for overloads is not well understood. Seasonal transmission switching models that are capable of answering these questions do not exist today, thereby emphasizing the need for further research and development in the area of seasonal transmission switching.

2.4 Conclusion

Topology control actions have been suggested to mitigate many power systems related problems. However, most of those studies are either based on DCOPF or assumes fixed generator dispatch, which has limited the spread of topology control in power system operations. Even though, today, system operators do change system topologies for short term application, these topology control actions are based on operators' prior knowledge or some add-hoc methods. To overcome this issue research presented in this report introduces a robust optimization based topology control methodology, which suggests the topology control actions, that are valid for a range of operating states, are guaranteed DC feasible for the entire uncertainty set.

Chapter 3

REVIEW OF OPTIMAL POWER FLOW AND UNIT COMMITMENT

3.1 Introduction

The electric industry is comprised of four major components: generation, transmission, distribution, and the load. The traditional operation of the electrical bulk power system is that the operator will dispatch the generation at minimum generation cost to meet the load (while maintaining reliability), while keeping the remaining assets fixed, for example, system topology. National directives and modern technologies are aimed to create flexibility in all components of the grid, resulting in a smarter and more efficient electric network. Modeling of deferrable load, would create a more flexible and smarter grid. Harnessing the flexibility in the network topology, i.e., flexible alternating current transmission systems (FACTS) devices and topology control, would further add an additional layer of control on the transmission side.

The remaining chapter is structured as follows: Section 3.2 describes the basic economical dispatch problem. Section 3.3 gives a brief description of AC optimal power flow. The detail formulation of DC optimal power flow is presented in Section 3.4. The security constraint unit commitment formulation, to generate starting point for all numerical results presented in this thesis, is presented in Section 3.5. The day-ahead unit commitment procedure used in Mid-continental Independent System Operator (MISO) is presented in Section 3.6.

3.2 Economic Dispatch

Economic dispatch is an optimization problem that finds the minimum operation cost for generation dispatch in order to meet the load on the system while adhering to the minimum and maximum generator capacity constraints. In the US Energy Policy Act of 2005 [31], the term is defined as "the operation of generation facilities to produce energy at the lowest cost to reliably serve consumers, recognising any operational limits of generation and transmission facilities." In general, for the economic dispatch problem, the network flow constraints are not considered; therefore, sometimes it is called an unconstrained economic dispatch problem. Hence, the economic dispatch problem provides a lower bound on the optimal power flow problem. Economic dispatch is a sub-problem of the unit commitment (UC) problem. Unit commitment determines a generator's ON or OFF status, its associated dispatch considering its minimum and maximum capacity, ramp rates, up and down time constraints, no load and start-up costs, as well as its available reserve. The generic economical dispatch problem is presented in (3.1)-(3.5), which consists of generator capacity constraint (3.2), generator ramping constraints (3.3) and (3.4), and energy balance constraint (3.5). The objective of the economical dispatch problem is presented in (3.1). The objective of the economical dispatch problem is to simultaneously minimize the total generation cost and to meet the load demand of a power system over some appropriate period while satisfying various constraints represented by (3.2)-(3.5). In some cases, instead of using a linearized cost function more complex quadratic cost function is used as shown in [32]. Note that in traditional economic dispatch problem generator ramping constraints are not considered; they are included in the formulation only when the temporal behaviour of the system is considered.

$$\min_{\forall g} \; c_g P_g \tag{3.1}$$

$$\text{s.t. } 0 \leq P_g \leq P_g^{max}, \forall g \tag{3.2}$$

$$P_g \geq \overline{P_g} - R_g^-, \forall g \tag{3.3}$$

$$P_g \leq \overline{P_g} + R_g^+, \forall g \tag{3.4}$$

$$\sum_{\forall n} P_g = \sum_{\forall n} d_n \tag{3.5}$$

3.3 AC Optimal Power Flow

The majority of the electric grid operates based on an alternating current (AC) setting; however, there are a few high voltage direct current (DC) lines in the electric grid. The flow of electric energy follows Kirchhoff's laws. The ACOPF problem is the optimization problem that models how electric power transfers across the AC electric grid and it is used to dispatch power optimally. In 1962, J. Carpentier first introduced the concept of ACOPF [33] and proved that it is a very difficult problem to solve. The ACOPF optimization problem is a non-convex optimization problem, which contains trigonometric functions in some of the constraints as shown in (3.6) and (3.7), which are similar to those given in [34]. Equation (3.6) represents the real power flow P_k, across the line k, from bus m to bus n, and equation (3.7) represents the reactive power flow Q_k, across the line k, from bus m to bus n.

$$P_k = V_m^2 G_k - V_m V_n (G_k \cos(\theta_m - \theta_n) + B_k \sin(\theta_m - \theta_n)), \forall k \tag{3.6}$$

$$Q_k = -V_m^2 B_k - V_m V_n (G_k \sin(\theta_m - \theta_n) - B_k \cos(\theta_m - \theta_n)), \forall k \tag{3.7}$$

The term, V_m, V_n represents the bus voltages and θ_m, θ_n represents the bus voltage angles. Additional constraints that are required for the ACOPF problem include the constrains on the magnitude of the voltage variables, constraints on the angle difference between

two connected buses, operational constraints on the generators, capacity constraints on the transmission lines, and node balance constraints. The voltage and trigonometric functions add non-convexities in (3.6) and (3.7); these non-convex transmission constraints add computational complexities to the ACOPF problem. To deal with these computational issues, different solution methods are proposed to solve ACOPF problem. For instance, in [33] Karush-Kuhn-Tucker (KKT) conditions are used to solve ACOPF problem. A detail review of ACOPF until 1991 is presented in [35], where more than 300 articles are reviewed; the authors concludes that the ACOPF problem is a computationally challenging problem and that it can be difficult to solve due to ill-conditioning and convergence issues.

To overcome the computational difficulties of ACOPF problem, it is common, both in academic literature and in the industry, to use a linear approximation of the ACOPF problem. The first assumption is made with regards to the voltage variables, V_n and V_m. In a per unit based power flow calculation, the bus voltage levels are close to unity; therefore, it assumed that all voltage variables are equal to one. The assumption removes some of the nonlinearities within (3.6) and (3.7).

The next assumption comes from the fact that the bus angle difference between two connected buses is generally very small. This simplification allows the approximation of the trigonometric functions in (3.6) and (3.7); the Sine of a small angle difference is approximated by the angle difference itself, and the Cosine of a small angle difference is approximately one. Using these voltage and angle difference assumptions, the G_k terms in (3.6) are removed and, similarly in (3.7), B_k terms are removed.

Another simplification made to the ACOPF formulation is with regards to the reactive power Q_k within the system. For computational simplicity in ACOPF approximation reactive power terms are ignored. To simplify the ACOPF problem further, resistance of transmission lines are assumed to be zero, which makes the susceptance equal to the inverse of the reactance. The resultant OPF model is known as the DCOPF model. In general, the

traditional DCOPF formulation is a lossless model; however, there are ways to modify the traditional DCOPF formulation to account for losses [36]. Throughout this dissertation, the DCOPF problem is assumed to be a lossless model. The more recent work on ACOPF formulation and associated linearization, to overcome the computational issues, are presented in [37, 38, 39, 40, 41, 42, 43, 44, 45, 46, 47].

Note that, a DCOPF is an approximation to a ACOPF problem; therefore, the accuracy of DCOPF solutions varies over different networks, transmission elements, and loading levels [48]. However, the DCOPF simplifies the OPF problem to a great extent and makes the OPF problem computationally tractable. Therefore, in industry, the DCOPF formulation is used for many applications [49] such as unit commitment, planning studies, system operations, etc..

3.4 DC Optimal Power Flow

In the previous section, the description and complexities associated with ACOPF are presented. To overcome these computational difficulties, it is common, both in academic literature and in the industry, to use the linearized version of the ACOPF problem. This linearized ACOPF formulation is known as the DCOPF problem. With a linear cost function, the DCOPF problem is a linear program (LP); thus, it is much easier to solve than the non-convex nonlinear ACOPF problem. The simple DCOPF problem can be described as shown in (3.8)-(3.12). Constraint (3.8) represents the generator's minimum and maximum real power generation capacity, constraint (3.9) represents the DC approximation of AC power flow across the transmission line, constraint (3.10) represents the minimum and maximum power flow across the transmission line, the energy balance equation at each bus is presented by constraint (3.12).

$$\min_{\forall g} \; c_g P_g \tag{3.8}$$

$$\text{s.t. } 0 \leq P_g \leq P_g^{max}, \forall g \tag{3.9}$$

$$P_k = B_k(\theta_n - \theta_m), \; \forall k \tag{3.10}$$

$$P_k^{min} \leq P_k \leq P_k^{max}, \forall k \tag{3.11}$$

$$\sum_{k \in \delta^+(n)} P_k - \sum_{k \in \delta^-(n)} P_k + \sum_{\forall g(n)} P_g = d_n, \forall n \tag{3.12}$$

Constraint (3.9) represents the operational constraints for generator g; for the basic DCOPF formulation, as shown in (3.9), it is assumed that the generator's minimum operating level is zero. However, in reality, most of the generators do not have zero minimum operating levels. In may cases, generators have minimum operating levels as well as minimum economical levels, which dictates the minimum operating level for most of the generators. Therefore, to enforce the true minimum operating levels of generators, i.e., if their minimum operating level is not zero, requires the use of a binary unit commitment variable thereby changing the linear program into a mixed integer linear program. In section 3.5, the unit commitment problem is presented.

Constraint (3.10) represents the DC approximation of AC power flow across the transmission like k. The DC line flow, P_k, is equals to the susceptance times the angle difference. Note that, a limit on the angle difference is equivalent to a limit on P_k; therefore, by linearizing (3.6), there is no longer a need to include the angle difference constraints. Instead, the lower and upper bounds on real power flow across the line is represented by constraint (3.11) and can be adjusted to reflect whatever constraint produces a tighter bound on P_k: the thermal capacity of the line or the limit on the voltage angle difference across the two connected buses. In many cases, the capacity constraint on transmission line k is treated as a symmetric constraint, allowing it to be modeled as $P_k^{max} = -P_k^{min}$.

Constraint (3.12) is the node balance constraint, which states that the power flow into

a bus must equal the power flow out of a bus. Generator supplies at a bus and power coming into a bus, through transmission network, are treated as injections while the load at a bus and power going out of the bus, though transmission network, is considered as a withdrawal.

Note that, the DCOPF problem is an approximation to the ACOPF and, hence, does not represent the actual electric system. Several parameters, like reactive power and losses, are neglected in the DC model and remedies, such as proxy limits, have been proposed in the literature to deal with these shortcomings of DCOPF.

The network constraints in DCOPF can also be formulated using power transfer distribution factors (PTDFs). The basic formulation of PTDF's are presented in [32]. The benefit of PTDF based DCOPF formulation is that it simplifies the DCOPF problem; for a fixed topology, the flow on any transmission line can be determined using PTDFs and net bus injections. Another benefit of PTDF structure it that it allows to consider only the critical transmission lines in DCOPF problem. For computational simplicity, in industry, a simplified DCOPF problem is solve, where instead of solving detail DCOPF model a simplified DCOPF model with less number of network constraints is solved. In this reduced model can be obtained with PTDF based DCOPF formulation. In [50], detail procedure to determine subset of the network DC constraints that are active in order to reduce the DCOPF problem size is presented; in [50], these constraints are called as *umbrella constraints*. In general, in industry, the subset of transmission lines for DCOPF problem are determined based on historical data or operators' past knowledge.

The limitation of PTDF based formulation is that the PTDFs are determined considering a fixed topology; any change in system topology needs recalculation of PTDFs for accurate DC solutions. Therefore, in this research, PTDF based DCOPF formulation is not used; instead, the $B - \theta$ formulation, as shown in (3.10), is used. There has been recent development of a different transmission switching formulation, [51], which builds on the

work of a generalized line outage distribution factors, [52]. With the use of flow canceling transactions, [51] develops a framework that is able to capture the changes in the topology and compares it to the $B - \theta$ formulation used in many preceding transmission switching papers, as well as in this research. This formulation is likely to outperform the $B-\theta$ formulation when the number of monitored lines is relatively small, something that is common practice within optimal power flow problems today.

3.5 Unit Commitment

Over the past two decades there has been a great deal of research in power generation operations and planning. Generation unit commitment is a well-known, difficult, multi-period mixed integer programming problem to solve within the electric industry. The unit commitment problem is a day-ahead scheduling problem where the operator forecasts system demand and the state of the network for the following day and solves for the optimal commitment schedule for generators. The main objective of unit commitment problem is to obtain a generator schedule with lowest possible operating cost. In reality, most generators have non-zero minimum operating levels, which is a characteristic that requires a binary variable to model the state of the generator. This binary variable is referred to as the unit commitment binary variable, u_{gt}; it takes on a value of one when the unit is on and zero when the unit is off. Generators also have minimum up and minimum down time constraints. The minimum up (or down) time constraint states that once a generator is turned on (or off), it must remain on (or off) for a certain number of time periods. This operational restriction for generators also requires the inclusion of a binary variable to model the state of the generator. It is possible to formulate the minimum up and down time constraints with just the use of the unit commitment binary variables [14].

There are four main costs that are frequently associated with a generator: operating

cost, start-up cost, shut down cost, and no load cost. The operating cost represents the fuel cost of the generator and it is proportional to the amount of energy produced. Generators can also have start-up and shut down costs. They can be modeled without start-up and shut down binary variables; as a result, some unit commitment formulations do not include start-up or shut down binary variables. However, in [14], it is shown that the inclusion of these binary variables is beneficial in solving the unit commitment formulation. Consequently, start-up binary variables, v_{gt}, and shut down binary variables, w_{gt}, are included. The start-up binary variable takes on a value of one when the unit is turned on in period t and it takes on a value of zero otherwise. Similarly, the shut down binary variable takes on a value of one when the unit is turned off in period t and it takes on a value of zero otherwise. No load costs represent the cost to keep the generator on during a particular period. This cost is not a variable operating cost; rather, the no load cost is a fixed cost that is incurred during every period that the unit is operating (online).

Unit commitment problem is a classical problem in electrical engineering. In the literature, there are many proposed methods to solve generation unit commitment problems; the detailed literature review on unit commitment solution methods are presented in [53, 54, 55]. In this research, the unit commitment problem with mixed integer programming (MIP) formulation is used; the basic unit commitment formulation, used in [14], is modified for this research. In the past years, many independent system operators (ISOs) in the United States have adopted MIP approach for their generation unit commitment software [49, 56, 57].

The unit commitment model used in this research is presented in (3.13)-(3.31), where constraint (3.13) represents an objective, constraint (3.14) represents a node balance condition of OPF, line capacity constraint is represented by (3.15), generator capacity constraint is represented by (3.16), constraints (3.17)-(3.19) represent minimum up and down limitations of generator, generator ramping constraints are modeled by constraints (3.20)-(3.21),

system reserve requirements are modeled as shown in (3.22)-(3.27).

In the unit commitment model, the generators' minimum up and down time requirements are difficult to model; the detailed analysis of generators' minimum up and down time constraints are explained in [58]. The ramping constraints used in this research, shown in (3.17)-(3.19), are the same as used in [14].

$$\min \sum_{\forall t}\sum_{\forall g}(c_g P_{gt} + c_g^{SU} v_{gt} + c_g^{SD} w_{gt} + c_g^{NL} u_{gt}) \tag{3.13}$$

$$\text{s.t.} \sum_{\forall k \in \delta_n^+} B_k(\theta_{nt} - \theta_{mt}) - \sum_{\forall k \in \delta_n^-} B_k(\theta_{nt} - \theta_{mt}) + \sum_{\forall g(n)} P_{gt} = d_{nt}, \forall n, t \tag{3.14}$$

$$P_k^{min} \leq B_k(\theta_{nt} - \theta_{mt}) \leq P_k^{max}, \forall k, t \tag{3.15}$$

$$P_g^{min} u_{gt} \leq P_{gt} \leq P_k^{max} u_{gt}, \forall g, t \tag{3.16}$$

$$v_{gt} - w_{gt} = u_{gt} - u_{gt-1}, \forall g, t \tag{3.17}$$

$$\sum_{q=t-UT_g+1}^{t} v_{gq} \leq u_{gt}, \forall g, t \in \{UT_g, .., T\} \tag{3.18}$$

$$\sum_{q=t-DT_g+1}^{t} w_{gq} \leq 1 - u_{gt}, \forall g, t \in \{DT_g, .., T\} \tag{3.19}$$

$$P_{gt} - P_{gt-1} \leq R_g^{+} u_{gt-1} + R_g^{SU} v_{gt}, \forall g, t \tag{3.20}$$

$$P_{gt-1} - P_{gt} \leq R_g^{-} u_{gt-1} + R_g^{SD} w_{gt}, \forall g, t \tag{3.21}$$

$$r_{gt}^{sp} \leq P_g^{max} u_{gt} - P_{gt}, \forall g, t \tag{3.22}$$

$$r_{gt}^{sp} \leq R_g^{sp} u_{gt}, \forall g, t \tag{3.23}$$

$$\sum_{g} r_{gt}^{sp} \geq SP_t, \forall t \tag{3.24}$$

$$\sum_{g} r_{gt}^{sp} \geq P_{gt}, \forall g, t \tag{3.25}$$

$$r_{gt}^{nsp} \leq R_g^{nsp}(1 - u_{gt}), \forall g \in \{Fast\}, t \tag{3.26}$$

$$\sum_{g} r_{gt}^{nsp} \geq NSP_t, \forall t \tag{3.27}$$

$$\sum_{g} r_{gt}^{nsp} \geq P_{gt}, \forall g, t \tag{3.28}$$

$$0 \leq v_{gt} \leq 1, \forall g, t \tag{3.29}$$

$$0 \leq w_{gt} \leq 1, \forall g, t \tag{3.30}$$

$$u_{gt} \in \{0, 1\}, \forall g, t \tag{3.31}$$

Constraints (3.20)-(3.21) represent the ramping capability of generators, which considers the generator's capability to change its output in a specific time step. In general, in the day-ahead unit commitment problem, as well as in this formulation, the time step of one hour is considered; therefore, in constraints (3.20)-(3.21) one hour ramping capability of generators are presented.

Constraints (3.22)-(3.27) represents the spinning and non-spinning requirements, which are needed to overcome any contingencies within the system. Therefore, in practice, there are ancillary services to protect against contingencies, such as a fault on a line or a loss of a generator, as well as unexpected load fluctuations. In general, there are four types of ancillary services: regulation reserve, spinning reserve, non-spinning reserve, and replacement reserve. Regulation reserve is used to follow the changes in load, to account for the changes in the load and minor fluctuations caused by different types of loads and load cycles. In some markets regulation reserves are specified as a regulation up and regulation down, which are deployed based on automatic generation control (AGC) and it is replaced by spinning reserve after a short time interval, which is also know as making the area control error (ACE) to zero. Though spinning reserve can be used to replace regulation reserve, its primary purpose is to be available to mitigate contingencies within a specified amount of time. Spinning reserves are called upon to help prevent a blackout when there is a contingency; in many cases, spinning reserves are supplied by committed generators with high ramping capability. Similar to spinning reserve, the primary purpose of non-spinning reserve is to be available, within a specified amount of time, generally within 10

minutes, if called upon to help prevent a blackout when there is a contingency. The primary difference between spinning and non-spinning reserve is that non-spinning reserve is not required to be online. Non-spinning reserves are supplied by fast start units, such as fast gas turbine generators, which ramp to their set operating point within a few minutes when they are called to respond. The purpose of replacement reserve is to replace spinning and non-spinning reserve when they are exhausted to mitigate contingency, within thirty minutes after a contingency occurs, to help the system to achieve its required reliable operating state, i.e., N-1 state. In the unit commitment problem, presented in (3.13)-(3.31), only spinning and non-spinning reserve requirements are considered. The reserve requirements for the unit commitment problem is the sum of 5% of demand supplied by hydro generators, and 7% of demand supplied by non-hydro units or the single largest contingency, whichever is greater. It is assumed that at least 50% of total required reserves will be supplied by spinning reserves, and the rest will be supplied by non-spinning reserves. This assumption is in line with California independent system operator's guidelines for spinning reserve and non-spinning reserve [59].

3.6 Day-ahead Unit Commitment Procedure in Realistic Setting

The SCUC problem presented in Section 3.5 is a complex problem and can be solved (in its original form without any special solution method) only with smaller test systems. However, in real-life, the system size may have thousands of buses and many more branches. To solve the SCUC problem, for these large systems, a more complex solution method is needed. In [60], the day-ahead unit commitment procedure used at Mid-continental Independent System Operator (MISO) is presented. The resultant day-ahead procedure is reproduced in Fig. 3.1. At MISO, the day-ahead scheduling procedure is divided into four stages: pre-processing, unit commitment, deliverability test and operator review.

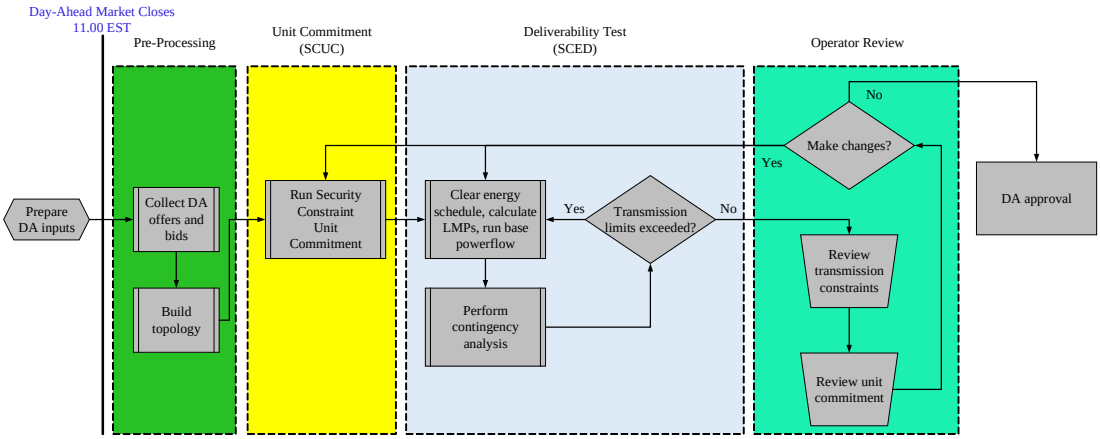

Figure 3.1: Day-Ahead Unit Commitment Procedure at MISO.

In the pre-processing stage, information collected from market participants are analyzed, along with the network topology, and passed on to the unit commitment stage. In the unit commitment stage, a SCUC problem is solved; this SCUC formulation is simple and primarily determines the generator schedule. The network information in the SCUC formulation is limited and mainly considers critical transmission elements. The solution of the unit commitment stage is passed on to the deliverability test stage. The deliverability test stage is SCED problem, which determines the feasibility of the generator schedule chosen in the unit commitment stage. The SCED model contains more network information determines energy schedule, LMPs and base case power flow. The deliverability test stage also performs the contingency analysis on the base case power flow and determines the solution solution quality in terms of N-1 requirements. Note that, in this case, system wide N-1 contingency analysis is not performed; only the critical contingencies are considered in the deliverability test. The solution obtained from the deliverability test stage is given it to operator review stage; in this stage, the solution obtained from the deliverability test stage is reviewed by the operator and necessary changes are made based on the solution quality and constraint violations. If the solution obtained, from the SCUC and the SCED problem, is not acceptable, the SCUC and the SCED problems is solved again. In many

cases this procedure is continued for 4-5 iteration and the resultant day-ahead solution is passed on the day-ahead approval. The input data and the output data, obtained from the MISO's day-ahead market tool, is presented in Table 3.1. This information is obtained from [60].

Table 3.1: Input Data and Output Solution from MISO's Day-Ahead Market Tool.

- Input Data	Output Solution
- Generator offers 3 Part - Load Bids fixed, price-sensitive - Virtual bids/offers - External transactions - Transmission network - Scheduled outages - HVDC schedule - Unit initial conditions - Unit physical characteristics - Loop flow assumptions - Interface limits - Constraints: flowgates, contingencies, phase shifter, facility ratings	- Day-ahead LMPs/ hour - Cleared energy (schedules/ participant/ location/ hour) - Physical and virtual bidders - External transactions - Unit commit schedules

3.7 Conclusion

The AC optimal power flow problem is a nonlinear non-convex problem, which is, in general, a complex problem to solve. To overcome this computational limitation, a linearized AC optimal power flow problem, known as the DC optimal power flow problem is used in many power system related studies. The benefit of using the DCOPF formulation

over the ACOPF formulation is that it is computationally light, computationally trackable, and can be scaled to larger size test cases with adding additional complexities. However, the DCOPF solution may not be accurate; in literature, it is shown that the gap between the DCOPF solution and ACOPF solution may be large and decisions based on a DCOPF solution may not be accurate and may be infeasible.

The unit commitment problem is a classical power system scheduling problem. To computationally track the unit commitment problem a linearized AC optimal power flow based formulation is used in the electrical industry. The solution of the unit commitment problem, presented in Section (3.5), is used as a input parameter for all the simulation studies presented in this thesis.

Chapter 4

ROBUST OPTIMIZATION

4.1 Introduction

The origin of robust optimization goes back to the early days of modern decision theories in the 1950's [61], where it was used to analyse the worst-case scenario of several uncertainties. In the 1970's, Soyster [62] proposed a worst-case model for linear optimization problem such that constraints are satisfied under all possible perturbations of the model parameters. Over the years, robust optimization techniques have been used in many areas, such as operations research [63, 64], control theory [65], logistics [66], finance [67], medicine [68], and chemical engineering [69].

In recent years, robust optimization has gained a great deal of attention in the electrical power system sector; for example, in [70] and [71], two-stage robust optimization techniques are used for unit commitment, which deal with the data uncertainty and attempt to find an optimal solution considering the worst-case uncertainty realization. The solution of the robust optimization problem is guaranteed to be feasible and optimal for a defined uncertainty set [72, 73]. Since the optimal solution is a hedge against the worst-case realization, the solution is often conservative. Robust optimization may not be preferred for many applications due to its conservative nature; however, it is in accordance with the power industry in regards to maintaining reliability.

4.1.1 The Need of Robust Optimization

LP is a type of optimization problem with a polynomial algorithm and generally it is in form of (4.1), where, x is a vector of decision variables such that $x \in \mathbb{R}^n$, cost is represented

by c such that $c \in \mathbb{R}^n$, A is an $m \times n$ constraint matrix, and $b \in \mathbb{R}^m$ is the right hand side vector of constraint matrix.

$$\min_x \{c^T x : \ Ax \leq b\} \tag{4.1}$$

The structure of the problem, given in (4.1), is such that there are m number of constraints and n number of variables. The data of the problem are the collection ($c,\ A,\ b$) and are collected in data matrix, D, as shown in (4.2). The dimension of this matrix is $(m+1) \times (n+1)$.

$$D = \left[\begin{array}{c|c} c^T & 0 \\ \hline A & b \end{array}\right] \tag{4.2}$$

Note that, in D, all the parameters are fixed and known prior to solving the LP problem. In most of the real world LP problem all this data is not known; the uncertainty in data is presented due to many reasons, some of them are listed below [74],

1. Prediction error- In many real-life mathematical problems, some of the data entries are unknown at the time problem formulation. Therefore, when the problem is solved, those data entries are estimated by their respective data forecasts. These data forecasts are not exact (by the definition of forecast), which introduces the prediction error. For instance, in case of day-ahead unit commitment problem, the system demand for the next day is unknown; therefore, it is forecasted using system demand forecasting methodologies [75]. It is well understood in the power industry that day-ahead system demand forecast is not accurate; hence, system operators consider operational reserves in day-ahead unit commitment problem to overcome this inaccuracy and the unpredicted nature of system demand in real-time implementation.

2. Measurement error- In some LP problems, the few parameters in the data matrix, D, are determined based on actual data measurement. Often these measurements are done off-line and may not be measured accurately. This introduces measurement errors in parameter calculations and may introduce considerable uncertainty into the LP problem solution. For instance, the susceptance of transmission lines in power transmission network are determined based on field measurements. In many cases, these measurements are not accurate or do not reflect the true value, as susceptance of transmission line depends on weather condition and changes over time due to operational wear and tear. Therefore, optimal power flow problems solved based on these susceptance values may results in sub-optimal or even infeasible solutions.

3. Implementation error- Sometimes the decision variables determined in a mathematical problem cannot be implemented exactly as they are computed. This practical implementation issue introduces implementation errors in solution. For example, in power system operations, the generators are scheduled and dispatched based on day-ahead unit commitment solution. However, sometimes, due to practical issues, generators deviate from the required set dispatch point; for instance, old generators may not ramp up and ramp down as expected or gas turbine generators fail to produce required power due to higher temperatures in the turbine. In these cases, system operators needs to update the generator dispatch based on present operating conditions.

Traditionally, LP problems are solved by ignoring the data uncertainty. The results obtained from the LP models are implemented or analyzed with small perturbations via sensitivity analysis. It has been shown that even with small perturbation of the data, the solutions from the deterministic LP models can be suboptimal and even infeasible in many real situations [73]. Therefore, consideration of uncertainties is critical in many practical applications.

4.2 Robust Optimization

In recent years, robust optimization has gained lot of attention. Robust optimization guarantees a feasibility, as well as optimality, of a solution for any possible realization in the modeled uncertainty set. This approach considers the worst-case realization of uncertainty within the pre-determined uncertainty set. The benefit of robust optimization is that it requires less probability information about uncertainty compared with the stochastic programming approach; however, the solution obtained from robust optimization is generally more conservative than the solution obtained from stochastic programming approach. Due to the conservativeness of robust optimization over stochastic programming, robust optimization has recently become more attractive as a mechanism to model uncertainty [76, 74, 77] in applications with high reliability requirements.

In addition, ensuring reliability and obtaining economically robust solutions are the primary concerns in the power systems sector. Little work has been done to examine the benefits of robust optimization in the electric power industry. Recently, more attention has been given to the application of robust optimization in the power systems sector by [71, 70, 78].

The generic form of deterministic MIP problem is presented in (4.3)-(4.8), where, x is a set of integer variables and y is a set of continuous variables. Other parameters, such as $A, a, B, b, c, E, e,\ F, f, H, h$, are data or parameters. The solution obtained from this MIP formulation is optimal/feasible only for the fixed values associated with parameters $A, a, B, b, c, E, e, F, f, H, h$. The basic topology control model, used in research, is a MIP problem. This can be represented in generic form as shown in (4.3)-(4.8), where, variable x represents the status of transmission line, i.e., line in service or line out of service, and variable y represents the set of other continuous variables, such as generator dispatch, line flows, and bus angles.

$$\min_{x,y} \quad c^T x + b^T y \tag{4.3}$$

$$\text{s.t.} \quad Fx \leq f \tag{4.4}$$

$$Hy \leq h \tag{4.5}$$

$$Ax + By \leq a \tag{4.6}$$

$$Ey = e \tag{4.7}$$

$$x \in \{0, 1\} \tag{4.8}$$

The objective of robust optimization problem is to determine the optimal solution considering the worst-case outcome under the assumed uncertainty set. The generic form of robust optimization problem is given in (4.9)-(4.14), which is a two-stage optimization problem. The first stage of the problem is to determine the solution associated with integer variables which are typically referred as design decisions ; the second stage is to find the worst-case cost or worst-case realization of the continuous variable, y, associated with the integer solution obtained in the previous stage. Traditionally, two-stage robust optimization is actually modeled as a three-stage problem with a middle stage of uncertainty scenario selection, as shown in (4.9)-(4.14). The formulation is attempting to determine an optimal solution of the design and operational cost against the worst-case uncertainty realization. The solution of the robust optimization problem is guaranteed optimal for a pre-defined uncertainty set [71, 70].

In (4.9), the term $y(d)$ is used to emphasize the dependency of continuous variable y on the uncertainty, d. The first minimization part of (4.9) minimizes the cost associated with the integer solution. The later part of (4.9), the max-min formulation, known as the evaluation part of robust structure, determines the worst-case cost of decision taken in first part of minimization problem. The evaluation part of the robust formulation is divided into two parts, which makes the entire robust optimization problem as a three-stage optimization

problem as shown in (4.9)-(4.14). In (4.9), the evaluation part of the robust formulation, i.e., max-min part of (4.9), is known as a robust counterpart of the robust optimization problem.

$$\min_{x \in \mathcal{X}} \quad \left(c^T x + \max_{d \in \mathcal{D}} \min_{y} b^T y(d) \right) \tag{4.9}$$

$$\text{s.t.} \quad Fx \leq f \tag{4.10}$$

$$Hy(d) \leq h \tag{4.11}$$

$$Ax + By(d) \leq a \tag{4.12}$$

$$Ey(d) = e \tag{4.13}$$

$$x \in \{0, 1\} \tag{4.14}$$

Traditionally, for robust optimization problems, the following assumptions are made prior to solving the problem, which are cited in [74].

1. All the entries in the first-stage decision variables are "here and now" decisions, which should get specific numerical values as a result of solving the problem, and before the actual data "reveals itself". The second-stage variables are "wait and see" decisions, which will be determined when the data realization is revealed. This assumption indicates that the first-stage solution of the robust optimization problem should be a fixed number/vector, which will be optimal and feasible to the entire uncertainty set with the adaptive second-stage solutions.

2. The decision maker is fully responsible for consequences of the decisions to be made when, and only when, the actual data is within the unspecified uncertainty set. This assumption indicates that the solution is guaranteed to be "robust" only to the uncertainties modeled within the uncertainty set.

3. The constraints in robust formulation are “hard”- we cannot tolerate violations of constraints, even small ones, when the data is within the uncertainty set. This assumption ensures the robustness property of robust optimization problem by enforcing all the constraints and not allowing any relaxations on a constraint level.

4.2.1 Uncertainty Modeling

Uncertainty modeling is a key part of robust optimization. In [70], polyhedral uncertainty sets are used to define demand uncertainties. System demand uncertainty, in [70], is modeled assuming that the system load has an upper, as well as a lower bound, and that the system-wide aggregate load has an upper bound, as shown in (4.15). Similar uncertainty set definition is used [71].

$$\mathcal{D} = \{d \in \mathbb{R}^{N_d} : \sum_{i \in N_d} \frac{|d_i - d_i^{fix}|}{\hat{d}_i} \leq \Delta, d_i \in [d_i - \hat{d}_i, d_i + \hat{d}_i],\ \forall i \in N_d\} \tag{4.15}$$

In (4.15), the set of nodes with uncertain demand is represented by N_d, d_i^{fix} represents the estimated or expected demand, d_i represents the realization in demand, the maximum deviation in demand at node i is represented by parameter $\hat{d}_i$ The total deviation in demand is also bounded by parameter Δ.

In Chapter 6-7 , a simplified uncertainty model is used to represent demand uncertainty. The polyhedral uncertainty set is presented in (6.1); if desired, a more complex polyhedral uncertainty sets can be used instead, as in [71].

$$\mathcal{D} = \{d \in \mathbb{R}^n : d_n^{fix} D_n^- \leq d_n \leq d_n^{fix} D_n^+,\ \forall n\} \tag{4.16}$$

In this uncertainty set, the system demand is bounded by its pre-determined lower and upper limits. The uncertainty description used in (4.16) is more conservative than the

uncertainty sets used in [70] and [71]. The size of the uncertainty set is defined by the parameters D_n^+ and D_n^-. When D_n^+ and $D_n^- = 1$, the uncertainty is zero and $\mathcal{D}$ is a singleton, i.e., $d_n = d_n^{fix}$. When $D_n^- \leq 1$ and $D_n^+ \geq 1$, the uncertainty set is a polyhedron and its size is defined by the values of D_n^+ and D_n^-.

Similarly, wind uncertainty is modeled as shown in (4.17). Renewable resources (in this case, wind generation), P_w, are assumed to vary within these pre-determined lower and upper limits, and the size of uncertainty set depends on the parameters D_w^- and D_w^+.

$$W = \{P \in \mathbb{R}^w : P_w^{fix} D_w^- \leq P_w \leq P_w^{fix} D_w^+, \ \forall w\} \tag{4.17}$$

4.3 Comparison Between Robust Optimization and Stochastic Optimization

Uncertainty is an important factor to be considered in the decision making processes. In traditional applications, the uncertainties were ignored or simplified due to computational difficulties. With the advance of the computational power, there are different ways to incorporate uncertainties in decision processes.

Stochastic programming has been one common approach to facilitate the decision processes with uncertainties. It typically assumes probability distributions for uncertain parameters, or incorporates a large number of scenarios, which leads to computationally challenging large scale optimization problems. In stochastic programming formulations, the objective is typically optimizing over the expectation over the uncertain parameters. The feasibility of the solutions is modeled either to be feasible to all scenarios or with probability guarantees. While it is generally difficult to know the exact distribution of the random parameters, sample based methods are popular in the stochastic programming literature. To achieve high probability guarantees, the sample size is typically large and leads to computational challenges of the stochastic programming approaches.

In (4.18), a generic form of stochastic optimization problem with probability constraints

is presented, where the uncertainty in optimization framework follows the probability distribution, when $\epsilon \ll 1$, the distribution of data (c, A, b) is represented by P. In simple cases, these uncertainties are modeled with known probability distribution functions; however, in more realistic cases, the probability distribution function is partially know. This may cause a problem in (4.18) such that the partial distribution of P is known and P belongs to a given family $\mathcal{P}$ of probability distributions on the space of the data (c, A, b). In this situations, the accuracy of stochastic optimization problem depends on the availability of possible scenarios and modeling details. If all the possible scenarios are modeled in stochastic framework, the optimization problem become cumbersome and may not be solvable. Therefore, there is a tradeoff between the number of scenarios modeled and the computational time/trackability. Another tradeoff is between the quality of stochastic solution and number of scenarios under consideration. The solution quality of stochastic optimization problem is directly related to number of scenarios under consideration. The primary barrier to stochastic programming is the tradeoff between the computational challenge and the quality of the solution; to get a more accurate solution, it would be preferable to represent additional uncertainties, but then this increases the model complexity, which makes it more difficult to obtain a quality solution.

$$\min_{x,t}\{t : Prob_{(c,A,b)\sim P}\{c^T x \leq t \;\&\; Ax \leq b\} \geq 1-\epsilon, \forall P \in \mathcal{P}\} \tag{4.18}$$

The robust optimization has gained substantial attention in recent years [71, 70, 78]. This approach is attractive in many aspects over stochastic optimization approach for the problems with high reliability requirements. The main benefit of robust optimization is that it requires moderate information about underlying uncertainties, such as range of uncertainty, type of uncertainty. The robust framework is flexible enough to model each type and size of uncertainty independently, as well as simultaneously. Robust optimization does

not requires probabilistic information about the uncertainty; the solution obtained from robust formulation is guaranteed to be optimal for the entire uncertainty set. Therefore, robust optimization modeling approach is favorable for the electric power sector where ensuring reliability is crucial. Furthermore, robust optimization requires less knowledge concerning the probability distribution as compared to stochastic programming and the computational complexity for robust optimization is typically smaller. In robust optimization, instead of assuming explicitly a probability distribution of uncertainty parameters, an uncertainty set is predetermined to cover the possible realizations. A solution model is robust if it is feasible for all the possible scenarios in the uncertainty set and is robust if it is close to the optimal solution for all the scenarios in the uncertainty set.

Smaller uncertainties can be analyzed by performing a sensitivity analysis [76]. The sensitivity analysis is a tool to analyze the stability properties of an already found solution; there are many application, in literature, which are based on sensitivity analysis to determine the solution quality/robustness. This approach has been used in many system control related problems; however, sensitivity analysis solution does not give guarantees associated with quality of solution and its effectiveness; plus, sensitivity analysis does not hold, if the expected uncertainty is relatively large. Therefore, implementation of solution sensitivity based methods are limited.

4.4 Conclusion

Uncertainty analysis plays an important role in decision making processes. By ignoring the uncertainty, a decision can be sub-optimal, or even infeasible. Stochastic optimization has been one common approach to incorporate uncertainties in decision making process.

This research focuses on robust optimization to understand and model the uncertainties in the decision making process. The solution obtained from robust optimization problem is guaranteed optimal/feasible for the entire uncertainty set. However, robust optimization

problems are computationally complex and require special solution techniques to solve the problem.

In recent years, robust optimization has gained attention in the electrical power system community. Robust optimization, would be suitable for power system related problems, as ensuring reliability and obtaining robust solutions are primary concerns in the power systems sector. However, little work has been done to examine the benefits of robust optimization in the electric power industry.

Chapter 5

OVERVIEW OF SYSTEM STABILITY STUDIES

5.1 Introduction

Power system stability is considered one of the important problems in power system operations. Power system stability has been studied since the 1920's, [79]. In the past, many blackouts has been caused by power system instability, underlining the importance of power system stability studies. In literature, transient instability has been considered a dominant stability problem. However, with increased number of generators and inter-connected system, other stability studies, such as frequency stability, voltage stability, etc., have also gained attention in recent years.

5.1.1 Need of Stability Studies with Topology Control

In [1], the power system stability is defined as "power system stability is the ability of an electric power system, for a given initial operating condition, to regain a state of operating equilibrium after being subjected to a physical disturbance, with most system variables bounded so that practically the entire system remains intact". This definition of power system stability motivates the need to check the system stability with topology control.

Topology control algorithms, presented in literature, are either based on ACOPF or DCOPF [21, 18, 14, 23, 80, 81, 51, 82]. However, in an optimization framework, there is no systematic way to insure system stability with topology control. In prior literature, topology control actions combined with stability constraints are proposed [83, 84], but these methodologies were never tested on realistic test cases. Therefore, solution obtained

from topology control algorithms must be tested to insure that the topology control action will not cause cascading events, or even a blackout.

5.2 Overview of Stability Studies

Power system stability may be broadly defined as the property of a power system that enables it to remain in a state of operating equilibrium under normal operating conditions and to regain an acceptable state of equilibrium after being subjected to a disturbance [85]. Under steady state conditions, there is equilibrium between input mechanical torque and output electrical torque of each machine, and the speed remains constant. If the system is perturbed, this equilibrium is upset, resulting in acceleration or deceleration of the rotors of the machines [86].

In an interconnected power system, the rotor angle stability of each synchronous machine defines its ability to restore equilibrium. Renewable resources, such as wind and solar, are inherently asynchronous in nature, as they do not have any rotating mass or inertia; they change the system dynamics with respect to the interaction of synchronous machine rotors among themselves. The mechanism associated with generation of electricity from wind and solar resources, together with their interface with the bulk power, contributes to change in system dynamics. At the same time, implementation of topology control for power system operation makes the power system stability studies critical. In [1], different stability studies are recommended for power system operation; they are classified based on nature, type of disturbance, as well as time span under consideration. Typically, stability studies are classified into three different categories: rotor angle stability, frequency stability, and voltage stability, as shown in Fig. 5.1. In this thesis, all three stability studies are considered to study the effect of topology control action on system stability/reliability.

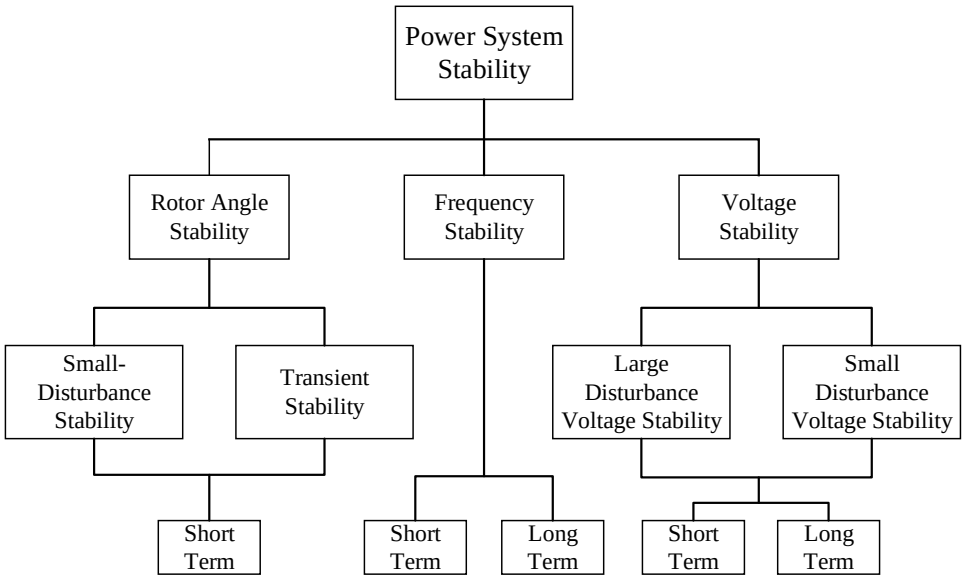

Figure 5.1: Classification of Power System Stability [1].

The mechanism by which interconnected synchronous machines maintain synchronism with one another is through restoring forces, which act whenever there are forces tending to accelerate or decelerate one or more machines with respect to other machines. The change in electrical torque of a synchronous machine following a perturbation can be resolved into two components [85]: (a) synchronizing torque component, which is in phase with the rotor angle perturbation, (b) damping torque component, which is in phase with the rotor speed deviation.

System stability depends on the existence of both components of torque for each of the synchronous machines. Lack of sufficient synchronizing torque results in instability through an aperiodic drift in rotor angle, while lack of sufficient damping torque results in oscillatory torque. For convenience in analysis and for gaining useful insight into the nature of stability problems, rotor angle stability is further categorized into transient stability and small signal stability.

5.2.1 Transient Stability

Transient stability is the ability of a power system to maintain synchronism when subjected to a severe disturbance such as a fault on transmission facilities, loss of generation, or loss of a large load. The system response to such disturbances involves large excursions of generator rotor angles, power flows, bus voltages and other system variables. The resulting system response is influenced by the nonlinear characteristics of the power system. If the resulting angular sepa-ration between the machines in the system remains within certain bounds, the system maintains synchronism. Transient stability depends on both the initial operating state of the system and the severity of the disturbance. Instability is usually caused due to insufficient synchronizing torque and results in aperiodic angular separation. The time frame of interest in transient stability studies is usually 3 to 5 seconds of the initial disturbance [85]. In a synchronous machine, if the rotor speed increases due to a disturbance, it causes a corresponding increase in rotor angle also. This increase in rotor angle results in an increase in electrical load on the generator. This load increase provides a synchronizing torque to the rotor and helps to bring the rotor back to synchronism. In the case of asynchronously connected wind generators, such synchronizing torque is not available to the rotor after a disturbance. Therefore, the transient stability of a system with appreciable wind resources is markedly different from a system with negligible wind resources.

5.2.2 Small Signal Stability

Small signal stability is the ability of the power system to maintain synchronism under small disturbances, which occur continually on the system because of small variations in loads and generations. The disturbances are considered sufficiently small for linearization of system equations to be permissible for purposes of analysis. Instability that may result can be of two forms: (i) steady increase in rotor angle due to lack of sufficient synchro-

nizing torque, or (ii) rotor oscillations of increasing amplitude due to lack of sufficient damping torque. The nature of system response to small disturbances depends on a number of factors including the initial operating conditions, the transmission system strength, and the type of generator excitation controls used [85].

In large power systems, the small-signal stability problem can be either local or global in nature. Local plant mode oscillations are associated with rotor angle oscillations of a single generator or a single plant against the rest of the system. Local problems may also be associated with oscillations between the rotors of a few generators close to each other. These oscillations have frequencies in the range of 0.7 to $2.0Hz$ [85]. On the other hand, global small-signal stability problems are caused by interactions among large groups of generators and have widespread effects. They involve oscillations of a group of generators in one area swinging against a group of generators in another area. Such inter-area oscillations have frequencies in the range of 0.1 to $0.7Hz$ [85].

5.2.3 Frequency Stability

Frequency stability is the ability of a power system to maintain steady frequency under a severe system upset resulting in a significant imbalance between generation and load caused by sudden loss of generation, contingency, implementation of topology control action, etc. The frequency stability of the system depends on the ability to maintain/restore equilibrium between system generation and load, with minimum unintentional loss of load. Instability that may result occurs in the form of sustained frequency swings leading to tripping of generating units and/or loads. Generally, frequency stability problems are associated with inadequacies in equipment responses, poor coordination of control and protection equipment, or insufficient generation reserve [85]. The timescale for frequency stability varies from fraction of seconds to several minutes.

5.2.4 Voltage Stability

Voltage stability refers to the ability of a power system to maintain steady voltages at all buses in the system after being subjected to a disturbance from a given initial operating condition [85]. It depends on the ability to maintain/restore equilibrium between load demand and load supply from the power system. Instability that may result occurs in the form of a progressive fall or rise of voltages of some buses. A possible outcome of voltage instability is loss of load in an area, or tripping of transmission lines and other elements by their protective systems leading to cascading outages [85].

5.3 Generator Modeling

5.3.1 Traditional Generators

In this research, stability studies are performed on IEEE-118 bus test case is given in [87]; however, the generation information for this test system is not available. Therefore, the generator mix of reliability test system 1996 (RTS) is used to create generator information for the IEEE-118 bus test case [87]. There are a total 71 conventional generators, and 9 wind injection locations.

The dynamic data for the IEEE-118 bus test case is not available; therefore, generator information from generators in the eastern interconnection, provided by Tennessee Valley Authority (TVA), are used to generate dynamic data. In this thesis, the detail listing of generator type and associated dynamic models, are presented in Table 5.1. The detail information about these dynamic models are given in PSLF manual [88].

Table 5.1: Traditional Generator Dynamic Model Information.

Generator Type	**TVA Reference**	**Generator Model**	**Excitor Model**	**Governor Model**
U12	343003-5	GENROU	SEXS	IEEEG1
U20	343003-7	GENROU	SEXS	IEEEG1
U50	505476-1	GENSAL	IEEET1	HYGOV
U76	349108-1	GENROU	ESDC1A	IEEEG1
U100	251939-1	GENROU	ESST4B	TGOV1
U155	383644-4	GENROU	IEEET1	IEEEG1
U197	315037-1	GENROU	ESST4B	GGOV1
U350	304869-1S	GENROU	IEEET1	IEEEG1
U400	256339-2	GENROU	EXST1	–

5.3.2 Full Converter Wind Turbine Generator (Type 4)

The IEEE-118 bus test case, used in this thesis, consists of 9 wind injection locations. It is assumed that all the wind generators are Type-4 wind generators.

The Type-4 design of wind turbine generator uses a conventional synchronous generator with a DC field or a permanent magnet to provide excitation. The advantage of this category of wind machine is the gearless design, since the generator is directly connected to the turbine and rotates at the same speed as that of turbine [89]. The generator is connected to the network through a back-to-back frequency converter, which completely decouples the generator from the network. Through this converter, the electrical output of the generator can be converted to system frequency over a wide range of electrical frequencies of the generator, enabling machine operation over a wide range of speeds. The schematic of the converter driven synchronous generator based wind turbine is as shown in Fig. 5.2

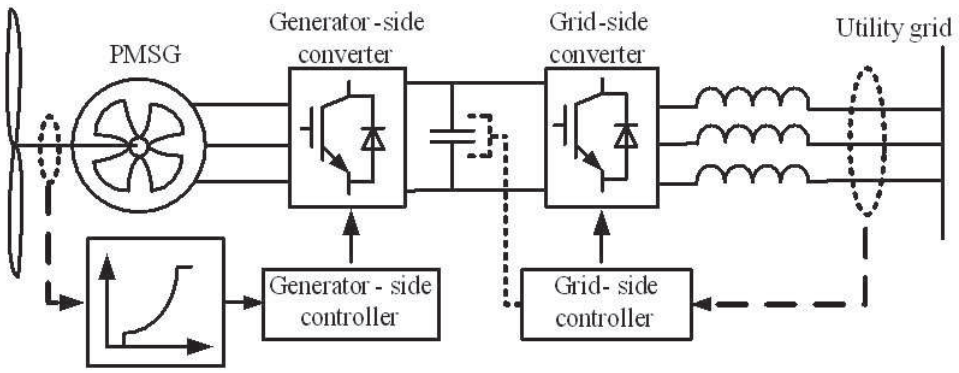

Figure 5.2: Full Converter Wind Turbine Generator (Type-4)

The dynamic data, for $1.5MW$ individual wind generator, given in [90], are used to model wind injection in this thesis.

5.4 Conclusion

System stability studies are critical for insuring power system reliability. The brief overview of stability studies are presented in this chapter. Power system stability is similar to the stability of any dynamic system, and has fundamental mathematical underpinnings. Precise definitions of stability can be found in the literature dealing with the rigorous mathematical theory of stability of dynamic systems.

Chapter 6

ROBUST CORRECTIVE TOPOLOGY CONTROL FOR SYSTEM RELIABILITY

6.1 Introduction

Even though the bulk power grid is one of the most complex systems to date, in practice, the modeling of the transmission network is simplified and limited attention is given to the flexibility in the network topology. Traditionally, transmission lines are treated as static assets, which are fixed within the network, except during times of forced outages or maintenance. This view does not describe transmission lines as assets that operators have the ability to control. Transmission switching has been studied since the 1980s and it was used as a tool to overcome various situations such as voltage violations, line overloads [2, 3, 4, 5], line losses and cost reduction [6, 7, 8], system security [9], or a combination of these [10, 11].

Recent work has demonstrated that TC can have significant operational as well as economic impacts on the way electrical power systems are operated today [14, 23, 91, 24]. The concept of a dispatchable network is presented in [20]. Additionally, optimal transmission switching using a direct current optimal power flow (DCOPF) formulation is presented in [91] and [21]; however, these models did not implicitly enforce N-1 reliability constraints. In [18], optimal transmission switching with an N-1 DCOPF formulation was tested on the IEEE 118-bus test case and on the RTS 96 test case. Reference [18] also indicates that substantial savings can be obtained by optimal transmission switching while satisfying N-1 reliability constraints.

There has been recent development of a different transmission switching formulation, [51], which builds on the work of on generalized line outage distribution factors, [52]. With

the use of flow canceling transactions, [51] develops a framework that is able to capture the changes in the topology and compares it to the $B - \theta$ formulation used in many preceding transmission switching papers as well as in this research. This formulation is likely to outperform the $B - \theta$ formulation when the number of monitored lines is relatively small, something that is common practice within optimal power flow problems today.

Past literature has shown that TC can be used to improve system operations and reliability. Such previous work has led system operators to adopt TC as a mechanism to improve voltage profiles, transfer capacity, and even improve system reliability [28, 92, 93]. However, the adoption of TC is still limited as there is a lack of systematic TC tools. Currently, the industry adoption and implementation of TC is based on ad-hoc methods or the operator's past knowledge. Alternatively, transmission switching decisions can be suggested by a mathematical decision support tool. Many factors have prevented TC from becoming a more widespread corrective action within system operations. For instance, there have been misconceptions that more transmission is always better than less, concerns over the switching actions' effect on stability, impacts on circuit breakers, computational complexities of TC algorithms, as well as additional concerns.

Corrective switching is one example of TC, which is implemented today [28]. These methods are based on operators' prior knowledge, as specified in [28] on page 107; such actions may also be based on historical information. Ideally, corrective switching algorithms should be solved in real-time. Once the disturbance occurs, the switching algorithm is executed to suggest switching actions to alleviate any constraint violations. This approach is beneficial since the current operating status is known, which ensures the accuracy of the solution. However, the challenge of real-time mechanisms is that they must be extremely fast while also ensuring AC feasibility, voltage stability, and transient stability. TC models could be solved offline by estimating the operating state of the system. However, deterministic offline mechanisms also have limitations since the operating state must be

predicted prior to the disturbance. The proposed offline corrective action is, thus, susceptible to its problematic reliance on perfect foresight. This rearch introduces the concept of robust corrective TC, which presents a solution to these current challenges.

Robust optimization has gained a great deal of attention in recent years; for example in [70], a two-stage robust optimization technique is used for unit commitment. It deals with data uncertainty and attempts to find an optimal solution considering the worst-case uncertainty realization. The solution of the robust optimization problem is guaranteed optimal for a defined uncertainty set [72, 73]. Since the optimal solution is a hedge against the worst-case realization, the solution is often conservative. Robust optimization may not be preferred for many applications due to its conservative nature; however, it is in accordance with the power industry in regards to maintaining reliability.

This research proposes the new concept of robust corrective TC. The main idea is to use transmission switching as a control tool to mitigate constraint violations with guaranteed solution feasibility for a defined uncertainty set. The switching solution obtained from the robust corrective TC formulation will work for all system states within the defined uncertainty set. The proposed robust corrective TC tool is tested as a part of contingency analysis, which is conducted after solving a day-ahead unit commitment problem; however, note that the concept of robust corrective TC is not restricted to such applications. The main concepts discussed in this chapter are summarized below.

1. Three corrective switching methodologies are identified: real-time corrective switching, deterministic planning based corrective switching, and robust corrective switching. Real-time corrective switching is the preferred process for corrective switching, but it requires extremely fast solution times. Thus, with existing technology, the implementation of real-time corrective switching is limited. With existing technology, deterministic planning based corrective switching can be implemented but it requires perfect foresight regarding future operating states. Therefore, implementation of de-

terministic planning based corrective switching is limited. To fill the technology gap between real-time corrective switching and deterministic planning based corrective switching, a robust corrective switching methodology is proposed.

2. A robust corrective TC formulation: the robust corrective switching model is a three-stage robust optimization problem. With a pre-determined uncertainty set regarding the nodal injections (or nodal withdrawals), the robust corrective switching model will determine the corrective switching action that will be feasible for the entire uncertainty set. The robust optimization model consists of a master problem and two subproblems. The master problem will determine the corrective switching action and the subproblems will determine the worst-case realization of demand within the uncertainty set (for the associated corrective switching action). The nodal injection uncertainty can be due to generation uncertainty (wind/renewables), demand uncertainty, area interchange uncertainty, as well as other causes of uncertainty. The robust corrective switching framework will work for all these different types of uncertainties. The detailed vision of the robust corrective switching framework as an end-to-end process is also presented.

3. A solution technique for solving the robust corrective switching model is presented: specifically, an iterative procedure is developed to solve the master problem and the subproblems. The master problem is a mixed integer programming (MIP) problem and the subproblems are reformulated into a single subproblem, which is a nonlinear problem. This new subproblem is converted from a nonlinear problem into a MIP problem. The proposed solution technique is tested on the IEEE 118-bus test case.

The chapter is structured as follows: a detailed framework of real-time corrective switching, deterministic planning based corrective switching, and robust corrective switching are presented in Section 6.2. The uncertainty modeling used in this chapter is described

in Section 6.3. The generic deterministic corrective switching formulation is given in Section 6.4. The detailed mathematical model for robust corrective switching is given in Section 6.5. The solution method for the corresponding problem is discussed in Section 6.6. The IEEE 118-bus test case is used for the robust corrective switching analysis and the results are presented in Section 6.7.

6.2 Corrective Switching Methodologies

Corrective transmission switching can be used as a control action to respond to an event. This research proposes a robust corrective switching methodology to respond to N-1 contingencies. This section analyzes two existing methods to determine potential corrective switching actions and compares them to the proposed robust corrective switching framework. Note that corrective transmission switching actions may or may not be combined with generation re-dispatch. For the proposed robust corrective switching procedure, generation re-dispatch is taken into consideration.

6.2.1 Real-time Topology Control

The real-time TC model determines the corrective action(s) to take as a response to an event, e.g., a contingency. The skeleton of the real-time TC scheme is shown in Fig. 6.1. When a particular contingency occurs, the corrective switching algorithm will determine the switching action in real-time based on the current system state. The resultant switching scheme will be tested to determine if the proposed topology is AC feasible and if the switching action causes instability. If the solution is feasible, it is implemented.

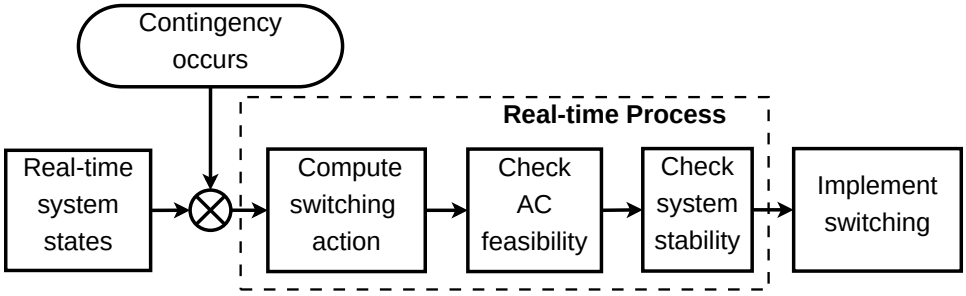

Figure 6.1: Real Time Topology Control Scheme.

Ideally, it is preferred to solve for the optimal switching action in real-time because more information is known about the operating state of the grid. However, during an emergency, it is paramount that a corrective action be taken as soon as possible in order to avoid a potential blackout. Real-time corrective switching is a non-convex, nonlinear, MIP problem. Such a problem cannot be solved in real-time with available tools today. Therefore, heuristics are necessary to generate potential solutions. There are many heuristics for transmission switching that have been previously proposed in literature [80, 82, 94, 95]. These heuristics can be used to find decent solutions faster than solving a MIP. However, there is still the overarching concern that they may not be fast enough for practical large-scale applications due to the extreme importance of implementing a solution as fast as possible during an emergency. DCOPF based heuristics would still need to be checked to see if they are AC feasible and any proposed action would need to be confirmed to not cause a stability concern. Therefore, it is difficult to establish the success rate of such heuristics due to the time sensitive nature of real-time corrective actions during emergency conditions. It is also difficult to predict the solution quality of switching actions proposed by heuristics. In [11], a real-time application of TC is proposed for an AC formulation and they have shown that this can be solved quickly but there is still the issue of transient stability of the switching action and the approach does not take into consideration generation re-dispatch.

Another drawback of such real-time corrective switching heuristics is that they assume

the operating state will not change. State estimation would be used to estimate the system state when the algorithm is executed. However, the actual system state when the action is implemented may be different than the assumed system state due to the time it takes to run the algorithm and check for AC feasibility and system stability. While such procedures can be adjusted to reflect multiple operational states, doing so adds additional complexity to the algorithm, which further exposes the approach to the risk that it may not solve fast enough. Overall, real-time TC mechanisms that rely on heuristics may be fast but there are still practical issues that they do not take into consideration. Thus, there is a need for TC actions that are robust against operating states in order to increase the likelihood of obtaining a feasible solution when implemented.

6.2.2 Deterministic Planning Based Topology Control

Today, there are special protection schemes involving corrective switching that are determined based on offline analysis, [28]. The main idea of deterministic planning based corrective switching is to determine the corrective switching action offline, e.g., in a day-ahead or a week-ahead timeframe, and then feed this information into a real-time dynamic security assessment tool that can determine if the switching action is feasible. For deterministic planning based corrective switching, an assumption regarding the system state is made and switching actions will be proposed in response to selected contingencies. Then, the switching schemes will be tested for AC feasibility and system stability based on the estimated, assumed system state(s). The benefit of such a procedure is that all of the heavy computational work is done offline. The resultant switching schemes are then fed into a real-time security assessment tool that functions like a lookup table. When the particular contingency occurs, a solution from the lookup table will be selected and tested for system feasibility based on the real-time system states. If a feasible solution is found, it is implemented; if a solution is not found, the operator can resort to traditional corrective

means, such as generation re-dispatch. The schematic of the deterministic planning based TC scheme is shown in Fig. 6.2.

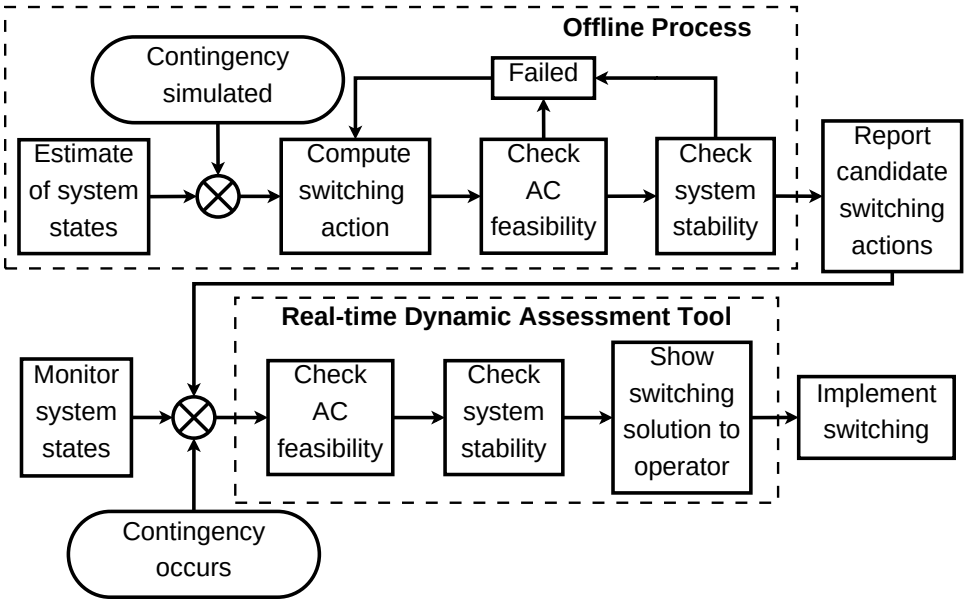

Figure 6.2: Deterministic Planning Based Topology Control Scheme.

The benefit of a planning based corrective switching approach is that the real-time procedures are minimal, resulting in a fast implementation of the action. However, the drawback is that a deterministic planning based corrective switching procedure requires perfect foresight of the system states. With a small deviation from the estimated operating state, the switching action may cause a blackout instead of preventing a blackout. However, most corrective switching schemes implemented in practice are developed offline [28, 92, 93]. For instance, on Page 8 of [92] it states, "Open or close circuits ... when previously documented studies have demonstrated that such circuit openings reliably relieve the specific condition." As a result, corrective switching is primarily limited to unique situations where the proper corrective action is obvious or it is already a well-known action due to the operator's prior knowledge and experience. In the literature, there are few mathematical models available that can be used to determine corrective switching schemes with guaranteed so-

lution feasibility for a range of operating states. In order to respond to this problem, robust corrective switching is proposed.

6.2.3 Robust Corrective Topology Control

This research proposes the robust corrective switching framework as a response to the limitations of real-time and deterministic planning based corrective switching. The proposed robust corrective switching methodology shown in Fig. 6.3 is a combination of real-time and planning based corrective switching methodologies. Due to robust optimization, the proposed robust corrective switching methodology is superior to deterministic policies with respect to solution reliability. The technology gap between real-time and deterministic planning based corrective switching scheme is reduced by doing most of the heavy computational work offline and the guarantee of solution feasibility for a range of operating states is achieved by developing an uncertainty set over estimated system states. The uncertainty set can be viewed as lower and upper bounds over the system parameters or a range of operating states. The TC algorithm will find the candidate switching actions based on modeled system states (with uncertainty) and a simulated contingency. The switching solutions generated by the TC algorithm will then be tested for AC feasibility and system stability. The resultant switching solutions will be considered as candidate switching solutions for the corresponding contingencies and will be used in connection with a real-time corrective switching algorithm. When a particular contingency occurs, the on-line dynamic security assessment tool will test the proposed robust switching actions to determine the appropriate switching action to take. This process can also be combined with previously proposed real-time corrective switching heuristics since combining these procedures together will increase the likelihood of finding a feasible corrective action fast enough.

The primary feature of robust corrective switching is that the solution is guaranteed to be feasible over a wide range of operating states. The uncertainty set may consist of

variable resources, such as generation uncertainty, wind/renewable generation uncertainty, demand uncertainty, and area interchange uncertainty. Furthermore, the TC algorithm can be used to generate multiple switching solutions for a particular contingency. Note that the presented solution method is designed to determine one TC solution at a time. However, by updating the solution method termination condition, the presented framework can be used to determine multiple TC solutions. Providing multiple potential corrective switching solutions to the operator provides added flexibility. This characteristic of robust corrective switching is critical as not all of the solutions generated by the TC algorithm may be AC feasible or pass the stability check. But due to multiple potential switching actions generated by the TC algorithm, it is more likely that at least one of them will produce a feasible operating solution.

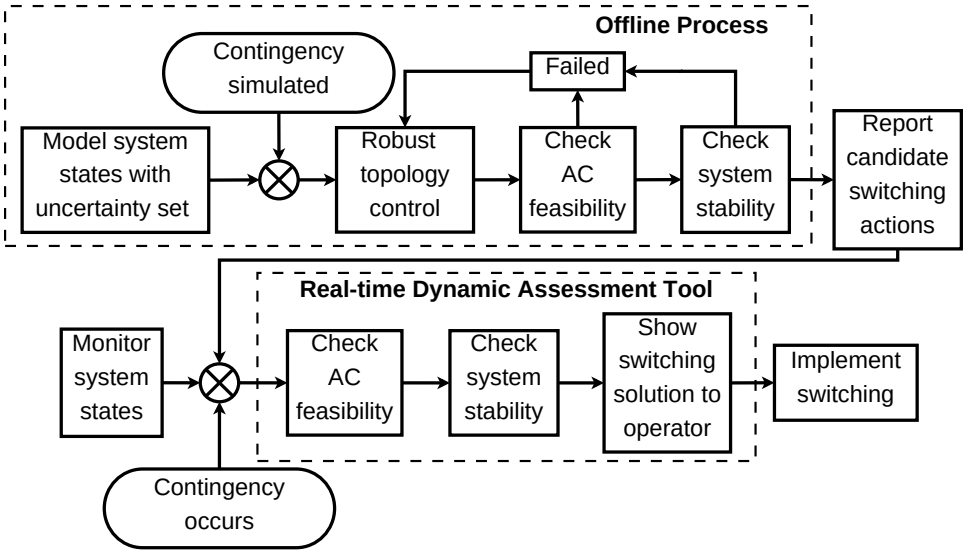

Figure 6.3: Robust Corrective Topology Control Scheme.

The timeline of the robust corrective switching scheme works as follows: after solving the day-ahead unit commitment problem, the robust corrective switching algorithm will determine the corrective switching schemes for possible contingencies. This can be seen as a form of contingency analysis, which has been modified to include robust corrective

switching and it checks for a robust N-1 solution. These switching actions will be tested for AC feasibility and system stability. All of these calculations will be done offline. Once a particular contingency occurs, the real-time dynamic security assessment tool will evaluate the switching solution (if any) based on the real-time system states. If any feasible solution is obtained, it will pass the possible switching actions to the operator. Next, the operator will decide whether to implement the switching solution. The benefit of the proposed procedure is that the robust corrective switching scheme obtained from this method does not rely on ad-hoc methods, which enables corrective switching to be more widespread in order to improve operations and reliability.

The robust corrective switching scheme in this research is based on a DCOPF framework and it guarantees the switching solution will be feasible for any operating state modeled by the uncertainty set. Since the optimal power flow (OPF) formulation is not an AC optimal power flow (ACOPF), the proposed solution must also pass an AC feasibility test. As a result, the guarantee that the solution is robust only holds for a DCOPF problem and is not guaranteed for the ACOPF problem. However, by developing a robust corrective switching formulation, we are able to improve the chances that the proposed switching action will, indeed, be feasible as compared to deterministic corrective switching DCOPF schemes. Typically, generation re-dispatch is required to obtain an AC feasible solution, which is one of the primary reasons why corrective switching schemes may be feasible for the DCOPF but are not AC feasible. However, the proposed robust corrective switching scheme is guaranteed to be feasible (for the DCOPF) for a wide range of operating conditions; this substantially increases the chances that the chosen topology solution will have an AC feasible solution since there are many DC solutions to start with. The proposed robust corrective switching procedure can be seen as a mathematical program that is equivalent to the practice used today by operators to identify candidate switching actions based on historical studies showing the action has worked under a variety of operating conditions.

Note that the procedure presented in Fig. 6.3 is used to determine corrective TC actions for a single contingency. For N different contingencies, the procedure described in Fig. 6.3 would be repeated N times.

In robust corrective TC methodology, it is assumed that with existing technology, the real-time dynamic assessment tool is fast enough to evaluate the TC action such that the TC solution can be implemented in realistic timescale. However, with larger test systems, it is possible that the computational time required for TC solution evaluation, for real-time application, may not be fast enough. To overcome this computational limitation modification to robust corrective TC methodology, presented in Fig. 6.4, is proposed. In this proposed TC solution evaluation process, after solving the off-line process, the candidate TC solutions are made available to real-time applications. In real-time, the real-time dynamic assessment tool will assess the feasibility of TC action by continuously simulating the contingency and its associated corrective TC action with real-time system states. When particular contingency occurs, the TC solution, evaluated in real-time dynamic assessment tool, is made available to operator for implementation. The benefit of this method is that the time required to implement corrective TC solution is minimal. However, evaluating all possible N-1 contingencies with associated TC solution, with real-time system states, might be computationally challenging; therefore, to minimize computational burden, only critical contingencies requiring TC action might be evaluated with real-time system states. This proposed method is similar to the contingency analysis tool, used today in industry, which monitors the critical contingencies, in continuous bases, with real-time system states, to insure N-1 contingency compliance. However, it should be noted that such an approach would limit the capability of corrective TC to mitigate contingencies, as not all the possible N-1 contingencies are considered for real-time TC solution evaluation. Another approach, to overcome computational limitation of real-time evaluation process, is to remove the TC solution evaluation process with real-time system states. In this approach, the TC solution

will be determined and tested with off-line process and implemented, in real-time, without any evaluations. The success of such a approach heavily depends on accuracy of off-line studies, which can be limit the implementation of corrective TC in power systems operation. Furthermore, in industry, today, most of the TC actions are determined and tested in off-line process [96].

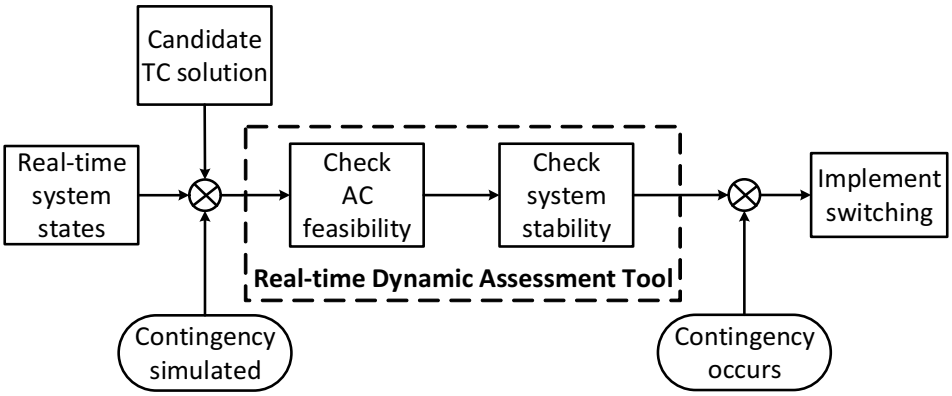

Figure 6.4: Modification to Real-Time Dynamic Assessment Tool

6.3 Modeling of Demand Uncertainty

Uncertainty modeling is a key part of robust optimization. In [70] and [71], polyhedral uncertainty sets are used to define demand uncertainties; they assume that each load has an upper and lower bound and that the system-wide aggregate load has an upper bound. In this research, a simplified uncertainty model is used to represent demand uncertainty. The polyhedral uncertainty set used in this chapter is presented in (6.1); if desired, more complex polyhedral uncertainty sets can be used instead, as in [71].

$$\mathcal{D} = \{d \in \mathbb{R}^n : d_n^{fix} D_n^- \leq d_n \leq d_n^{fix} D_n^+, \ \forall n\} \tag{6.1}$$

In this uncertainty set, the system demand is bounded by its pre-determined lower and upper limits. The uncertainty description used in (6.1) is more conservative than the uncertainty sets used in [70] and [71]. The size of the uncertainty set is defined by the parameters

D_n^+ and D_n^-. When D_n^+ and $D_n^- = 1$, the uncertainty is zero and $\mathcal{D}$ is a singleton, i.e., $d_n = d_n^{fix}$. When $D_n^- \leq 1$ and $D_n^+ \geq 1$, the uncertainty set is a polyhedron and its size is defined by the values of D_n^+ and D_n^-.

6.4 Deterministic Topology Control

Equations (6.2)-(6.7) represent the generic form of deterministic TC, which includes a DCOPF corrective switching formulation. In this formulation, vector c and b are cost vectors. The parameters $A,\ B,\ E,\ F,,\ f,\ H,\ h$ and g represent the system data. The system demand in this case is the forecasted demand and it is denoted by vector $\bar{d}$; each entry in $\bar{d}$ represents the forecasted demand at each bus, d_n^{fix}. Deterministic corrective switching is a MIP problem. The variable x represents the binary variable associated with the switching action, where $x = 1$ if the line is closed/in service or $x = 0$ if the line is open/out of service. The continuous variable y represents all of the OPF continuous variables, such as line currents, bus angles, and generator dispatch.

$$\min_{x,y} \quad c^T x + b^T y \tag{6.2}$$

$$\text{s.t.} \quad Fx \leq f, \tag{6.3}$$

$$Hy \leq h, \tag{6.4}$$

$$Ax + By \leq g, \tag{6.5}$$

$$Ey = \bar{d}, \tag{6.6}$$

$$x \in \{0, 1\} \tag{6.7}$$

6.5 Robust Corrective Topology Control Formulation

In the deterministic corrective transmission switching problem, the switching action is based on a single system state. However, in the robust TC problem, the switching action is determined based on a range of operating states. The objective of robust TC is to find a ro-

bust switching solution in response to a contingency while not allowing any load shedding for any realizable load within the uncertainty set. It should be noted that demand response can also be used as a control mechanism in response to a contingency; however, this option is not included in this research. Furthermore, in this chapter the TC problem is modeled as a feasibility problem; hence, vectors c and b in (6.2) are equal to zero.

The generic form of robust TC formulation is given in (6.8)-(6.13), which is a two part optimization problem. The first part of the problem is to find a transmission switching solution and the second part is to find the worst-case cost or worst-case realization of demand associated with the switching solution obtained in the previous stage. Robust optimization is seen as being more conservative than stochastic optimization since it minimizes the worst-case approach. While this is often seen as a drawback of robust optimization, this is exactly the motivation: to create a robust, reliable corrective switching methodology.

$$\min_{x \in \mathcal{X}} \quad \left(c^T x + \max_{d \in \mathcal{D}} b^T y(d) \right) \tag{6.8}$$

$$\text{s.t.} \quad Fx \leq f \tag{6.9}$$

$$Hy(d) \leq h, \tag{6.10}$$

$$Ax + By(d) \leq g, \tag{6.11}$$

$$Ey(d) = d, \tag{6.12}$$

$$x \in \{0, 1\} \tag{6.13}$$

When the system demand uncertainty is zero, the TC model presented in (6.2)-(6.7) is the same as the model given in (6.8)-(6.13). In (6.12), the term $y(d)$ is used to emphasize the dependency of continuous variable y on the demand uncertainty, d. The second part of the robust formulation is further divided into two parts and results into a three-stage optimization problem as shown in (6.14). The objective of a three stage robust problem is to find a feasible topology under the worst-case demand. The first stage will determine the

topology or switching action, whereas stages two and three will determine the feasibility of the switching action for the entire uncertainty set.

$$\min_{x \in \mathcal{X}} \quad \left(c^T x + \max_{d \in \mathcal{D}} \quad \min_{y \in \Omega(x,d)} b^T y \right) \tag{6.14}$$

$$\text{s.t. } Fx \leq f,\ x \in \{0,1\} \tag{6.15}$$

The set $\Omega(x,d)$ is a set of feasible solutions for a fixed topology and demand d, which is represented by $\Omega(x,d) = \{y : Hy \leq h,\ Ax + By \leq g,\ Ey = d\}$. In (6.14), the $\max_{d \in \mathcal{D}} \min_{y \in \Omega(x,d)} b^T y$ part of the problem determines the worst-case cost or demand associated with the switching solution (determined in the first stage) and can be combined together into one problem by taking the dual of $\min_{y \in \Omega(x,d)} b^T y$. The resultant problem is shown in (6.16)-(6.18).

$$\max_{d,\varphi,\lambda,\eta} \quad \lambda^T (Ax - g) - \varphi^T h + \eta^T d \tag{6.16}$$

$$\text{s.t.} \quad -\lambda^T B - \varphi^T H + \eta^T E = b^T, \tag{6.17}$$

$$d \in \mathcal{D},\ \lambda \geq 0, \varphi \geq 0, \eta\ free \tag{6.18}$$

$\varphi,\ \lambda$ and η are dual variables of constraints (6.4), (6.5), and (6.6) respectively. In (6.16), the term $\eta^T d$ is nonlinear. In [70], an outer approximation technique is used to solve this bilinear problem. In [70], the bilinear term, $\eta^T d$, is linearized using a first order Taylor series approximation as shown in (6.19), where $L(d,\eta)$ is a linearized approximation that is linearized across d_j and η_j. Furthermore, the resultant LP problem is solved by employing an iterative process between the outer approximation and the rest of the evaluation problem. The benefit of this method is that it is simple and the resultant optimization problem is a simplified LP. However, this method does not guarantee global optimality; therefore, the solution obtained from this outer approximation method only guarantees local optimality.

Furthermore, this approach assumes that the problem is feasible, the corrective TC problem is a feasibility problem and, thus, it requires a global solution. Therefore, the outer approximation technique is not suitable for the robust corrective switching problem. Hence, in this chapter, instead of using an outer approximation method, the bilinear term is defined by describing the extreme point of the uncertainty set.

$$L(d,\eta) = \eta_j^T d_j + (\eta - \eta_j)^T d_j + (d - d_j)^T \eta_j \tag{6.19}$$

Since the DCOPF problem is a convex problem, the new subproblem formulation presented by (6.16)-(6.18) can be reformulated into a MIP problem. By classifying all extreme points of the polyhedron representing the uncertainty set, we can guarantee a robust solution due to the convexity of the DCOPF problem, i.e., we can guarantee that all interior points are feasible if the robust solution is feasible for all extreme points of the polyhedron. This reformulation allows us to solve the nonlinear problem (6.16)-(6.18) by mixed integer programming while still being able to guarantee a global optimal solution. This reformulation procedure is also used in [71]. The MIP reformulation for the polyhedron representing the demand uncertainty is shown by (6.43)-(6.46).

The master problem is a MIP problem and represented by (6.20)-(6.21) and the subproblem is represented by (6.16)-(6.18).

$$\min_{x \in \mathcal{X}} \quad c^T x \tag{6.20}$$

$$\text{s.t.} \quad Fx \leq f, \; x \in \{0,1\} \tag{6.21}$$

The robust corrective switching formulation used in this chapter is presented in (6.23)-(6.35), with an objective presented by (6.22). The formulation includes generator limit constraints (6.23)-(6.24), generator contingency ramp up and ramp down constraints (6.25)-(6.26), line limit constraints (6.27)-(6.28), transmission switching constraints (6.29)-(6.30),

the node balance constraint (6.31), and demand uncertainty (6.32)-(6.33). The maximum number of line switchings per solution are limited by parameter M in (6.34). In this research, only one corrective line switching solution is considered to be implemented in the post-contingency state.

$$\min_{Z_K \in \mathcal{X}} \left(0 \; + \; \max_{d \in \mathcal{D}} \; \min_{P_g, P_k, \theta_n \in \Omega(Z_k, d)} 0 \right) \tag{6.22}$$

$$\text{s.t.} - P_g \geq -P_g^{max} u_g, \; \forall g \tag{6.23}$$

$$P_g \geq P_g^{min} u_g, \; \forall g \tag{6.24}$$

$$- P_g \geq (-R_g^{+c} - P_g^{uc}), \; \forall g \tag{6.25}$$

$$P_g \geq (-R_g^{-c} + P_g^{uc}), \; \forall g \tag{6.26}$$

$$- P_k \geq -P_k^{max} Z_k N1_k, \; \forall k \tag{6.27}$$

$$P_k \geq -P_k^{max} Z_k N1_k, \; \forall k \tag{6.28}$$

$$P_k - B_k(\theta_n - \theta_m) + (1 - Z_k N1_k) M_k \geq 0, \; \forall k \tag{6.29}$$

$$P_k - B_k(\theta_n - \theta_m) - (1 - Z_k N1_k) M_k \leq 0, \; \forall k \tag{6.30}$$

$$\sum_{\delta(n)^+} P_k - \sum_{\delta(n)^-} P_k + \sum_{\forall g(n)} P_g = d_n, \forall n \tag{6.31}$$

$$d_n \leq d_n^{fix} D_n^+, \; \forall n \tag{6.32}$$

$$d_n \geq d_n^{fix} D_n^-, \; \forall n \tag{6.33}$$

$$\sum_{\forall k} (1 - Z_k) \leq M \tag{6.34}$$

$$Z_k \in \{0, 1\}, \; P_g, \; P_k, \; \theta_n \;\; free \tag{6.35}$$

The complete robust corrective switching problem is split into two parts: a master problem, and a subproblem. The master problem is $\min_{Z_K \in \mathcal{X}} 0$ with constraints represented by (6.34)-(6.35), which determine the topology. The subproblem is a two part optimization problem, which determines the worst-case demand for a particular topology. The first part

of the subproblem is represented by an objective $\max_{d \in \mathcal{D}}$ with constraints (6.32)-(6.33), which determines the worst-case system demand within the uncertainty set. The second part of the subproblem is represented by the objective $\min_{P_g, P_k, \theta_n \in \Omega(Z_k, d)} 0$ with constraints (6.23)-(6.31). This second part of the subproblem is a DCOPF formulation that evaluates the feasibility of the system demand, which is selected in the first part of the subproblem.

The objective of the third stage's dual is given in (6.36), where $\alpha_g^+, \alpha_g^-, \Omega_g^+, \Omega_g^-, F_k^+, F_k^-, S_k^+, S_k^-, L_n$ are dual variables associated with constraints (6.23)-(6.31) respectively. When the second stage and the third stage of the subproblem are combined together, the term $d_n L_n$ in (6.36) makes the objective nonlinear. The nonlinearity of the dual objective is removed by restructuring the nonlinear problem into a MIP problem. The resultant subproblem is given in (6.37)-(6.46), where the dual formulation of the third stage subproblem is combined with the demand uncertainty.

$$\begin{aligned} \max \; & -\sum_{\forall g} P_g^{max} u_g \alpha_g^+ + \sum_{\forall g} P_g^{min} u_g \alpha_g^- \\ & + \sum_{\forall g} (-R_g^{+c} - P_g^{uc}) \Omega_g^+ + \sum_{\forall g} (-R_g^{-c} + P_g^{uc}) \Omega_g^- \\ & - \sum_{\forall k} P_k^{max} Z_k N1_k (F_k^+ + F_k^-) + \sum_{\forall n} d_n L_n \\ & - \sum_{\forall k} (1 - Z_k N1_k) M_k (S_k^+ + S_k^-) \end{aligned} \tag{6.36}$$

A big-M formulation is used to represent the extreme points of the polyhedron representing the uncertainty set. The drawback of such an approach is that it causes a poor relaxation. To overcome this problem, CPLEX's indicator constraint modeling approach is used to model (6.43)-(6.47).

$$\max \; -\sum_{\forall g} P_g^{max} u_g \alpha_g^+ + \sum_{\forall g} P_g^{min} u_g \alpha_g^- \tag{6.37}$$
$$+\sum_{\forall g}(-R_g^{+c} - P_g^{uc})\Omega_g^+ + \sum_{\forall g}(-R_g^{-c} + P_g^{uc})\Omega_g^-$$
$$-\sum_{\forall k} P_k^{max} Z_k N1_k (F_k^+ + F_k^-) + \sum_{\forall n} \eta_n$$
$$-\sum_{\forall k}(1 - Z_k N1_k) M_k (S_k^+ + S_k^-)$$

$$\text{s.t.} \; -\alpha_g^+ + \alpha_g^- - \Omega_g^+ + \Omega_g^- + L_n = 0, \; \forall g \tag{6.38}$$

$$-F_k^+ + F_k^- + S_k^+ - S_k^- + L_n - L_m = 0, \; \forall k \tag{6.39}$$

$$-\sum_{\delta(n)^+} B_k S_k^+ + \sum_{\delta(n)^-} B_k S_k^+ + \sum_{\delta(n)^+} B_k S_k^- - \sum_{\delta(n)^-} B_k S_k^- = 0, \; \forall n \tag{6.40}$$

$$\alpha_g^+, \alpha_g^-, \Omega_g^+, \Omega_g^- \geq 0, \; \forall g \tag{6.41}$$

$$F_k^+, F_k^-, S_k^+, S_k^- \geq 0, \; \forall k \tag{6.42}$$

$$\eta_n - L_n d_n^{fix} D_n^+ + (1 - D_n) M_n \geq 0, \; \forall n \tag{6.43}$$

$$\eta_n - L_n d_n^{fix} D_n^+ - (1 - D_n) M_n \leq 0, \; \forall n \tag{6.44}$$

$$\eta_n - L_n d_n^{fix} D_n^- + D_n M_n \geq 0, \; \forall n \tag{6.45}$$

$$\eta_n - L_n d_n^{fix} D_n^- - D_n M_n \leq 0, \; \forall n \tag{6.46}$$

$$D_n \in \{0, 1\} \tag{6.47}$$

6.6 Solution Method for Robust Corrective Topology Control

The robust TC problem is a three-stage problem with a master problem and two subproblems. However, it is reformulated into a two-stage problem with a master problem and a subproblem. The solution method proposed in this research is an iterative process between the master problem and the subproblem. The master problem is a MIP, which determines the system topology. The subproblem is a nonlinear problem, which is converted

into a MIP and it searches for the worst-case demand for the particular topology. For the proposed solution method, it is assumed that the unit commitment problem is solved prior to solving the robust corrective switching problem.

6.6.1 Initialization

The unit commitment problem is first solved with the fixed, initial topology. The solution of this unit commitment problem, the unit commitment status, the generators' scheduled dispatch, and the acquired reserves, are fed into the robust TC framework. The first step of solution method is to solve the dual problem given by (6.48), where $\overline{Z}_k$ represents the initial topology. The model presented in (6.48) is the dual of the DCOPF problem. The dual variables of constraints (6.38)-(6.40) are P_g, P_k, θ_n respectively. If the problem is infeasible, then the proposed unit commitment solution is not N-1 reliable and a cut must be added to the master problem in the form of (6.50). The proposed approach will then search for a robust corrective switching action that enables the solution to be N-1 compliant, if such a solution exists.

$$\begin{aligned}
\max \; & -\sum_{\forall g} P_g^{max} u_g \alpha_g^+ + \sum_{\forall g} P_g^{min} u_g \alpha_g^- \\
& + \sum_{\forall g} (-R_g^{+c} - P_g^{uc}) \Omega_g^+ + \sum_{\forall g} (-R_g^{-c} + P_g^{uc}) \Omega_g^- \\
& - \sum_{\forall k} P_k^{max} \overline{Z}_k N1_k (F_k^+ + F_k^-) + \sum_{\forall n} d_n L_n \\
& - \sum_{\forall k} (1 - \overline{Z}_k N1_k) M_k (S_k^+ + S_k^-) \\
\text{s.t. } & (6.38) - (6.42)
\end{aligned} \tag{6.48}$$

6.6.2 Master Problem: Topology Selection

The master problem is a MIP problem and its objective is to determine the system topology. The master problem contains a topology selection formulation and combinatorial cuts. The master problem is represented by (6.49)-(6.52). For iteration $j \geq 1$,

$$\min \ 0 \tag{6.49}$$

$$\text{s.t. } 1 \leq \sum_{\overline{Z}_{k,l}=0} Z_k + \sum_{\overline{Z}_{k,l}=1} (1 - Z_k), \ \forall l \leq j \tag{6.50}$$

$$\sum_{\forall k} (1 - Z_k) \leq M \tag{6.51}$$

$$Z_k \in \{0, 1\} \tag{6.52}$$

At each iteration, the master problem finds a feasible solution and then passes Z_k to the subproblem as an input parameter. The solution Z_k will be evaluated for the worst-case scenario in the subproblem. If the master problem is infeasible, this states that all of the possible topologies are infeasible and there is no feasible switching action for the defined uncertainty set, as shown in stage 1 of Fig 6.5.

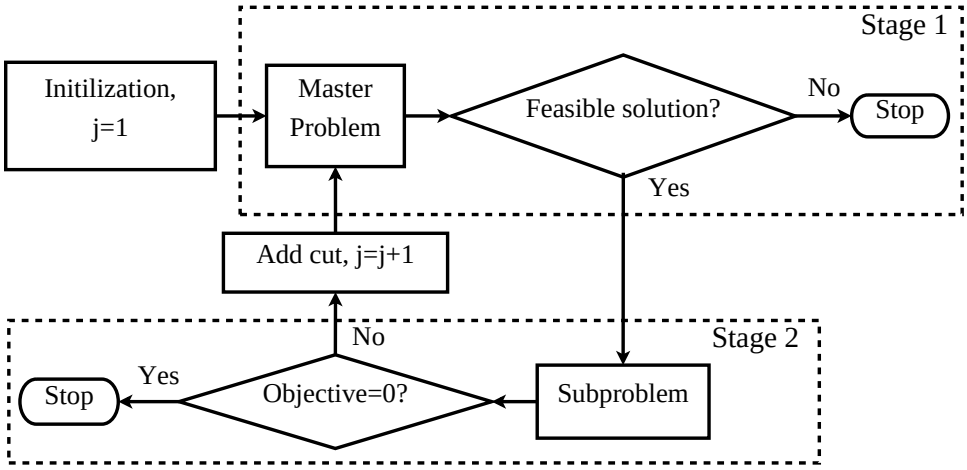

Figure 6.5: Flowchart for Robust Corrective Topology Control.

6.6.3 Subproblem: Worst-case Evaluation

The objective of the subproblem is to determine the worst-case demand associated with the topology (determined in the master problem). The subproblem is a MIP and presented in (6.37)-(6.47). If the subproblem is feasible and the objective is equal to zero, then it proves that, for a given topology, there is no system demand within the uncertainty set that will produce an infeasible OPF solution. In other words, the corresponding topology is feasible for the entire uncertainty set; hence, a robust solution is obtained. On the other hand, if the subproblem's objective is non-zero, then the corresponding topology is infeasible for a particular demand within the uncertainty set. Hence, that topology is discarded and a feasibility and/or combinatorial cut is applied to the master problem in form of (6.50). Equation (6.50) is known as a combinatorial cut, which prevents the master problem from choosing any prior binary Z_k solution that is known to be infeasible. The master problem is solved again and the process continues till the robust solution is found or all possible topologies are confirmed to be infeasible. The solution method for the robust TC problem is summarized in Fig. 6.5.

6.7 Numerical Results: Demand Uncertainty

The computational study for robust corrective switching is performed on the IEEE 118-bus test case. The test case consists of 54 generators, 118 buses, and 186 transmission lines. The IEEE 118-bus test case given in [87] does not have generator information. Therefore, generator information from the Reliability Test System-1996 [87] is used. The fuel costs given in [23] are used to calculate generator operating costs. The basic unit commitment model presented in [14] is adopted. A 24-hour unit commitment problem is solved. The reserve requirement for the unit commitment problem is the sum of 5% of demand supplied by hydro generators and 7% of demand supplied by non-hydro units or the single largest

contingency, whichever is greater. It is assumed that at least 50% of total required reserves will be supplied by spinning reserves and the rest will be supplied by non-spinning reserves. This assumption is in line with CAISO's guidelines for spinning reserve and non-spinning reserve [59]. The hour 16 solution of the unit commitment problem is used for deterministic as well as robust corrective switching analysis. The IEEE 118-bus test case in [87] does not have emergency transmission rating. Therefore, it is assumed that the emergency thermal rating for the transmission elements is 125% of the steady state operating limits.

6.7.1 Deterministic Corrective Switching

In the deterministic corrective switching analysis, the demand uncertainty is assumed to be zero. The switching action is determined with the static demand levels used in the unit commitment problem. It is observed that 10 transmission contingencies (out of 186) can only be alleviated if transmission switching is combined with generation re-dispatch, i.e., generation re-dispatch on its own cannot satisfy these 10 transmission contingencies. The generation re-dispatch allows each unit to change within 10 minutes of its ramping capability. This result is important because, traditionally, such contingencies are mitigated by expensive generation re-dispatch. Moreover, these 10 transmission contingencies have multiple corrective switching actions. The ability of the corrective switching algorithm to generate multiple solutions for a single contingency is critical from a system operations point of view. The corrective switching formulation is based on a DC framework. Therefore, the solution needs to be tested for AC feasibility and system stability requirements. Hence, the probability of having at least one AC feasible and stable corrective switching solution is higher if the corrective switching algorithm generates multiple corrective solutions.

It is also observed that the solution for corrective transmission switching will not always be 'to open the congested line', but frequently it will be 'to open a lightly loaded line'. This

demonstrates that the commonly held assumption that congested lines are the top candidate lines for switching is not always correct. Furthermore, such examples demonstrate the need for systematic tools for TC.

6.7.2 Robust Corrective Switching Analysis

For robust corrective switching analysis, $\pm 14.3\%$, i.e., $\pm 324.5MW$, demand uncertainty is assumed. For computational simplicity, the demand uncertainty is assumed only on 50% of the system MW demand involving roughly half of the load buses. It is also assumed that all of the system reserves are available within 10 minutes and the generators are allowed to change their outputs within each generators' 10 minutes ramp rate. Of the 186 transmission contingencies, 159 can be alleviated by dispatching reserves alone. While corrective switching is not required for these 159 contingencies, TC can still be useful in response to these contingencies because it can reduce the need for a costly system re-dispatch; furthermore, the TC algorithm provides multiple feasible switching solutions for these 159 transmission contingencies. The 7 transmission contingencies listed in Table 6.1 require corrective transmission switching actions in order to avoid load shedding, i.e., generation re-dispatch alone was not sufficient to respond to the contingencies. Note that these robust corrective switching solutions involve both corrective switching and generation re-dispatch.

The first column of Table 6.1 represents the transmission contingency and the second column represents the corresponding corrective switching actions. All 7 of these transmission switching contingencies can only be alleviated if corrective transmission switching is employed. For instance, a contingency on line 111 can only be mitigated by switching line 108 or 109 combined with generation re-dispatch. No feasible solution is available with generation re-dispatch alone due to network congestion. The switching solutions for the other 6 transmission contingencies are documented in Table 6.1.

Table 6.1: Robust Corrective Switching Solution with Demand Uncertainty.

Line Contingency	**Switching Solution(s)**	**Number of Deterministic Solutions**
63	64	3
111	108, 109	163
115	33, 34, 35, 38, 51, 78, 86, 112, 121, 132, 141	165
116	141	151
120	132	162
148	137, 138, 139, 140, 141, 143, 153, 157, 158, 159, 160, 161, 162, 163, 165, 166, 167, 168, 169, 173	163
154	139, 140, 153, 155, 157, 158, 159, 160, 161, 163,165, 167, 169, 173	166

The contingencies of line $111,\ 115,\ 148,$ and 154 have multiple robust corrective switching actions. Table 6.1 shows that there can be multiple switching solutions for a single contingency. Similarly, one switching action may alleviate multiple contingencies. For instance, the robust switching solution to open line 141 mitigated 3 transmission contingencies. This result shows the potential of robust corrective switching to generate multiple candidate switching solutions for a real-time dynamic security assessment tool to evaluate switching actions for real-time operations.

In the last column of Table 6.1, the number of deterministic corrective switching solutions, for a particular contingency, is presented. It shows that the number of possible deterministic corrective switching solutions is much more as compared to the number of robust solutions. However, the robust solutions guarantee solution feasibility over a wide range of operating states whereas the deterministic solutions do not guarantee solution fea-

sibility if there is any change in the operating state. Therefore, the possibility of having a successful corrective action with the deterministic corrective switching solutions is far less than the potential success rates for the robust corrective switching solutions.

For a contingency on line 63, with the initial topology no feasible solution is obtained with a fixed demand. Hence, the unit commitment solution is not N-1 compliant. However, with the robust corrective switching framework, an N-1 feasible solution exists; furthermore, the robust corrective switching framework is able to produce an N-1 feasible solution that is robust against the demand uncertainty. This result is extremely important and powerful as we have proven that TC can take a solution that is N-1 infeasible for a deterministic fixed demand and make it N-1 feasible even with a high level of demand uncertainty. Indeed, the assumption that transmission switching must degrade system reliability is false. Furthermore, in prior research, TC has shown considerable operational benefits and cost savings [14]. The detail analysis for cost savings, obtained from robust corrective TC methodology, is presented in Chapter 7.

The computational time for $\pm 14.3\%$ uncertainty set is about 10 minutes per contingency with a 2.93 GHz, Intel i-7 processor with 8 GB RAM. It is also observed that the computational time increases with small increases in the uncertainty set. For instance, a 1% decrease in uncertainty causes a 13% drop in computational time.

6.8 Numerical Results: Wind Uncertainty

In this section, robust N-1 system reliability studies with wind uncertainty are presented. For these studies the robust corrective topology control methodology, presented in Section 6.6, are modified to account for the wind uncertainty. In this section, the wind uncertainty is modeled as shown in (6.53). Polyhedral uncertainty sets are used to capture the intermittency of renewable resources, as shown in (6.53); the renewable resources (in this case, wind generation) are assumed to vary within these pre-determined lower and upper

limits and the size of uncertainty set depends on the parameters D_w^- and D_w^+. Furthermore, $D_w^- \leq 1$ and $D_w^+ \geq 1$. In this analysis, the wind uncertainty is assumed to be $\pm 20\%$; therefore D_w^-=0.8 and D_w^+=1.2.

$$W = \{P \in \mathbb{R}^w : P_w^{fix} D_w^- \leq P_w \leq P_w^{fix} D_w^+, \ \forall w\} \tag{6.53}$$

In order to address the wind uncertainty, the robust corrective topology control formulation is updated; the master problem is same as shown in (6.49)-(6.52) and the subproblem is as shown in (6.54)-(6.59). In the subproblem, the wind generation is modeled as a negative load, which is a standard practice in industry to model renewable generation. The solution method to solve the robust corrective topology control problem, presented in Section 6.6, is used to solve this problem.

$$\max \; -\sum_{\forall g} P_g^{max} u_g \alpha_g^+ + \sum_{\forall g} P_g^{min} u_g \alpha_g^- \tag{6.54}$$
$$+ \sum_{\forall g} (-R_g^{+c} - P_g^{uc}) \Omega_g^+ + \sum_{\forall g} (-R_g^{-c} + P_g^{uc}) \Omega_g^-$$
$$- \sum_{\forall k} P_k^{max} Z_k N1_k (F_k^+ + F_k^-) + \sum_{\forall n} \eta_n$$
$$- \sum_{\forall k} (1 - Z_k N1_k) M_k (S_k^+ + S_k^-)$$

$$\text{s.t. } \eta_n - L_n (d_n - \sum_{\forall w(n)} P_w^{fix} D_w^+) + (1 - D_n) M_n \geq 0, \; \forall n \tag{6.55}$$

$$\eta_n - L_n (d_n - \sum_{\forall w(n)} P_w^{fix} D_w^+) - (1 - D_n) M_n \leq 0, \; \forall n \tag{6.56}$$

$$\eta_n - L_n (d_n - \sum_{\forall w(n)} P_w^{fix} D_w^-) + D_n M_n \geq 0, \; \forall n \tag{6.57}$$

$$\eta_n - L_n (d_n - \sum_{\forall w(n)} P_w^{fix} D_w^-) - D_n M_n \leq 0, \; \forall n \tag{6.58}$$

$$D_n \in \{0, 1\} \tag{6.59}$$

$$(6.38) - (6.42)$$

In general, TC algorithms are either based on the ACOPF or the DCOPF [97, 11, 91, 98]. However, in an optimization framework, there is no systematic and highly accurate method to insure system stability with TC. In prior literature, TC actions combined with stability constraints are proposed [83, 84]. Furthermore, in a robust corrective TC problem, as shown in [97], there is no simple method to insure AC feasibility of TC actions. The robust corrective TC methodology, which is used in this chapter, is based on the DCOPF. Therefore, the TC solution obtained from the robust corrective TC algorithm is tested for the AC feasibility and the system stability, to ensure that the TC action will provide AC feasible and stable operating point. Therefore, in this Section TC solutions, obtained from the robust corrective TC algorithm, are tested for AC feasibility. In Section 6.9, TC solutions,

obtained from the robust corrective TC algorithm, are considered for stability studies.

The robust corrective TC methodology for system reliability is presented in [97]. The security constraint unit commitment solution is used as an initial operating condition for all the studies presented in this chapter. The branch data for the IEEE-118 bus test case is given [87]; however, the generation information for this test system is not available. Therefore, the generator mix of reliability test system 1996 is used to create generator information for the IEEE-118 bus test case [87]. There are total 71 conventional generators and 9 wind injection locations, with peak demand of 4004 MW. The load profile and wind forecast is obtained from the California Independent System Operator (CAISO) duck chart [99].

A 24 hour security constrained unit commitment (SCUC) is solved and the SCUC solution is used as a starting point for all the simulations presented in this chapter. The basic SCUC model and the fuel costs, given in [14], are used to calculate generator operating costs. The reserve requirements for the SCUC are modeled as sum of 5% of demand supplied by conventional generators and 10% of demand supplied by wind units or the single largest contingency, whichever is greater. On top of that, at least 50% of total required reserves will be supplied by spinning reserves and the rest will be supplied by non-spinning reserves. A similar assumption is cited in CAISO's guidelines for spinning reserve and non-spinning reserve [59]. Note that the corrective TC actions may or may not be combined with generator re-dispatch. However, for the robust corrective TC procedure generator re-dispatch is taken into consideration. Furthermore, in this N-1 analysis, only one simultaneous TC actions considered.

6.8.1 Robust N-1 Analysis

To see the effect of higher penetration of renewable resources on the system reliability, the N-1 contingency analysis with the robust corrective TC is presented in this chapter. The basic model and solution method is the same as [97]. For analysis purposes, the wind

uncertainty is assumed to be 20%.

The comprehensive N-1 reliability study with the robust corrective TC for the IEEE-118 bus test system is presented in Fig. 6.6. In this analysis 5492 contingencies (generator and transmission combined) over 24 hours are considered. From this analysis, it is observed that $\sim 72.7\%$ contingencies does not requires TC to mitigate contingencies with a base case wind forecast and with a wind uncertainty. Initial topology along with generation re-dispatch is sufficient to mitigate these contingencies. With a base case wind forecast, $\sim 25\%$ contingencies can be mitigated with initial topology and generation re-dispatch; however, with a wind uncertainty, initial topology and generation re-dispatch alone is insufficient to mitigate these contingencies. To mitigate these $\sim 25\%$ contingencies, TC along with generation re-dispatch is required. Furthermore, for $\sim 1.5\%$ contingencies, with a base case wind forecast, initial topology and generation re-dispatch is sufficient to mitigate contingencies. However, in presence of wind uncertainty, these $\sim 1.5\%$ contingencies cannot be mitigated with a single TC action along with generation re-dispatch. In this case, a single TC action has shown no benefit for contingency mitigation. For $\sim 0.8\%$ contingencies, with the initial topology no feasible solution is obtained with a base case wind forecast. Hence, the unit commitment solution is not N-1 compliant. However, with a corrective TC action along with generation re-dispatch, an N-1 feasible solution exists; furthermore, the robust corrective TC is able to produce an N-1 feasible solution that is robust against the wind uncertainty. This result is extremely important and powerful as we have proven that TC can take a solution that is N-1 infeasible for a deterministic fixed wind forecast and make it N-1 feasible even with a high level of wind uncertainty. Indeed, the assumption that TC must degrade system reliability is false.

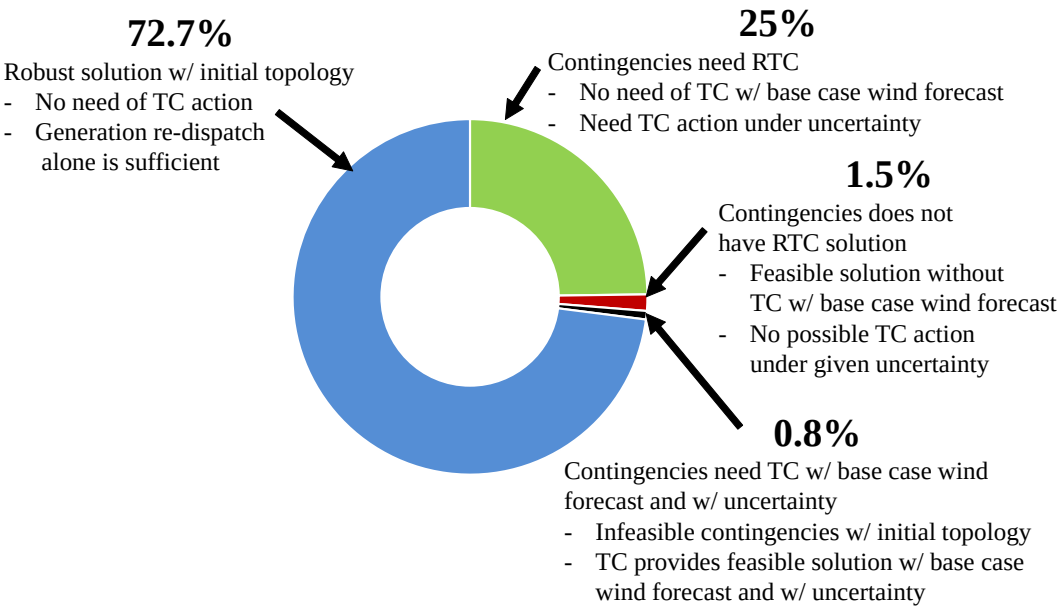

Figure 6.6: Comprehensive N-1 Analysis with Robust Corrective Topology Control on the IEEE-118 Bus Test Case.

The N-1 analysis of the IEEE-118 bus test system with CAISO's duck chart demand and wind forecast is presented in Fig. 6.7. In this analysis, contingencies, which can be mitigated by 10 minute generator re-dispatch alone, are not considered and are considered as trivial cases; these are cases that do not require corrective TC actions. Contingencies that require a corrective TC action, along with 10 minute generator re-dispatch, are considered nontrivial cases and are presented in Fig. 6.7; the bar chart in Fig. 6.7 shows the number of nontrivial contingencies for a 24 hours period. During high wind generation and low demand periods, such as hours 1-2, 13-15, and 23-24, the numbers of contingencies requiring corrective TC for N-1 reliability are much higher. In these hours, the system cannot avoid load shedding for most of the N-1 contingencies with generator re-dispatch alone, if the forecasted renewable output deviates by 20% from its base value. Furthermore, during these hours of operations, the system has sufficient amount of reserves to overcome

the single largest contingency; however, due to network congestion, these reserves cannot be delivered with the initial topology. The corrective TC actions essentially redirects the power flow within the network so that the system reserves can be delivered to mitigate contingencies. In this analysis, only one corrective TC action per contingency is considered. Similar conclusions are drawn with the IEEE-118 bus test system with a traditional demand/wind profile.

The computational time for these simulations on a 2.93 GHz, Intel i-7 processor with 8 GB RAM computer is about 5 seconds per iteration.

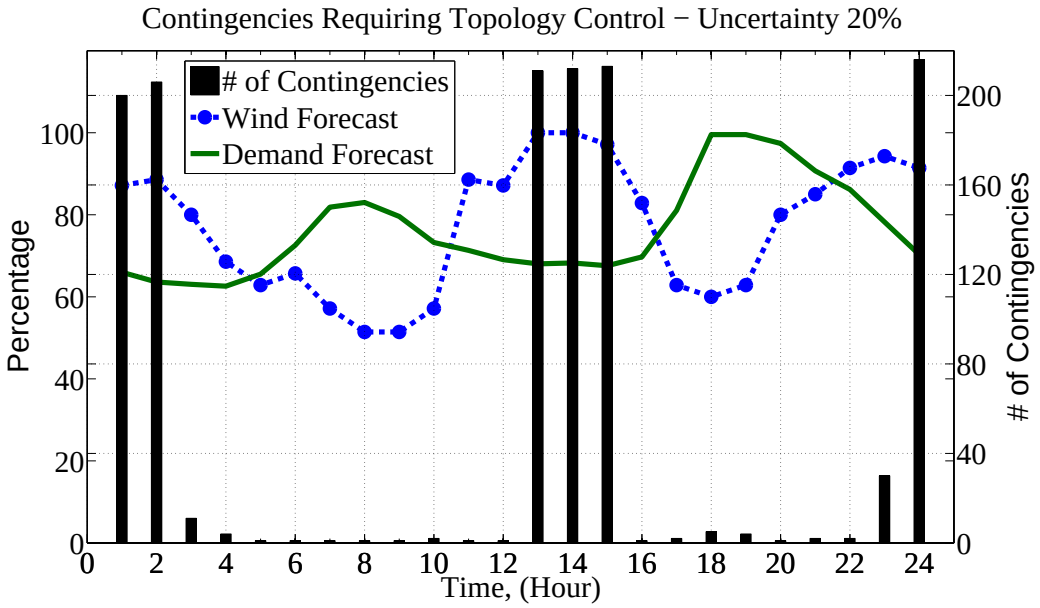

Figure 6.7: N-1 Analysis with Robust Corrective Topology Control on the IEEE-118 Bus Test Case.

6.8.2 AC Feasibility of Topology Control Solution

The robust corrective TC formulation used in [97] is based on a DC approximation. Therefore, a corrective TC solution obtained from this algorithm must be tested for AC feasibility. The basic AC optimal power flow (ACOPF) formulation presented in [13] is used to check AC feasibility of the TC solutions obtained from the robust TC algorithm.

The commercially available nonlinear solver KNITRO [100] is used to solve the AC feasibility problem. The DC solution obtained from a TC algorithm, such as a generator's real power output, line flows, etc., are used as a starting point for the AC feasibility test. Fig. 6.8 shows the base case bus voltages and the bus voltages with TC action for an hour of peak demand (i.e., hour 18) with contingency of "loss of line $\#119$". Fig. 6.8 shows that bus voltages do not change much with the corrective TC action; in fact, with TC, bus voltages are closer to unity (the ideal voltage scenario) compared with its pre-contingency state. The bus angle differences for the same base case condition and post-contingency simulation are presented in Fig. 6.9, which shows that bus angle differences do not change much with the proposed corrective TC action. The maximum bus angle difference for this test case is about ± 15 degrees, which is less than its approximate stability limit of ± 30 degrees.

To check for the overall AC feasibility of the corrective TC solutions, for the IEEE-118 bus test case with the CAISO duck chart, more than 3000 TC solutions are tested. Out of those 3000 DC robust solutions, $\sim 90\%$ of the TC solutions, obtained from a robust corrective switching algorithm, produce AC feasible solutions. This result is very critical from system operations point of view, as this result fills the gap between the disconnected DC formulation and an AC operation. Similarly, with the IEEE-118 bus test system using traditional demand/wind profile, $\sim 85\%$ of robust DC TC solutions provides an AC feasible corrective TC solution for the base case operating point. The computational time for an AC feasibility test on a 2.93 GHz, Intel i-7 processor with 8 GB RAM computer is about 4 seconds per contingency.

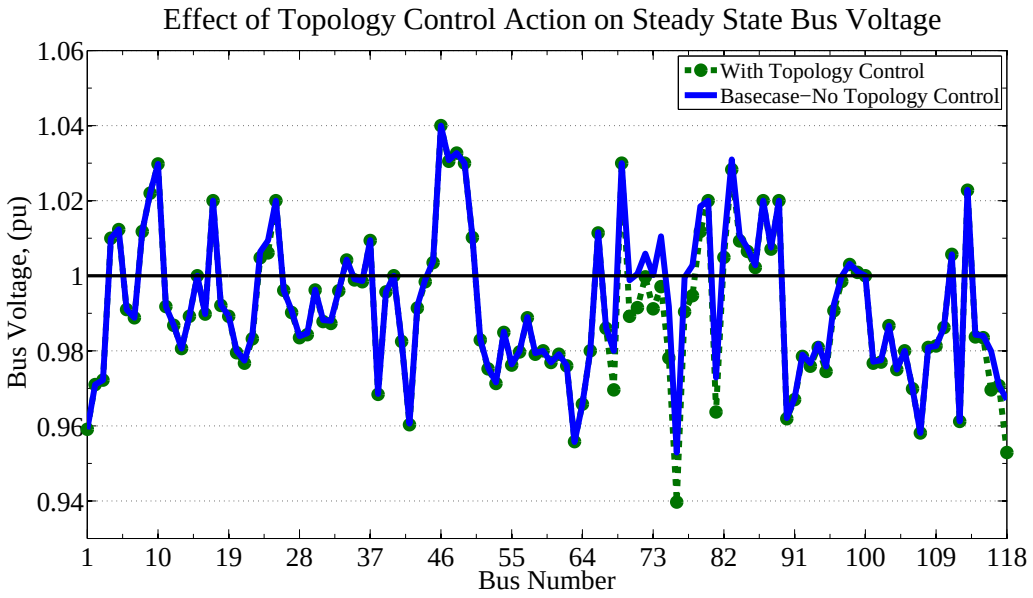

Figure 6.8: Bus Voltages (in pu) With and Without Topology Control Action.

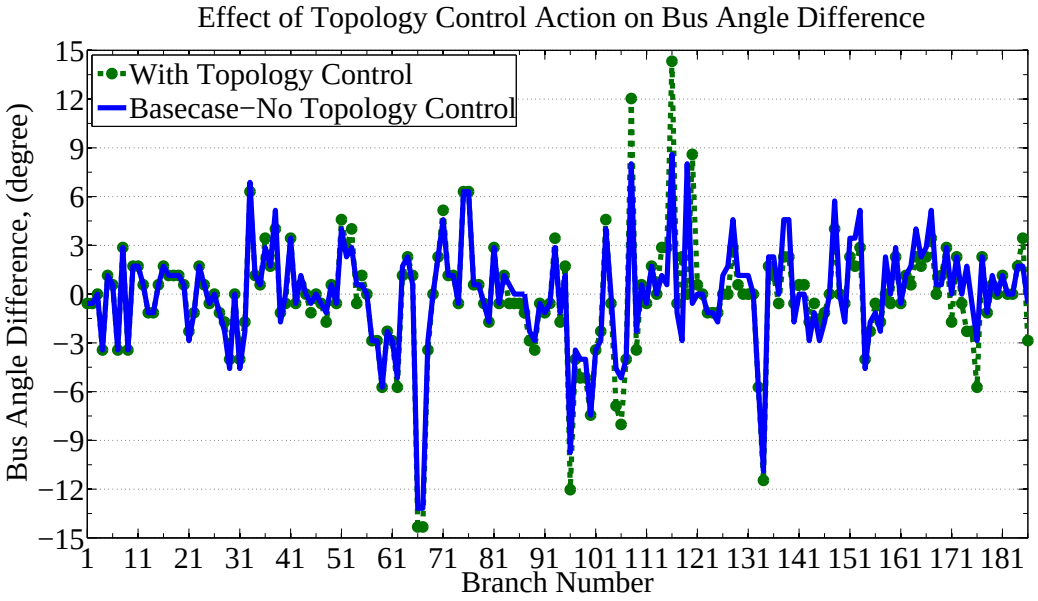

Figure 6.9: Bus Angle Difference (in Degree) for All the Transmission Elements With and Without Topology Control Action.

6.9 Stability Study with Robust Corrective Topology Control Actions

In this section, different stability studies are conducted to analyze the TC solutions for the IEEE-118 bus test system presented in Section 6.8. For discussion purposes, results associated with the peak load hour (hour 18) with base case wind forecast are presented in this chapter. The dynamic data for the IEEE-118 bus test case is not available; therefore, generator information from generators in the eastern interconnection of the United States are used to generate dynamic data. The dynamic data, for 1.5 MW individual wind generator, given in [90], are used to model wind injection in this analysis.

Small signal eigenvalue studies are carried out on this test case, with SCUC dispatch solution, for hour 18. The real part of the smallest eigenvalue obtained from this study is ~ -112 and the real part of largest eigenvalue is ~ -0.01. This study shows that all eigenvalues are negative and lie on the left hand side of the s-plane indicating that the given system is stable. This result shows that the given system is small signal stable and will remain stable for small perturbations in the operating state. This analysis is carried out using SSAT [101].

6.9.1 Generator Contingency

To demonstrate the effect of TC, on system reliability under loss of generation condition, the scenario described in Table 6.2 is simulated. The loss of wind represented by this scenario is equivalent to loss of $\sim 2\%$ of total generation. Note that, in the western interconnection, for many stability related studies, the worst-case scenario is the loss of two Palo Verde nuclear units [102], which is about 2% of total online generation.

The effect of TC action on system frequency is presented in Fig. 6.10. Due to the sudden drop of wind generation, the system frequency drops below 59.8 Hz and recovers to ~ 59.88 Hz using system inertia. After implementing the line switching action, the sys-

tem frequency improves and reaches to ~ 59.89 Hz. This small improvement in frequency happens because TC action decrease the losses in the system, which can be viewed as increased in generation. At t=160 sec., the generators are re-dispatched to overcome the loss of renewable generation. After generation re-dispatch, at last, the frequency improves and settle downs to ~ 59.97 Hz. In this analysis, 10 minutes ramping capability of generators are considered and it is assumed that after each 60 sec. the real power supplied by generators is available online. This additional generation is obtained from generators providing spinning reserves.

The effect of the TC on bus voltage stability is also studied. In the above scenario, the loss of wind on bus voltages are not significant; however, the TC alters the voltages on buses close to line switching action. The magnitude of change in voltage is highest on buses that are connected to the switched line.

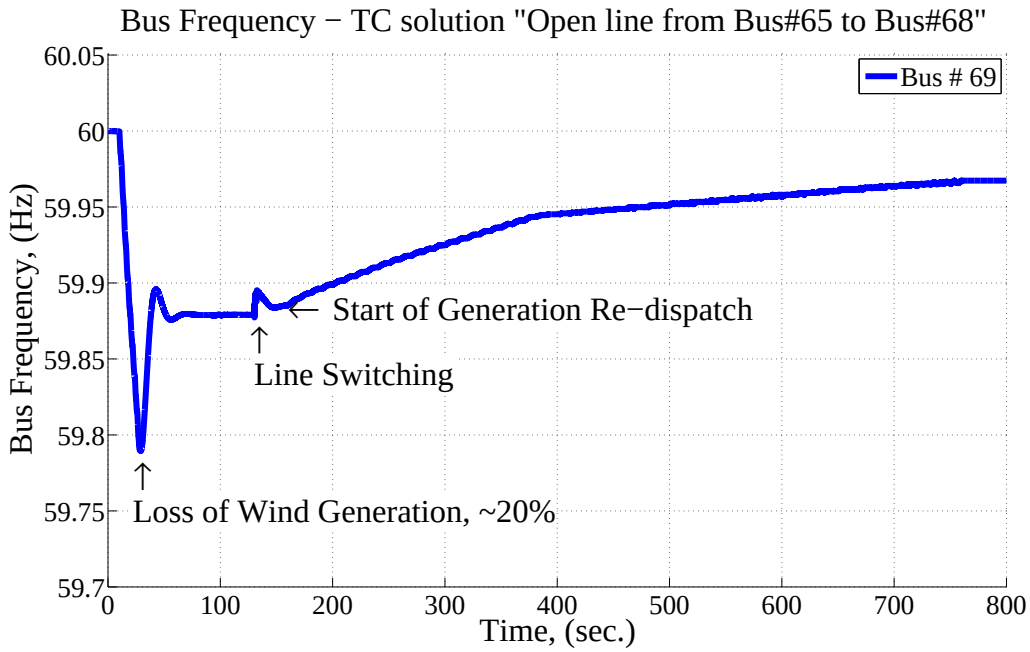

Figure 6.10: Effect of TC on System Frequency Under Generator Contingency.

Table 6.2: Scenario to Study the Effect of TC on System Reliability Under Generator Contingency

Time	Event
10-12 sec.	Loss of wind generation (20%)
130 sec.	Topology control solution implemented (open line between Bus$\#$65-Bus$\#$68)
160-760 sec.	Generators are dispatched based on ramping capability

Furthermore, the small signal analysis after TC and generation re-dispatch indicates that the change in dominant poles of the system are $<2\%$, as compared with the pre-contingency steady state condition. This study shows that a single TC action does not affect small signal stability of the system.

6.9.2 Transmission Contingency

In bulk power system, occurrence of transmission contingencies are relatively more than generator contingencies. In this chapter, the effects of TC under transmission contingencies are also studied. Furthermore, the robust corrective TC algorithm can produce multiple switching solutions for a single contingency [97]; at the same time, single TC action can mitigate multiple contingencies. To demonstrate this feature of corrective TC, in this chapter, the same TC action is used to mitigate generation as well as transmission contingencies. To demonstrate the effect of TC, on system reliability when there is a transmission contingency, the scenario described in Table 6.3 is simulated. Note that the generator dispatch is kept constant and not allowed to deviate from its desired dispatch point.

Table 6.3: Scenario to Study the Effect of TC on System Reliability Under Transmission Contingency

Time	Event
10 sec.	Transmission contingency (Loss of line between Bus#69-Bus#77)
70 sec.	Topology control solution implemented (open line between Bus#65-Bus#68)

The effect of transmission contingency and its associated corrective TC action on system frequency is shown in Fig. 6.11. Due to the transmission contingency, the system frequency deviates and settles down after a transient decay; the maximum deviation in the frequency due to the contingency is ~ 60.03 Hz. After implementation of TC action and the transients, the system frequency settles down to 60 Hz.

Fig. 6.12 shows the voltage contour plots for the pre-contingency, contingency, and post-contingency states for a subsection of the IEEE-118 bus test system. The pre-contingency state voltages, around the contingency affected area, are presented in Fig. 6.12-(a). In the pre-contingency state, all the voltages are within 0.95-1.05 pu and there is no congestion within the network around the contingency affected area. However, in the contingency state, as shown in Fig. 6.12-(b), the network flow change. This change in power flow results in congestion of network, which affects the deliverability of resources and causes under-voltage situation in some areas. In the post-contingency state, implementation of TC inherently removes the congestion and improves deliverability of resources in the affected area, as shown in Fig. 6.12-(c). Note that, in Fig. 6.12, for simplicity, only a subsection of the IEEE-118 bus test system is shown.

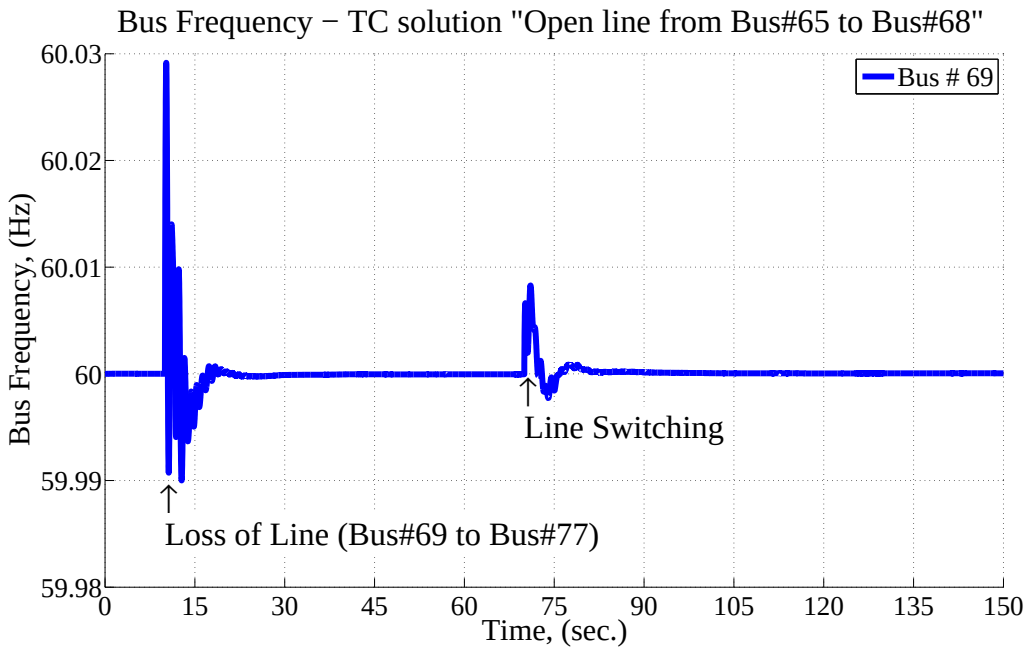

Figure 6.11: Effect of TC on System Frequency Under Transmission Contingency.

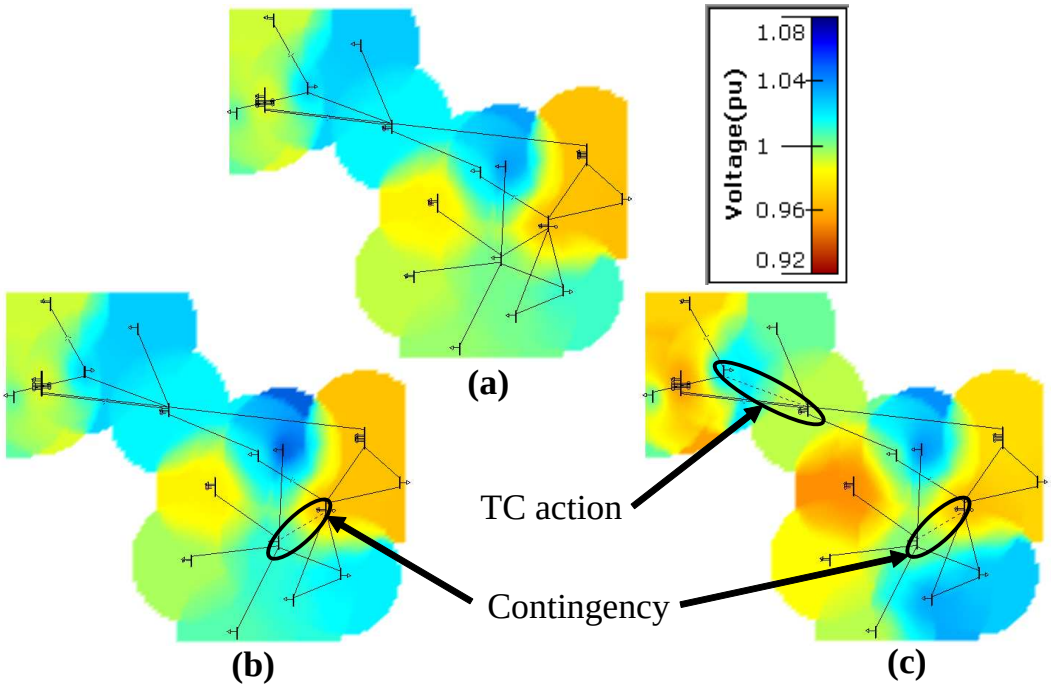

Figure 6.12: Voltage Contours Under Transmission Contingency.

The small signal analysis after TC indicates that the change in dominant poles of the system are $<1.5\%$, as compared with the pre-contingency steady state condition. This study shows that a single TC action does not affect small signal stability of the system.

Furthermore, for IEEE-118 bus test case, $\sim 65\%$ transmission and generation contingencies with corrective TC have passed stability check and produced stable operating point. In this analysis, ~ 200 transmission and generation contingencies are simulated.

6.10 Conclusion

In this chapter, three different corrective switching methodologies are presented: real-time, deterministic planning based, and robust corrective switching. Real-time corrective switching is very difficult to implement with existing technology due to a lack of computational power and the practical barriers of needing to ensure AC feasibility, voltage stability, and transient stability. Deterministic planning based corrective switching can be solved offline, but such an approach relies on predicting the operating state. Furthermore, the deterministic planning based methods cannot guarantee solution feasibility over a wide range of system states. The proposed method of robust corrective switching fills the technology gap between the real-time and the deterministic planning based corrective switching methodologies. The offline mechanism of robust corrective switching generates multiple solutions and can be implemented in real-time with the help of a real-time dynamic security assessment tool. As a result, the proposed robust corrective switching model provides a mathematical decision support tool that integrates TC into every day operations by being able to guarantee robust solutions.

While deterministic corrective switching frameworks may suggest many potential switching solutions, the empirical results presented in this research show that many of these solutions will be infeasible for minor changes in the operating state. In contrast, the robust corrective switching scheme presented in this chapter guarantees solution feasibility for a

wide range of system states, given a DCOPF formulation. In addition, the robust corrective switching formulation demonstrates the ability of generating multiple corrective switching actions for a particular contingency. Moreover, a single resulting corrective switching solution is capable of mitigating multiple contingencies.

Day-ahead unit commitment problems with proxy reserve requirements do not guarantee N-1 feasibility. Contingency analysis is used to determine whether there are contingencies that cannot be satisfied by the unit commitment solution. When this happens, unit commitment must be resolved or the operator will employ out-of-market corrections to obtain a feasible N-1 solution. The results have shown that robust corrective TC can be used to reduce the occurrence of contingencies that are not satisfied by the re-dispatch capabilities of the unit commitment solution alone. Furthermore, the numerical results prove that TC does not necessarily degrade system reliability; on the contrary, it can help the system to achieve N-1 feasibility even with uncertainty.

While transmission switching exists today, it is used to a limited extent; historical information or the operators' prior knowledge are the primary mechanisms to establish and implement corrective switching as opposed to using a mathematical framework to identify corrective switching actions. The electric grid is one of the most complex engineered systems to date. Relying on only prior observations to determine potential corrective switching actions limits our capability to harness the existing flexibility in the transmission network. Systematic procedures that are capable of capturing such complexities should be preferred over such limited methods. Furthermore, the hardware requirements to implement TC (circuit breakers) already exist, leaving only the need to develop the appropriate decision support tools, which are low in cost, to obtain such benefits.

Chapter 7

ENHANCEMENT OF DO-NOT-EXCEED LIMITS WITH ROBUST CORRECTIVE TOPOLOGY CONTROL

In recent years, the penetration of renewable resources in electrical power systems has increased. These renewable resources add more complexities to power system operations, due to their intermittent nature. As a result, operators must acquire additional reserves in order to maintain reliability. However, one persistent challenge is to determine the optimal location of reserves and this challenge is exacerbated by the inability to predict key transmission bottlenecks due to this added uncertainty. This chapter presents robust corrective topology control as a congestion management tool to manage power flows and the associated renewable uncertainty. The proposed day-ahead method determines the maximum uncertainty in renewable resources in terms of do-not-exceed limits combined with corrective topology control. The day-ahead topology control formulation is based on the direct current optimal power flow; therefore, topology control solutions obtained from these algorithms are tested for AC feasibility and system stability. The numerical results provided are based on the IEEE-118 bus test case and the Tennessee Valley Authority (TVA) test system.

7.1 Introduction

The penetration of stochastic resources (e.g., variable wind and solar power) has increased in past years. These intermittent semi-dispatchable, or sometimes non-dispatchable, resources add more complexity to power system operations. In general, in most optimal dispatch models, conventional fossil-fuel power plants are dispatched to a fixed operating point, known as a desired dispatch point (DDP). Furthermore, it is assumed that each con-

ventional fossil-fuel generator will stay at its instructed fixed operating point over a specified time period. However, it is problematic to make this assumption for semi-dispatchable renewable resources due to their inherent intermittent and unpredictable nature. Therefore, system operators may instruct renewable power producers to stay within a desired dispatch range as opposed assuming, within their optimization problems, that these uncertain resources will operate at a fixed operating point. Within the Independent System Operator of New England (ISONE), this dispatch range is known as a do-not-exceed (DNE) limit for intermittent renewable power producers. The DNE limit defines a continuous set of potential dispatch solutions for the renewable resource and the bounds of the DNE limit are meant to be set such that if the renewable resource stays within the specified DNE limits (i.e., the upper and lower bounds), then the system will remain in a secure and reliable operating state. Such DNE limits are determined by constructing a robust optimization problem; the DNE limits are represented by an uncertainty set, which states that the uncertain resource can operate at any value within this continuous feasible set. Furthermore, the operator could also determine the maximum bounds for this uncertainty set by which the system can still absorb the variable production of the renewable resource without sacrificing system reliability.

Robust optimization has shown promising results in recent years to address issues associated with modeling uncertainty and decision making under uncertainty. In [70], a two-stage robust optimization technique is used to solve the unit commitment problem. Robust optimization deals with the data uncertainty and tries to find an optimal solution considering the worst-case uncertainty realization, within the defined uncertainty set. The solution of the robust optimization problem is guaranteed to be feasible for a pre-defined uncertainty set [97, 72, 73]. Another way to treat uncertainty is to use stochastic programming techniques; however, stochastic programming approach only provides probabilistic robustness and a solution is robust only to the scenarios that are modeled in the stochastic framework.

Therefore, in this paper, robust optimization techniques are used over the stochastic programming approach, to determine DNE limits since robust optimization provides a robust guarantee against the entire uncertainty set.

In this chapter, corrective topology control (TC) is used to determine DNE limits for renewable resources. Traditionally, TC is considered as a corrective mechanism, to overcome many power systems operational issues. In [97, 24], a detailed review of current industrial practices for TC are presented. In [96], a comprehensive list of corrective TC actions used at PJM are listed. In prior literature, TC has also been proposed to mitigate many power system related issues. In [2, 3, 4, 5, 11], TC is used to overcome voltage violations and line overloads. TC has shown benefits, to reduce line losses [6, 7, 8], to improve system security [9], and/or a combination of these [10]. TC has also shown significant improvement in operational flexibility [97] and cost saving [14, 23, 91, 24, 20, 21]. In general, TC is a congestion management tool; the implementation of corrective TC action alters the transmission network, which changes the line flows across the branches and reduces violations caused due to network congestion. In recent years, a number of heuristics to determine TC actions are investigated; in [82, 51, 81], different TC heuristics are discussed in order to improve the TC solution quality and the computational time.

TC algorithms are either based on the AC optimal power flow (ACOPF) or the DC optimal power flow (DCOPF) [97, 11, 91]. However, in an optimization framework, there is no systematic and highly accurate method to insure system stability with TC. In prior literature, TC actions combined with stability constraints are proposed [83, 84]; however, these methodologies were never tested on realistic test cases. Therefore, solutions obtained from TC algorithms must be tested to insure that the TC action will not cause a blackout. In [1], different stability studies are recommended for power system operation; they are classified based on the nature and the type of the disturbance as well as the time span under consideration. Typically, stability studies are classified into three different categories: rotor angle

stability, frequency stability, and voltage stability. In this chapter, all three stability studies are considered to study the effect of corrective TC actions on system stability/reliability.

The main contributions of this chapter are listed below.

1. TC is applied to facilitate the integration of renewable resources by enhancing DNE limits. A multistage (day-ahead and real-time) framework is proposed. In the day-ahead operational planning stage, DNE limits are determined for the system with and without TC. The DNE limits with TC provide the system operator more flexibility to manage the uncertain renewable resources and the DNE limits without TC can be used to define the trigger as to when it is necessary to implement the corrective TC action in order to maintain system reliability. The multistage framework manages some of the computational complexities by moving part of the computational process to the day-ahead time stage and then to reconfirm the accuracy of the day-ahead time stage solution with the real-time operating state. The day-ahead and the real-time based robust topology control (RTC) DNE limit procedure is novel and flexible enough to consider different types of uncertainties, such as uncertainty in generation, uncertainty in renewable resource, and demand uncertainty, simultaneously.

2. The RTC DNE limit problem is formulated, which is a three stage robust optimization problem with a structured uncertainty set definition. The robust DNE limit problem is not a standard robust optimization problem; for a standard robust optimization problem, the uncertainty set, i.e., the DNE limit, is known prior to solving the robust optimization problem. However, the DNE limit problem can be transformed into a standard robust optimization problem. The DNE limit problem is then combined with transmission topology control, which increases the the computational complexity.

3. A multistage solution method is developed to solve the RTC DNE limit problem. The RTC DNE limit problem is transformed into a two stage problem. The uncertainty

set, i.e., the DNE limit, for the RTC DNE limit problem is determined by an iterative procedure. The proposed solution method for the RTC DNE limit problem requires fewer iterations to find the solution as compared with the solution method used in [97].

4. The RTC DNE limit problem and its associated solution method is validated on a smaller test system, the IEEE-118 bus test case and a realistic test system, the Tennessee Valley Authority (TVA) test system. The realistic results demonstrate the benefits of the RTC on renewable integration and system operations. Limited prior work on TC has been done for realistic systems.

5. The majority of prior work on TC does not confirm that the switching solutions are AC feasible or does not cause instability. In this chapter a more thorough assessment of the potential for TC by confirming whether the solutions are AC feasible and stable. Different stability studies are carried out and the effects of the TC actions on system stability are presented.

The rest of the chapter is structured as follows: the robust corrective TC methodology to determine DNE limits is described in Section 7.2. The RTC DNE limit formulation is presented in Section 7.3. The solution method for the RTC DNE limit algorithm is presented in Section 7.4. The associated simulation results for the RTC DNE limit algorithm, on the IEEE-118 bus test system and the TVA test system, are presented in Section 7.5. In Section 7.6, results related to different stability studies associated with TC actions are presented. Section 7.7 provides the conclusions and discusses potential future work.

7.2 Do-Not-Exceed Limits: Robust Corrective Topology Control Methodology

This chapter proposes a two stage approach to determine the DNE limits, with and without TC. The proposed methodology, shown in Fig. 7.1, is divided into two parts: a day-ahead process and a real-time process. In the day-ahead process, after solving the day-ahead security constrained unit commitment (SCUC) problem, the solution will be used to determine DNE limits, which includes information about generator status, generator dispatch, and operational reserve. The standard SCUC procedure at Midcontinent Independent System Operator (MISO) is presented in [60]. In Fig. 7.1, after solving the day-ahead SCUC problem, the resultant solution will be passed to the RTC DNE limit algorithm. The RTC DNE limit algorithm determines the DNE limits (with and without TC). The TC solution and associated DNE limits, obtained from the RTC DNE limit algorithm, will be tested for AC feasibility and stability. The resultant TC solutions will be stored for real-time use if needed. In real-time, TC actions are implemented if the renewable generation goes outside of the DNE limit without TC actions, i.e., the boundary of the DNE limits without TC actions, define the necessary trigger as to when to implement the TC actions. In real-time, the DNE limits (with and without TC) will be continuously re-evaluated based on the real-time system states and the updated renewable forecasts. If the real-time energy management system (EMS) determines the need to implement the corrective TC action, then a resulting signal will be passed to the operator.

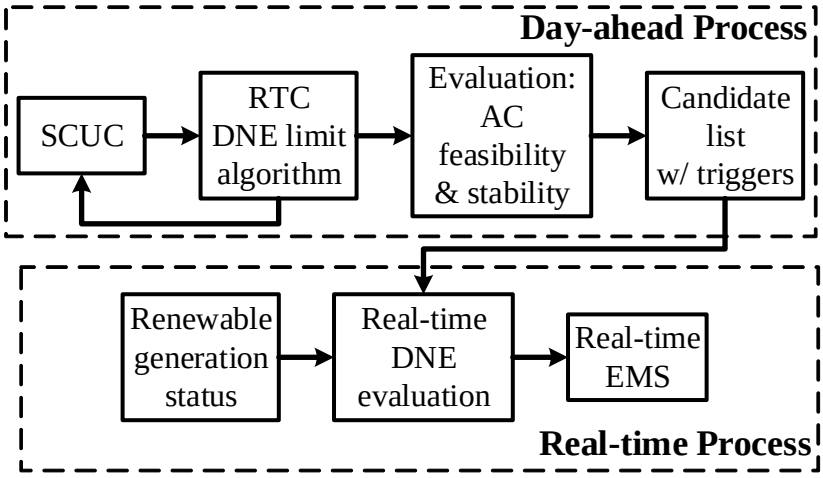

Figure 7.1: Day-ahead to real-time process for DNE limits with RTC.

The RTC DNE limit algorithm determines the DNE limits with and without corrective TC for the specified SCUC solution. The difference in these DNE limits is caused by network congestion that inhibits deliverability of reserves. The differences in the DNE limits also identify the necessary triggers as to when to implement the corrective TC action. If the DNE limits, with and without TC, are smaller than the anticipated range of potential renewable production, then the operator can rerun the SCUC to commit additional units in order to hedge against the higher resource uncertainty. Note that, the robust DNE limit algorithm relies on a DC approximate power flow and, thus, it does not guarantee a robust AC power flow solution but it substantially improves the reliability of the day-ahead schedule by accounting for renewable uncertainty. The resultant DNE limits and its associated TC actions will be sent to the EMS to be used in real-time.

In real-time, the day-ahead DNE limits with and without TC are continuously evaluated with real-time system states and updated renewable forecasts. Furthermore, the AC feasibility and stability checks are also performed. If the real-time renewable generation crosses the DNE limits specified without TC, determined by the real-time evaluation process, the TC solution will be passed on to the real-time EMS, for implementation. Note

that this process is described as a two-stage (day-ahead and real-time) process; however, the DNE limits and RTC solutions can be updated more frequently, e.g., hour-ahead, to create a multistage process.

One benefit of the proposed robust DNE limit process is that, in the day-ahead time-frame, the system operator will have an estimate of the DNE limits, with and without TC. If the day-head DNE limits are less than the expected uncertainty in the renewable generation, the operator can update the SCUC solution at the day-ahead time stage. Currently, there are no such systematic procedures available for day-ahead operations, which determines the effect of renewable generation on SCUC solution [60]. Furthermore, the TC solutions are determined in the day-ahead framework, which can be useful to improve reliability coordination of neighboring entities. The benefit of real-time process is that the real-time DNE limit evaluation process is computationally light, as most of the complex part of determining DNE limits with TC are performed within the day-ahead process. Therefore, with the existing computational capabilities, the RTC DNE limit procedure can be implemented.

In this chapter, the detailed formulation and associated solution method of the RTC DNE limit algorithm are presented. Furthermore, the entire day-ahead procedure is simulated and tested on two different test cases.

7.3 DNE Limits Model

In [103], a procedure to determine the DNE limits for a real-time application is presented. This procedure determines the DNE limits, without TC, based on available capacity of conventional generators with automatic generation control (AGC) and 10 minutes ahead wind forecast. In [103], the DNE limits problem is solved after determining the real-time economical dispatch, which includes the DDP for conventional generators. To improve the computational time, it assumed that only conventional generators, with AGC, would respond to the change in the wind generation, while other conventional generators would

maintain DDP. For real-time applications, to have a fast solution time, considering only AGC generators to respond to wind deviations is justifiable. However, at other scheduling time stages, assuming that most of the conventional generators will not move and cannot move away from their DDP is not a valid assumption as there are many changes that can occur between look-ahead time stages and real-time (e.g., forecasts will be updated, generator availability and system topology may change). Hence, in a day-ahead or an hour-ahead time stage, assuming only the generators with AGC over the short term ramping capabilities of all the conventional generators may result in a poor solution quality as it will not accurately capture the quantity and locational aspect of resources. Furthermore, in [103], a shift factor based network model is used to model line flows, which allows to monitor subset of transmission lines while determining the DNE limits. In [103], only a handful of critical transmission paths are monitored for the line flow violations, which simplifies the DNE limit problem and reduces the computational time. However, this simplification may result in inaccurate solution as change in wind and corresponding AGC injection may cause line flow violations on unmonitored transmission lines. Therefore, to obtain a quality solution at the day-ahead timeframe, a more complex mathematical model is proposed in this chapter, which models renewable generation uncertainties along with a nodal optimal power flow (OPF) structure within a robust optimization framework.

The uncertainty in renewable generation is captured by constructing a polyhedral uncertainty set around the wind generation, as shown in (7.1) and (7.2). The size of the uncertainty set depends on φ_w^- and φ_w^+, as shown in (7.1); by simplifying (7.1), φ_w^- is always less than or equal to 1 and φ_w^+ is always greater than or equal to 1. The uncertainty set definition, used in this chapter, is defined in (7.2), where the uncertainty set, $\mathcal{U}$, is defined by variables φ_w^- and φ_w^+. In (7.2), renewable resources (in this case, wind generation) are assumed to vary between the lower limit, φ_w^-, and the upper limit, φ_w^+. A similar uncertainty set definition is used in [97], which is a more conservative uncertainty set definition

as compared with the uncertainty set definitions used in [70, 72, 73, 104].

$$\mathcal{O} := \{\varphi_w^-, \varphi_w^+ \in \mathbb{R}^{2w} : P_w^{min} \leq P_w^{fix}\varphi_w^- \leq P_w^{fix}, \forall w \tag{7.1}$$
$$P_w^{fix} \leq P_w^{fix}\varphi_w^+ \leq P_w^{max}, \forall w\}$$
$$\mathcal{U} := \{P_w \in \mathbb{R}^w : P_w^{fix}\varphi_w^- \leq P_w \leq P_w^{fix}\varphi_w^+, \forall w\} \tag{7.2}$$

Note that, in the RTC DNE limits problem, φ_w^- and φ_w^+ are not constant; in fact, it is the solution of the problem, i.e., the DNE limits. Therefore, the RTC DNE limit problem is more difficult to solve as compared with standard robust optimization problems discussed in [97, 70, 72, 73, 104]. In [97, 70, 72, 73, 104], a robust optimization problem is solved considering the predetermined uncertainty set; the solution obtained from these standard optimization problems are robust against the predetermined uncertainty set. For the RTC DNE limit problem, uncertainty sets are not constant. In fact, the objective is to determine the uncertainty set and associated TC action that will be robust (i.e., feasible) for the entire uncertainty. This feature makes the RTC DNE limit problem difficult to solve and demands a complex solution methodology to solve the problem within tractable time span.

The RTC DNE limit problem is a three stage optimization problem and it is represented by (7.3)-(7.16); the first minimization part of the RTC DNE limit problem is a MIP problem, which determines the system topology and the uncertainty set. The second part of the RTC DNE limit problem chooses the worst-case realization of renewable generation from the uncertainty set, determined based on the solution from the first part of the problem. The last part of the RTC DNE limit problem is a power flow (PF) problem, which determines the feasibility of the worst-case realization of renewable generation, determined in second part of the RTC DNE limit problem, with the TC action, determined in the first stage of the RTC DNE limit problem. Furthermore, the last minimization problem, i.e., the PF problem, is a feasibility problem. The max-min parts of the formulation form a

robust counterpart of the RTC DNE limit problem; when combined, they determine the feasibility of worst-case realization of renewable generation associated with the chosen TC solution. In this formulation, generator capacity constraints are modeled as shown in (7.4) and (7.5). To respond to the change in the renewable generation, conventional generators' ramping capabilities are used and are modeled as shown in (7.6) and (7.7); in this chapter, at the day-ahead time stage, generators' 10 minutes ramp up and ramp down capabilities are considered. Transmission line flows are modeled as shown in (7.8)-(7.11). The node balance constraints are represented by (7.12). The number of simultaneous TC actions are controlled by constraint (7.15); in (7.15), the user defined parameter, M, controls the number of simultaneous TC actions. Furthermore, in this chapter, only one simultaneous TC action is considered (M=1).

$$\min_{\substack{Z_k,\varphi_w^-,\\ \varphi_w^+}} \left(\sum_{\forall w} (\varphi_w^- - \varphi_w^+) + \max_{P_w} \min_{P_g,P_k,\theta_n} 0 \right) \tag{7.3}$$

$$\text{s.t.} - P_g \geq -P_g^{max} u_g, \ \forall g \tag{7.4}$$

$$P_g \geq P_g^{min} u_g, \ \forall g \tag{7.5}$$

$$- P_g \geq (-R_g^{+c} - P_g^{uc}), \ \forall g \tag{7.6}$$

$$P_g \geq (-R_g^{-c} + P_g^{uc}), \ \forall g \tag{7.7}$$

$$- P_k \geq -P_k^{max} Z_k, \forall k \tag{7.8}$$

$$P_k \geq -P_k^{max} Z_k, \forall k \tag{7.9}$$

$$P_k - B_k(\theta_n - \theta_m) + (1 - Z_k) M_k \geq 0, \forall k = (n, m) \tag{7.10}$$

$$P_k - B_k(\theta_n - \theta_m) - (1 - Z_k) M_k \leq 0, \forall k = (n, m) \tag{7.11}$$

$$\sum_{\delta(n)^+} P_k - \sum_{\delta(n)^-} P_k + \sum_{\forall g(n)} P_g + \sum_{\forall w(n)} P_w = d_n, \forall n \tag{7.12}$$

$$P_w^{min} \leq P_w^{fix} \varphi_w^- \leq P_w^{fix} \leq P_w^{fix} \varphi_w^+ \leq P_w^{max}, \forall w \tag{7.13}$$

$$P_w^{fix}\varphi_w^- \leq P_w \leq P_w^{fix}\varphi_w^+, \ \forall w \tag{7.14}$$

$$\sum_{\forall k}(1 - Z_k) \leq M \tag{7.15}$$

$$Z_k \in \{0, 1\} \tag{7.16}$$

The RTC DNE limit model presented in (7.3)-(7.16) can be represented by a generic robust optimization formulation as shown in (7.17)-(7.24). In a generic representation, l represents the binary decision variable, within set $\mathcal{L}$, such as TC decision variable Z_k. In (7.17)-(7.24), x represents the continuous decision variables, within set $\mathcal{X}$, such as uncertainty set defining variables φ_w^- and φ_w^+. Similarly, in (7.17)-(7.24), y represents the continuous decision variables, within set Y, such as power flow decision variables P_g, P_k, and θ_n. The worst-case realization of the renewable generation, within the uncertainty set $\mathcal{V}$, is represented by variable υ. Furthermore, the size of the uncertainty set $\mathcal{V}$ depends on variable x. Similarly, the size of the uncertainty set Y depends on variables υ and l. The objective cost function for the OPF problem is represented by b. In RTC DNE limit formulation, the OPF problem is a feasibility problem; therefore, in (7.17), the parameter b is set to be zero. In matrix representation, the system parameters in matrix form are represented by **A, C, E, G, H, K, Q, R, T** and the system parameters in vector form are represented by c, d, e, j, r, s.

$$\min_{\substack{x\in\mathcal{X}\\ l\in\mathcal{L}}} (f(x) + \max_{v\in\mathcal{V}(x)} \min_{y\in Y(v,l)} b^T y) \tag{7.17}$$

$$\text{s.t. } \mathbf{A}x \leq c \tag{7.18}$$

$$\mathbf{C}l \leq d \tag{7.19}$$

$$\mathbf{E}y \leq e \tag{7.20}$$

$$\mathbf{T}x + \mathbf{R}v \leq s \tag{7.21}$$

$$\mathbf{G}l + \mathbf{H}y \leq j \tag{7.22}$$

$$\mathbf{Q}v + \mathbf{K}y = r \tag{7.23}$$

$$l \in \{0, 1\} \tag{7.24}$$

The robust counterpart of the RTC DNE limit formulation, is formed by the max-min section of the formulation, which are LP problems that can be combined into a single optimization problem. In [97], a detail procedure to transform a three stage robust optimization problem into a two stage optimization is presented. In this procedure, the third stage of the minimization problem, i.e., the OPF problem, is transformed into the dual form LP problem and combine with the second stage maximization problem. The dual form of the OPF problem is merged with the second stage in order to properly preserve the worst-case scenario setting of the robust optimization problem; additional information about transforming a three stage robust optimization problem into a two stage optimization problem is presented in [70, 104, 74, 97]. The resultant two stage problem, in a generic form, is given in (7.25)-(7.27), where μ, λ, η are the dual variables of the constraints represented by (7.20), (7.22) and (7.23). For additional details about transforming a three stage robust optimization problem into a two stage robust optimization problem, refer to the Appendix.

$$\min_{\substack{x\in\mathcal{X}\\ l\in\mathcal{L}}} f(x) + \max_{\substack{\upsilon,\mu,\\ \lambda,\eta}} \lambda^T(\mathbf{G}l - j) - \mu^T e + \eta^T(r - \mathbf{Q}\upsilon) \tag{7.25}$$

$$\text{s.t. } -\mu^T\mathbf{E} - \lambda^T\mathbf{H} + \eta^T\mathbf{K} = b^T \tag{7.26}$$

$$\mu \geq 0, \lambda \geq 0, \upsilon \in \mathcal{V} \tag{7.27}$$

$$(7.18), (7.19), (7.21), (7.24)$$

In (7.25), the minimization problem, the master problem, determines the TC action and the uncertainty set; the maximization problem, the sub-problem, determines the robustness properties of the chose TC solution in the master problem. The sub-problem is a nonlinear problem, due to the $\eta^T\mathbf{Q}\upsilon$ term in (7.25), and can be transformed into a MIP problem using a big-M formulation [97].

7.4 Solution Method: RTC DNE Limit Algorithm

The reformulated RTC DNE limit problem is a two-stage optimization problem: a master problem and a sub-problem, as shown in (7.25)-(7.27). In [97], the topology selection problem, a master problem, is a MIP problem, which is computationally inefficient, for larger test systems. In [19], a sensitivity based greedy algorithm is derived and used to determine TC action for real-time emergency situations; the detail study of this greedy TC heuristic method on a large scale Polish system is presented in [98]. In this chapter, a sensitivity based rank list approach, presented in [19], is proposed over the master problem presented (7.17)-(7.19). The rank list suggestions are based on a sensitivity analysis of an OPF problem, as shown in (7.28)-(7.36). The rank list formulation consists of generator capacity constraint (7.29), generator ramping constraints (7.30) and (7.31), transmission line constraints (7.32)-(7.34), and node balance constraint (7.35). The objective of rank list formulation, presented by (7.28), is to maximize the demand serve considering the expected

extreme renewable generation, i.e., P_w^{rl}. To determine the lower bound of DNE limits P_w^{rl} is set to $P_w^{fix}\varphi_w^-$ and to determine the upper bound of DNE limits P_w^{rl} is set to $P_w^{fix}\varphi_w^+$.

$$\max \sum_{\forall n} d_n^{rl} \tag{7.28}$$

$$\text{s.t. } P_g^{min} \leq P_g^{rl} \leq P_g^{max},\ \forall g \tag{7.29}$$

$$P_g^{rl} \leq R_g^{+c} + P_g^{uc},\ \forall g \tag{7.30}$$

$$P_g^{rl} \geq P_g^{uc} - R_g^{-c},\ \forall g \tag{7.31}$$

$$P_k^{rl} \leq P_k^{max} Z_k, \forall k \tag{7.32}$$

$$P_k^{rl} \geq P_k^{min} Z_k, \forall k \tag{7.33}$$

$$P_k^{rl} - B_k(\theta_n^{rl} - \theta_m^{rl}) = 0, \forall k = (n, m) \tag{7.34}$$

$$\sum_{\delta(n)^+} P_k^{rl} - \sum_{\delta(n)^-} P_k^{rl} + \sum_{\forall g(n)} P_g^{rl} + \sum_{\forall w(n)} P_w^{rl} = d_n^{rl},\ \forall n \qquad (\tau_n) \tag{7.35}$$

$$0 \leq d_n^{rl} \leq d_n,\ \forall n \tag{7.36}$$

The rank list problem is arranged such that for a fixed initial topology, the dual variable of (7.35), i.e., τ_n, provides information about the marginal change in the objective with respective marginal change in the state of the transmission line. Note that the change in transmission line state, i.e., in service or out of service, is binary; however, the information obtained from the rank list formulation is based marginal change in the transmission line state. Therefore, rank list approach provides only suggestions for possible TC action and does not guarantee the solution feasibility. However, the rank list approach is still preferred over the MIP formulation for TC selection; as solving MIP based formulation is computationally challenging as compared with the linear programming based rank list formulation. The rank list is generated by estimating the benefit of TC action, using (7.37), and arranging

the possible TC actions in descending order.

$$\sigma_k = P_k^{rl}(\tau_n - \tau_m) \tag{7.37}$$

In (7.37), the benefit of TC solution is represented by σ_k, the line flow across the branch is represented by P_k^{rl}. τ_n and τ_m represent the dual variables of the node balance constraints for nodes n and m, where node n is the "to" bus and node m is the "from" bus for line k. Furthermore, with the IEEE-118 bus test case, it is observed that, with the rank list based master problem, the number of iterations required to determine DNE limits can be reduced by $\sim 80\%$ compared with the MIP based master problem.

Note that the solution method, presented in this section, is to determine the lower bound of the DNE limits. The same solution method can be updated to determine the upper bound of the DNE limits; the only change would be in the uncertainty set update section of the solution method.

Initialization: It is assumed that the SCUC problem is solved prior to solving the RTC DNE limit algorithm. The solution of SCUC problem, such as generator status and associated dispatch, renewable generation, system demand, is used as an input parameter to the RTC DNE limit algorithm. The detail solution method is presented in Fig. 7.2. To initialize the RTC DNE limit algorithm assume φ_w^+ to be 1 and φ_w^- to be 0; furthermore, for algorithm termination condition assume, ϵ to be very small number, L_b to be 0, and U_b to be 1. The uncertainty set is updated outside of the robust framework, as shown in Fig. 7.2. For simplicity, it is assumed that all the renewable injections will vary with the same percentage across all the renewable injection nodes. Therefore, to determine the lower bound of DNE limits φ_w^+ is set to 1 for all w and to determine the upper bound of DNE limits φ_w^- is set to 1 for all w.

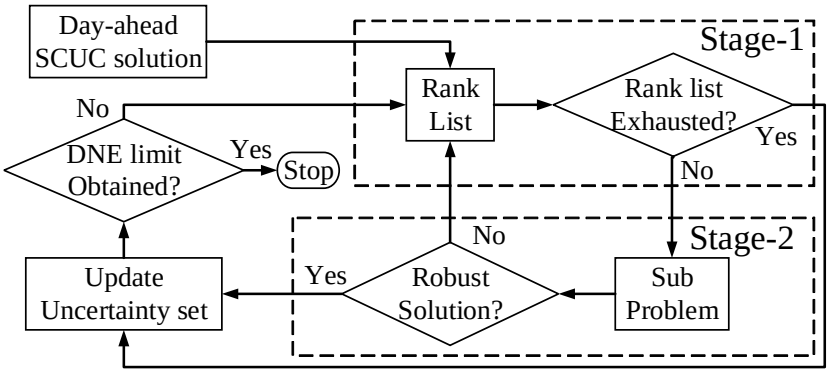

Figure 7.2: Solution method to determine DNE limits with robust corrective TC.

Stage-1: The stage-1 problem determines the system topology, which will be evaluated for its robustness properties in the stage-2 of this solution method. The TC solutions are generated in form of the rank list, using (7.37). If a feasible topology is obtained from the rank list, the resultant topology will be passed to the stage-2 problem. If the rank list is exhausted, which indicates that there is no feasible TC action available based on the incumbent SCUC solution and the chosen uncertainty set; therefore, at the next iteration, the uncertainty set will be reduced.

Stage-2: The sub-problem determines the feasibility of the worst-case renewable resource realization, for a chosen TC action and generation dispatch. The generic form of the sub-problem formulation is presented in (7.25)-(7.27). The actual formulation of the sub-problem is given in (7.38)-(7.48), where $\alpha_g^+, \alpha_g^-, \Omega_g^+, \Omega_g^-, F_k^+, F_k^-, S_k^+, S_k^-, L_n$ are the dual variables of constraints (7.4)-(7.12), respectively. The uncertainty set is defined using a big-M formulation, as shown in (7.42)-(7.45). The D_n is a binary variable, which is used to evaluate extreme points of a polyhedron uncertainty set. The sub-problem chooses the variable D_n, such that it will maximize the sub-problem objective function (7.38).

$$\max \sum_{\forall g}(u_g(-P_g^{max}\alpha_g^+ + P_g^{min}\alpha_g^-) - (R_g^{+c} + P_g^{uc})\Omega_g^+ + (-R_g^{-c} + P_g^{uc})\Omega_g^-) - \sum_{\forall k}((P_k^{max} Z_k(F_k^+ + F_k^-) + (1 - Z_k)M_k(S_k^+ + S_k^-)) + \sum_{\forall n}(L_n d_n - \eta_n) \quad (7.38)$$

$$\text{s.t. } -\alpha_g^+ + \alpha_g^- - \Omega_g^+ + \Omega_g^- + L_n = 0, \ \forall g \quad (7.39)$$

$$-F_k^+ + F_k^- + S_k^+ - S_k^- + L_n - L_m = 0, \ \forall k \quad (7.40)$$

$$\sum_{\delta(n)^+} B_k(S_k^- - S_k^+) + \sum_{\delta(n)^-} B_k(S_k^+ - S_k^-) = 0, \ \forall n \quad (7.41)$$

$$\eta_n - L_n \sum_{\forall w(n)} P_w^{fix}\varphi_w^+ + (1 - D_n)M_n \geq 0, \ \forall n \quad (7.42)$$

$$\eta_n - L_n \sum_{\forall w(n)} P_w^{fix}\varphi_w^+ - (1 - D_n)M_n \leq 0, \ \forall n \quad (7.43)$$

$$\eta_n - L_n \sum_{\forall w(n)} P_w^{fix}\varphi_w^- + D_n M_n \geq 0, \ \forall n \quad (7.44)$$

$$\eta_n - L_n \sum_{\forall w(n)} P_w^{fix}\varphi_w^- - D_n M_n \leq 0, \ \forall n \quad (7.45)$$

$$\alpha_g^+, \alpha_g^-, \Omega_g^+, \Omega_g^- \geq 0, \ \forall g \quad (7.46)$$

$$F_k^+, F_k^-, S_k^+, S_k^- \geq 0, \ \forall k \quad (7.47)$$

$$D_n \in \{0, 1\} \quad (7.48)$$

After solving the sub-problem, if a robust solution is obtained, i.e., the objective of the sub-problem is equals to zero, which indicates that the chosen TC solution satisfies the entire uncertainty set, and in the next iteration the uncertainty set will be increased. If the sub-problem failed to obtain a robust solution, i.e., the objective of the sub-problem is not equal to zero, the resultant TC action will be discarded and the next TC action listed in the rank list will be tested.

The benefit of this solution method is that the stage-2 problem is independent of the stage-1 problem. Stage-1 of the solution method determines the entire rank list, for a given renewable generation, based on a LP based rank list formulation. After stage-1, each suggested TC action in the rank list can be tested sequentially, as shown in Fig. 7.2, or can be distributed to multiple computer/cores at the same time. Therefore, the sub-problem can be parallelized for solution speedup, which will help with scalability. However, in this chapter, the solution method is not parallelized and the numerical results, presented in Section 7.5, are based on sequential implementation of algorithm.

Uncertainty set update: To simplify the RTC DNE limit problem, in this chapter, it is assumed that all the renewable generation deviates uniformly over all the renewable injection nodes. We acknowledge that such an approximation is conservative; however, it simplifies the problem significantly. The future work will involve eliminating this approximation and developing a more accurate solution method.

If the uncertainty set is updated due to the exhaustion of the rank list, this indicates that there is no available TC action that could satisfy the given uncertainty set. Therefore, in this case, the lower bound of the uncertainty set, i.e., φ_w^-, should be increased using (7.49) and the upper of the uncertainty set, i.e., φ_w^+, remains the same. Furthermore, the terminational conditions are also updated; the lower bound, L_b, is updated to new φ_w^- and the upper bound, U_b, remains the same.

If the uncertainty set is updated due to the robust solution obtained from stage-2, which indicates that there is a possible TC action that could satisfy the given uncertainty set. Therefore, in this case, the lower bound of the uncertainty set, i.e., φ_w^-, should be reduced using (7.50) and the upper of the uncertainty set, i.e., φ_w^+, remains the same. Furthermore, the terminational conditions are also updated; the new upper bound, U_b, is equals to L_b

(previous iteration) and the new lower bound, L_b, is equals to new φ_w^-.

$$\varphi_w^- = L_b + \delta(U_b - L_b) \tag{7.49}$$

$$\varphi_w^- = L_b - \delta(U_b - L_b) \tag{7.50}$$

Note that optimal determination of δ, in each iteration, is outside the scope of this research and is an interesting future research direction. However, in this chapter, the parameter δ is set to 0.5.

Algorithm termination: After updating the lower and the upper bound of termination condition, i.e., L_b and U_b respectively, if the difference between the L_b and U_b is less than the termination condition, ϵ, terminate the algorithm and the resultant robust uncertainty set along with the associated TC action will be the solution for the RTC DNE limit problem. Furthermore, after updating the lower and the upper bounds of the termination condition, if the difference between the L_b and U_b is more than the termination condition, ϵ, continue the solution method and solve the stage-1 problem with an updated uncertainty set.

Note that the TC actions are controlled by the stage-1 problem; to determine the DNE limits without TC, the stage-1 problem should be eliminated from the solution method. The rank list approach should be removed and the initial topology should be passed on to the stage-2 problem.

7.5 Numerical Results: Robust DNE Limits

In this section, the RTC DNE limit algorithm is tested on the IEEE-118 bus test case and the TVA test system.

7.5.1 IEEE-118 Bus Test Case

The branch data for the IEEE-118 bus test case is given [87]; however, the generation information for this test system is not available. Therefore, the generator mix of reliability

test system 1996 (RTS) is used to create generator information for the IEEE-118 bus test case [87]. There are total 71 conventional generators and 9 wind injection locations, with peak demand of $4004MW$. The load profile and wind forecast is obtained from California Independent System Operator (CAISO) duck chart [99].

A 24 hour SCUC problem is solved and the SCUC solution is used as a starting point for all the simulations presented in this chapter. The basic SCUC model and the fuel costs, given in [14], are used to calculate generator operating costs. The reserve requirements for the SCUC are modeled as sum of 5% of demand supplied by conventional generators and 10% of demand supplied by wind units or the single largest contingency, whichever is greater. On top of that, at least 50% of total required reserves will be supplied by spinning reserves and the rest will be supplied by non-spinning reserves. A similar assumption is cited in CAISO's guidelines for spinning reserve and non-spinning reserve [59].

The DNE limits for the IEEE-118 bus test case, with and without corrective TC actions, are presented in Fig. 7.3. The total penetration wind resources, on MW generation, is about 22%. In this chapter, conventional generators' 10 minutes ramping capabilities are used to respond to intermittencies in renewable generation. In Fig. 7.3, the bar chart shows the amount of available reserve generation that cannot be used to increase the DNE limits. Fig. 7.3 shows that, with corrective TC, during some of the low wind periods, such as hours 1,2, 7-10, 18 and 19, the lower bound of DNE limit with TC can be increased by $\sim 18\%$ as compared with DNE limits without corrective TC. In this case, due to higher congestion in initial topology, the generators ramping capabilities are not utilized to its limit. With TC, the congestion within the system is reduced, which results in an increase in transfer capability across the network and subsequent DNE limits. In hours, 3-6, 11-17 and 20-24, the lower bound of DNE limit obtained with and without TC are same; for these hours, the DNE limits are bounded by the availability of reserves. In this case, the initial topology is sufficient to deploy reserves in event of drop of renewable generation. However, in these

cases, robust DNE limits algorithm also suggests multiple TC solutions, which gives more options to system operator to choose from in real-time implementation. Furthermore, during hours 1-6, 11-16 and 20-24, the upper bound of DNE limit with TC can be increased by $\sim 74\%$ as compared with DNE limits without corrective TC. Furthermore, for the entire 24 hours, it is observed that the upper bound of DNE limits never goes beyond maximum real power supplied by wind generators; it is due to the smaller size of test system. However, on a realistic test case, the upper bound of DNE limit would be constrained by the physical limitations of wind generators to produce real power. Furthermore, for the entire 24 hours, the DNE limits with TC can be increased by $\sim 22\%$ from the DNE limits determined without TC.

In the IEEE-118 bus test case, the peak demand occurs during hour 18 and hour 19, as shown in Fig. 7.3. In this case, from hour 16 to hour 18, the system demand increases by 29% and wind generation decreases by 22%. Therefore, to meet the system demand in peak hours, the slow start units will be committed during hour 13-16, resulting in the higher amount of available generation in these hours. However, due to the congestion within the network, this additional available generation could not be utilized to increase the upper bound of DNE limit. In these situations, the TC action shows great benefit to system operation as it helps to reduce congestion within the network, which results in increase in DNE limits. Furthermore, the computational time, required to determine DNE limit is ~ 3 seconds per iteration; the master problem requires ~ 1 sec. and the sub-problem requires ~ 2 sec. Note that parallelization techniques can be used to improve the computational performance; however, such testing is outside the scope of this chapter.

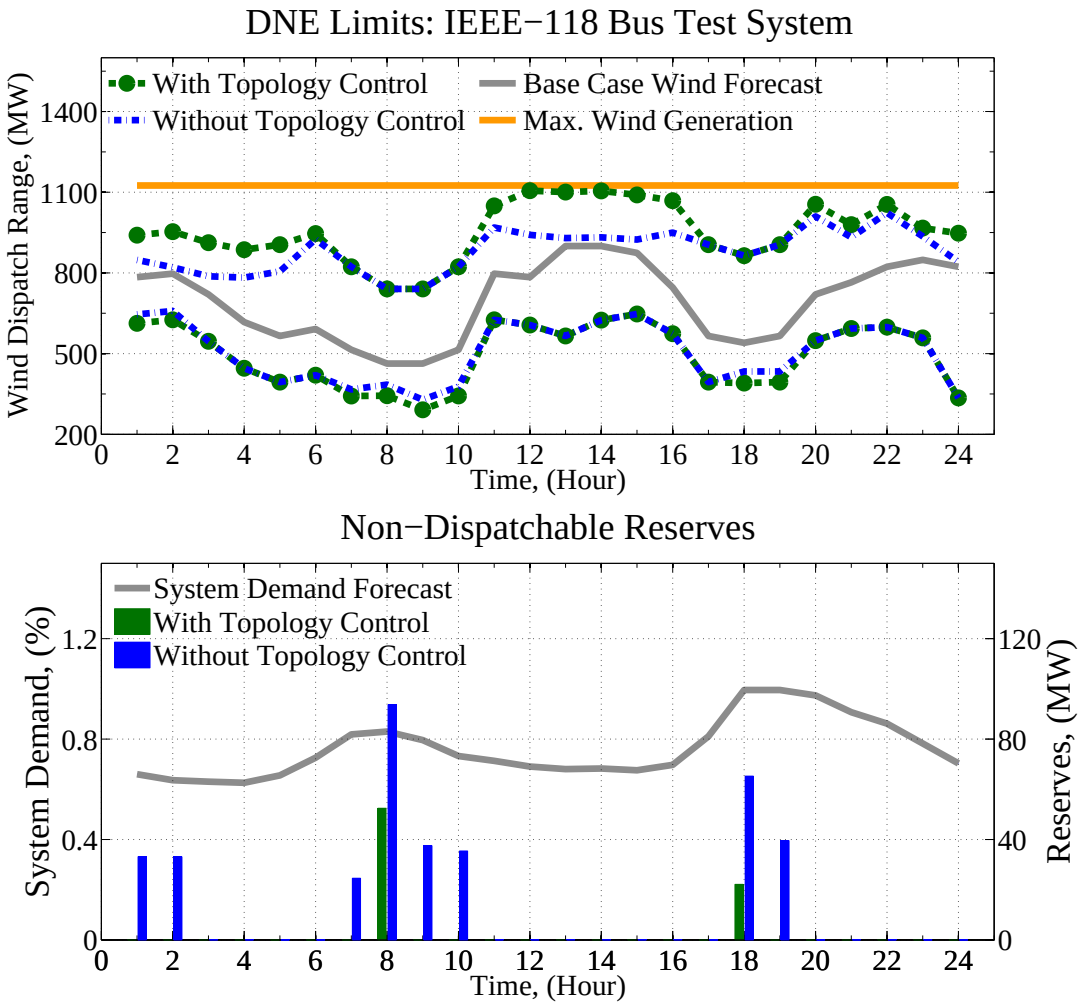

Figure 7.3: DNE limits with the IEEE-118 bus test case and utilization of reserves.

In the past, with TC, significant savings were obtained for the IEEE 118-bus test case [91]. While costs are not included in the proposed formulation, by improving this stage of the multistage scheduling process, it is possible to reduce the overall cost to operate the system reliably. Denote the DNE limit obtained when topology control is used as DNETC. This DNE limit is a larger uncertainty set than the DNE limit determined when topology control is not implemented. If the operator decides to protect the system against DNETC without implementing topology control, then there will have to be either generation re-dispatch or additional units committed because the original topology was only able to re-

liably handle a smaller uncertainty set. Thus, if DNETC is forced to be achieved without TC, the operational cost would be increased by at least 6%; this is determined by solving a robust unit commitment problem where both additional commitments and de-commitments are allowed in reference to the original unit commitment schedule (the schedule that was used within the original DNE limit problem). If only additional commitments are allowed, then the cost increase is estimated to be $\sim 14\%$. The solution method presented in [70] is used to solve the robust unit commitment problem; however, instead of the outer approximation method, suggested in [70], a big-M method is used to define the uncertainty set. This result proves that TC not only helps to integrate renewable resources, by increasing the DNE limits, but also provides substantial cost savings in system operations. Furthermore, the TC solutions, obtained from the RTC DNE limit algorithm, are tested for AC feasibility on base case wind forecast. The ACOPF model presented in [13] is used to test the AC feasibility of the TC solution. In this case $\sim 90\%$ of TC solutions have produced AC feasible solution; for this analysis >1000 TC solutions are tested for AC feasibility.

7.5.2 TVA Test System

The TVA test system consists of 1779 nodes, 1708 transmission lines, 321 traditional generators, 299 two-winding transformers, 98 three-winding transformers, and 178 switched shunts. The TVA test system does not have wind generation; therefore, for analysis purposes, 10 different wind injection locations are considered. The wind forecast is obtained from the NERL western wind resource database, profile case$\#12514$ for 20^{th} December 2005 [105]. A 24 hours SCUC model is solved using same reserve requirement rules, used in the IEEE-118 bus test case, and used as a starting point to determine RTC DNE limits. For entire 24 hours, the total wind penetration on MW basis is $\sim 26\%$. Fig. 7.4, shows the DNE limits on the TVA test systems. In this case, for 24 hours, the DNE limit obtained with TC are $\sim 19\%$ more than the DNE limit obtained without TC.

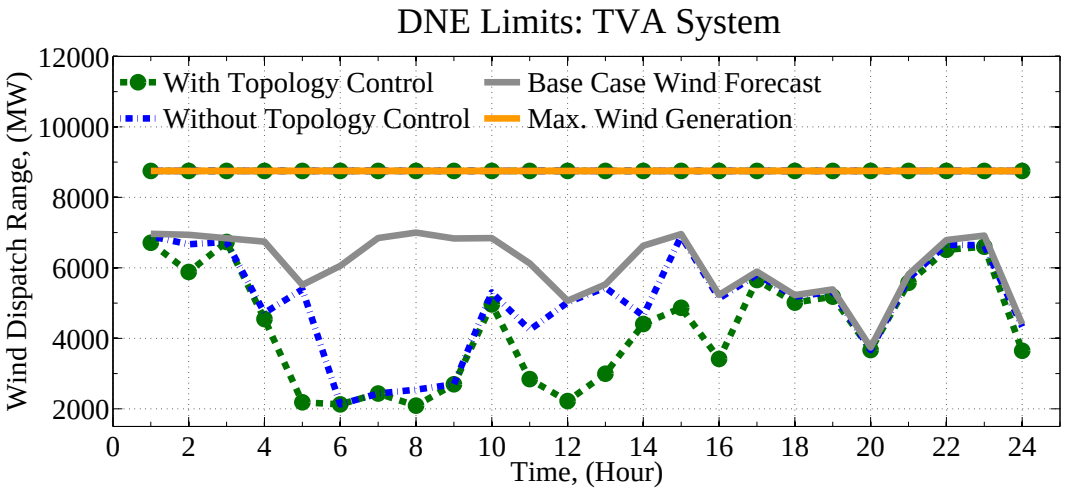

Figure 7.4: DNE limits with the TVA test system.

In the TVA test system, for all the 24 hours, the lower bound of DNE limit obtained with TC is more than the lower bound of DNE limit obtained without TC. For all 24 hours, the lower bound of DNE limit obtained with TC is $\sim 66\%$ more than the lower bound of DNE limit obtained without TC, as shown in Fig. 7.4. This result highlights the benefit of robust TC for renewable resource integration. In general, TC provides better control over the available resources and utilizes the existing infrastructure, without adding additional installation cost. Furthermore, for all 24 hours, the upper bound of DNE limit is bounded by maximum real power supplied by wind generators. This result proves the initial intuition about the upper bound of DNE limit. For a realistic test case, it may not be critical to determine upper bound of DNE limit, with and without TC, as it is mainly bounded by install capacity of the wind generation. An upper limit for renewable penetration reflects a situation where renewable generation exceeds the forecasted level. For the upper limit to be anything other than the capacity indicates the following possibilities: i) the limitations of delivering the energy to the load locations, i.e., transmission congestion, ii) the unavailability of enough ramping capability with conventional units, or iii) the minimum physical operating levels with conventional generators are reached. If the renewable gen-

eration is controllable and the renewable generation spillage is allowable then the upper bound of DNE limits would always be the installed capacity as renewable generation can be reduced. Note that in this case also determining the upper bound of DNE limit without such an assumption of spillage is critical as this would then define trigger to implement spillage. Computational time required to determine DNE limits, on the TVA system, is ~ 36 seconds per iteration; the master problem requires ~ 10 sec. and the sub-problem requires ~ 26 sec.

The TC solution obtained from the RTC DNE limit algorithm for TVA system, are tested for the AC feasibility on base case wind forecast. For the TVA system, 84% of TC solution obtained from the RTC DNE limit algorithm have produced AC feasible solution; for this analysis ~ 70 TC solutions are considered.

7.6 Stability Study with Robust Corrective Topology Control Actions

In this section, the RTC DNE limit solutions for IEEE-118 bus test system, presented in Section 7.5, are tested for different stability studies. For discussion purposes, results associated with the peak load hour (hour 18) are presented in this chapter. The dynamic data for the IEEE-118 bus test case is not available; therefore, generator information from generators in the eastern interconnection are used to generate dynamic data. The dynamic data, for $1.5MW$ individual wind generator, given in [90], are used to model wind injection in this analysis.

To demonstrate the effect of TC, on system reliability, scenario described in Table 7.1 are tested. The presented scenario represents the worst-case wind scenario for the given operating condition; the loss of wind represented by this scenario is equivalent to loss of $\sim 2\%$ of total generation. Note that, in the western interconnection, for many stability related studies, the worst-case scenario is the loss of two Palo Verde nuclear units [102], which is about 2% of total online generation.

Table 7.1: Scenario to Study the Effect of TC on System Reliability.

Time	Event
10-12 sec.	Loss of wind generation ($\sim 17\%$)
120 sec.	Topology control solution implemented (open line between Node#65-Node#68)
150-750 sec.	Generators are dispatched based on ramping capability

The effect of TC action on system frequency is presented in Fig. 7.5. Due to the sudden drop of wind generation, the system frequency drops below $59.8Hz$ and recovers to $\sim 59.88Hz$ using system inertia. After implementing the line switching action, the system frequency improves and reaches to $\sim 59.89Hz$. This small improvement in frequency happens because TC action decrease the losses in the system, which can be viewed as increased in generation. At t=150 sec., the generators are re-dispatched to overcome the loss of renewable generation; in this analysis, 10 minutes ramping capability of generators are considered. After generation re-dispatch, at last, the frequency improves and settle downs to $\sim 59.97Hz$.

Small signal (SS) eigenvalue studies are carried out on this test case, with SCUC dispatch solution, for hour 18. The SS eigenvalue studies are carried out at two instances: before the loss of renewable generation, i.e., at time = 0 sec. in Fig. 7.5, and at the end of generation re-dispatch, i.e., at time = 800 sec. in Fig. 7.5. Before the loss of wind generation, the real part of the smallest eigenvalue, obtained from the small signal study, is ~ -112 and the real part of largest eigenvalue is ~ -0.01. This study shows that all the eigenvalues are negative and lie on the left hand side of the s-plane indicating that the given system is stable. The SS eigenvalue analysis, at the end of generation re-dispatch, shows that the maximum change in dominant eigenvalues is $\sim 2\%$. This result shows that with TC action the given system is small signal stable and will remain stable for small perturbations

in the operating state. This analysis is carried out using SSAT [101].

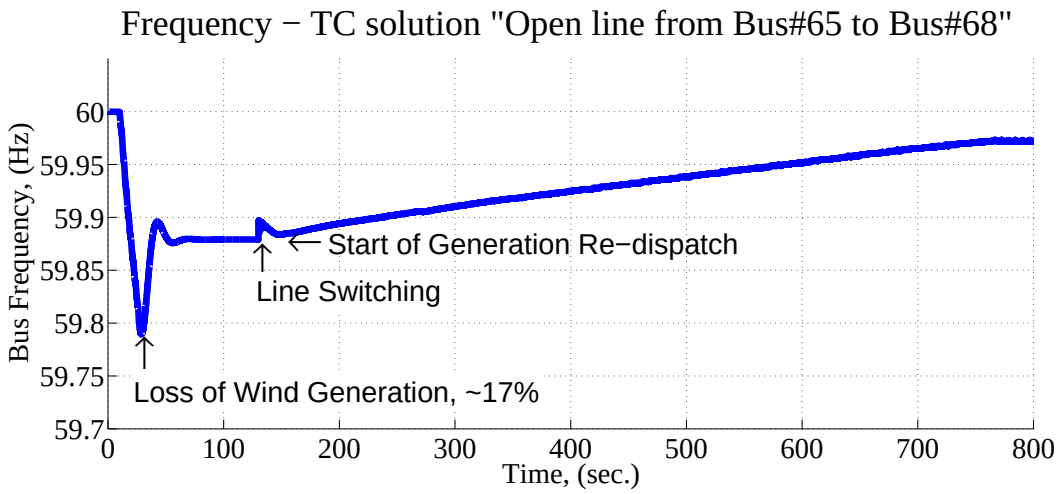

Figure 7.5: Effect of TC on System Frequency.

The relative rotor angle of generators nearer to topology control action are presented in Fig. 7.6. The effect of loss of wind generation on generator's rotor angle is relatively smaller than the implementation of topology control action, as the loss of wind generation is not close of these buses. On other hand, the topology control action is close to these buses; therefore, the effect of loss of wind generation, on generators relative rotor angle, is smaller compared to topology control action. The real power supplied by these generators are also presented in Fig. 7.7.

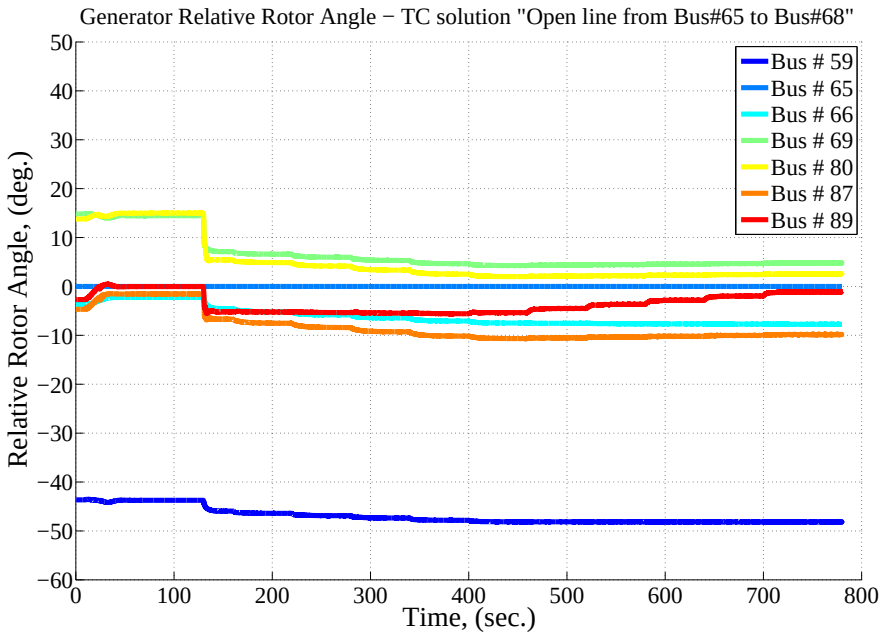

Figure 7.6: Generator Relative Rotor Angle - TC Solution “Open Line From Bus-65 To Bus-68”

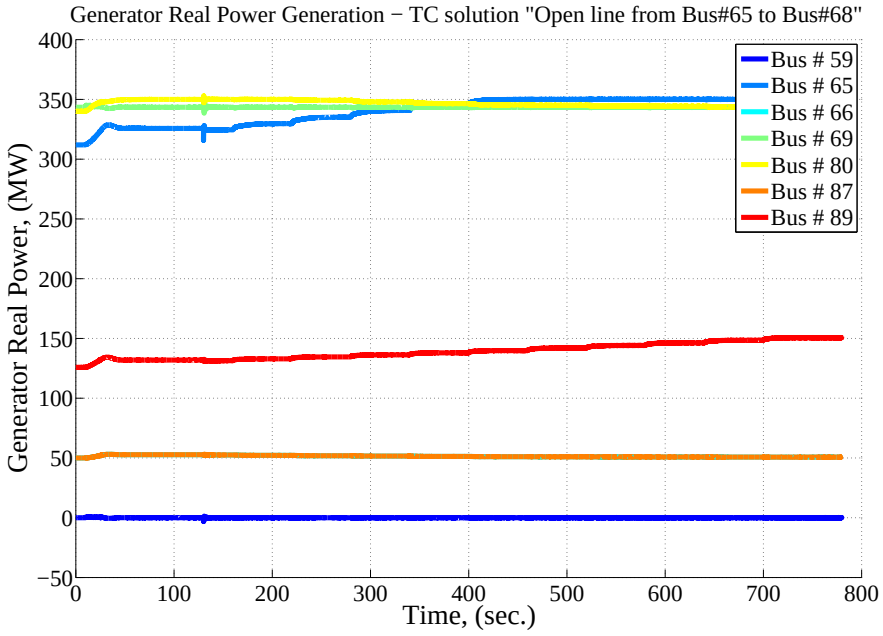

Figure 7.7: Generator Real Power Generation - TC Solution “Open Line From Bus-65 To Bus-68”

The effect of the TC on bus voltage stability is also studied. In the above scenario, the loss of wind on bus voltages are not significant; however, the TC alters the voltages on buses close to line switching action. The magnitude of change in voltage is highest on buses that are connected to the switched line, as shown in Fig. 7.8.

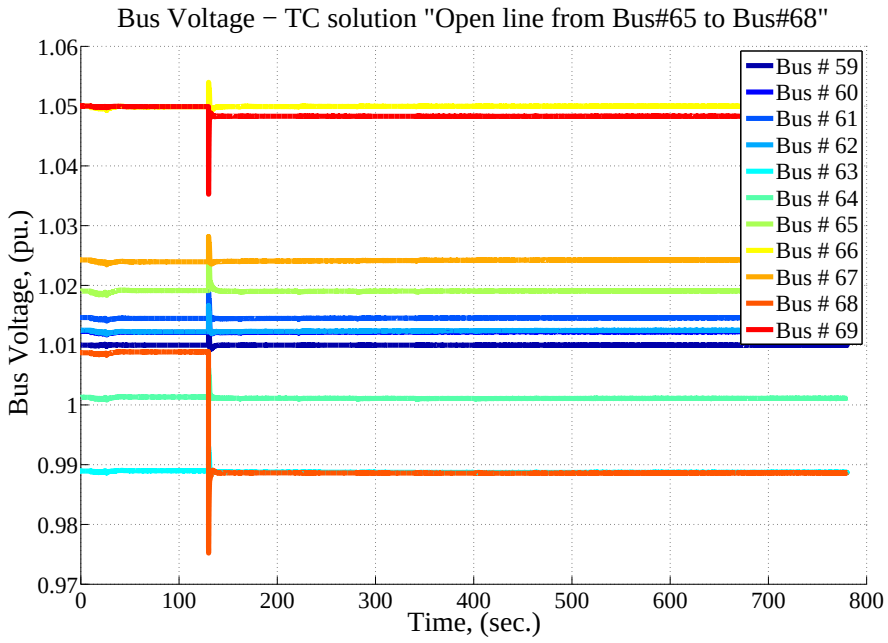

Figure 7.8: Bus Voltage - TC Solution “Open Line From Bus-65 To Bus-68”

7.7 Conclusion

The penetration of renewable resources in electrical power systems has increased in recent years. This increase in intermittent renewable resources is forcing a change in regards to the way bulk power systems are operated today. This chapter shows the usefulness of TC for integration of renewable resources.

In case of renewable resource integration, the determination of DNE limits is critical; in this chapter, a systematic procedure to determine DNE limit is presented. With corrective TC, the DNE limits can be increased by 22-26%, as compared with no topology control

actions. At the same time, TC can lower the operational cost by at least 6%. The RTC DNE limit algorithm is based on a DCOPF; therefore, the TC solutions obtained from this algorithm must be checked for AC feasibility; on the IEEE-118 bus test case, $\sim 90\%$ of TC solutions obtained from the RTC DNE limit algorithm are AC feasible.

The stability studies, presented in this chapter, demonstrated that the TC solution obtained from the RTC DNE limit algorithm can pass AC feasibility and stability tests. Furthermore, $\sim 66\%$ of TC solutions obtained from the RTC DNE limit algorithm pass the stability check. At the same time, these results show that TC does not deteriorate the system stability; on the contrary, when TC is done properly, it can help to maintain stable operations.

Future work will involve testing of the robust topology control algorithm on real-life test cases along with investigation of the benefits of parallel computation of the robust topology control algorithm.

7.8 Appendix

The presented model is a three-stage robust optimization problem that is reformulated into a two-stage robust optimization problem as shown in Fig. 7.9. The proposed robust optimization problem structure is similar to other robust optimization problems solved in prior literature [70, 103, 104]. One key difference is that the final stage of the proposed DNE limit problem is a linear feasibility problem as compared to a linear optimization programming problem as is the case in [70, 103, 104]. Note that, while our final stage is a linear feasibility problem, the solution approach is not distinct from other work that has a linear optimization problem (a non-zero objective) in the final stage; all linear optimization problems can be converted into a linear feasibility problem that will either produce the global solution to the original problem or say that the original problem is infeasible. This is possible by modeling the linear equality and inequality requirements of primal feasibility,

dual feasibility, and strong duality as these three conditions are both necessary and sufficient for optimality [106]. Thus, any such robust optimization problem that has its final stage as a linear program, that linear program can be transformed into a linear feasibility problem. While the proposed model has a fixed objective for the final stage, it can still return two outcomes: i) either zero stating that there is a feasible solution or ii) infinity stating the problem is infeasible. To adequately capture the appropriate characteristics of the final two stages, which can be interpreted as an attacker-defender (max-min) problem, even though the final stage is a feasibility problem, it still requires to take its dual (step 1 in Fig. 7.9) so that final two stages can merge properly into the one problem (step 4 in Fig. 7.9). This is the same approach as what is seen in [70, 103, 104] as it preserves the desired attacker-defender structure. Simply changing the final stage problem from min 0 to max 0 will not preserve the robust optimization structure; if such a trivial reformulation were otherwise possible, it would also be possible in such work as in [70, 103, 104] as well since all linear programs can be transformed into linear feasibility problems.

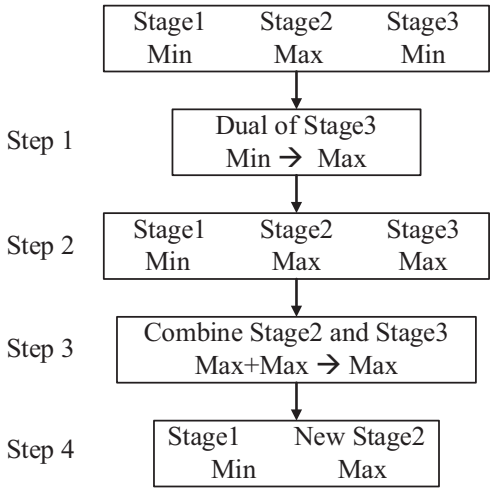

Figure 7.9: Transformation of a three stage robust optimization problem into a two stage robust optimization problem.

The presented robust min-max-min structure, in this chapter, is the appropriate structure to solve the DNE limit problem. This min-max-min structure guarantees the solution feasibility for the entire uncertainty set, i.e., the DNE limits.

Chapter 8

ZONAL DO-NOT-EXCEED LIMITS WITH ROBUST CORRECTIVE TOPOLOGY CONTROL

The penetration of renewable resources in electrical power systems has increased over the years. This increased levels of intermittent resources adds complexities in power system operations. At the Independent System Operator of New England (ISONE), in real-time operation, the renewable resources are integrated into the system using do-not-exceed (DNE) limits. The determination of DNE limits, in real-time, is challenging; to reduce the computational time, approximations are made and mathematical models are simplified. In this chapter, a zonal approach is proposed to determine DNE limits, which reduces the network model into few interlinked zones. The approximations with the zonal approach do not affect the quality of solution to a great extent. However, they reduce the computational time so that the zonal DNE limits approach may be implemented in real-time. The DNE limits determined with the zonal approach are compared with the detail nodal DNE limits on a smaller IEEE-118 bus test case and a realistic system provided by Tennessee Valley Authority (TVA).

8.1 Introduction

As the penetration of stochastic resources (e.g., variable wind and solar power) increases in power systems, the challenge to maintain a continuous supply of electrical energy, at minimal cost, has increased. Traditionally, economic dispatch models, used in system operations, are deterministic and do not optimize system resources while explicitly accounting for uncertain resources. In order to reduce operational costs, while maintaining reliability, uncertainty modeling plays an important role in the decision making process; by

ignoring uncertainty, the operational decision can be suboptimal or even infeasible.

Today, in most optimal dispatch models, conventional fossil-fuel generators are dispatched to a fixed operating point known as desired dispatch point (DDP). In these models, it is assumed that the conventional generators can operate at a fixed operating point for the desired time period. However, this assumption cannot be made for semi-dispatchable or non-dispatchable renewable resources because of their inherent intermittent nature and limited operational control. Therefore, in such cases, system operators instruct renewable power producers to operate within the desired dispatch range, so that these uncertain resources will be at a fixed operating point. At the Independent System Operator of New England (ISONE), this dispatch range is known as a do-not-exceed (DNE) limit for intermittent wind power producers [103]. The DNE limit defines a continuous set of potential dispatch solutions for the renewable resource; this continuous set of dispatch solutions that can be viewed as an uncertainty set. The bounds of the DNE limit are meant to be set such that if the renewable resource stays within the specified DNE limits (i.e., the upper and lower bound), then the system will remain in a secure and reliable operating state [103].

In ISONE's DNE limit formulation, only generators with active automatic generation control (AGC) are considered to respond to intermittencies in wind generation [103]. In real-time application, such approximation is justified because expected uncertainty in renewable generation is relatively smaller in real-time operating state. However, traditionally, AGC is used for load following and addressing small perturbations in system operation. If all available AGC is used to address renewable generation intermittency, additional resources may be required for load following and system perturbations. In [103], details about these additional resource requirements are not presented but these additional resources can be obtained with more frequent and more accurate dispatch instruction to conventional generators or by committing additional generators [107]. Furthermore, in [103], the DNE limits are determined close to real-time operation, where more accurate

information about the quantity and location of AGC is available. However, in day-ahead or hour-ahead timeframe, the AGC based approach restrict the capabilities of DNE limits, as generator output or DDP changes over time due to change in system demand and renewable generation. At the same time, in day-ahead timeframe, accurate determination of AGC, in terms of location and quantity, is difficult and may result in inaccurate DNE limits.

Past research has shown benefits of topology control (TC) for system operation and reliability. Today, most of the TC decisions are determined based on operators' past knowledge or other ad-hoc methods. The review of current TC related industrial practices are discussed in [97] and [24]; furthermore, at PJM, TC actions are included in the transmission manual as corrective solutions for reliable power system operations [96]. In literature, TC has been proposed to mitigate many power system related issues. In [11, 2, 3, 4, 5], TC is used to overcome voltage violations and line overloads; in [6, 7, 91, 14], TC is used for line losses and operational cost reduction. TC is also proposed to improve system security and operational flexibility [97, 8, 19]. TC has shown significant improvement in operational flexibility [97] and cost saving [23, 21, 18, 14]. TC has also shown benefits in transmission planning studies [27].

Robust optimization has shown promising results in recent years to address issues associated with modeling uncertainty and decision making under uncertainty. In [70] and [104], a two-stage robust optimization technique is used to solve the unit commitment problem. Robust optimization deals with the data uncertainty and tries to find an optimal solution considering the worst-case uncertainty realization. The solution of the robust optimization problem is guaranteed to be optimal for a defined uncertainty set [97], [70, 104, 72, 73]. Since the optimal solution is a hedge against the worst-case realization, the solution is often conservative and probably expensive. For the application of power system reliability, such a robust policy is preferred due to the enormous costs of a potential blackout.

In general, TC algorithms are either based on the AC optimal power flow (ACOPF)

or the DC optimal power flow (DCOPF) [97, 11, 91]. However, in a robust optimization framework, there is no simple method to insure AC feasibility of TC actions. The zonal DNE limit formulation, presented in this chapter, is based on DCOPF; therefore, the TC solution, obtained from the zonal DNE limit problem, is tested for the AC feasibility to ensure that the TC action will provide AC feasible operating point.

The main contribution of this chapter is summarized below.

1. Identified the limitations of the DNE limits procedure used by ISONE. The AGC based DNE limit procedure may not be sufficient to determine the DNE limits in day-ahead timeframe. In this chapter, a more generic methodology to determine the DNE limits is presented.

2. Addressed the scalability issue of the robust DNE limit problem. In this chapter, a zonal DNE limit procedure is proposed, over the detailed nodal approach, to determine DNE limits.

3. Formulated the zonal DNE limit problem using robust optimization techniques. The proposed solution method to determine the DNE limits is a two stage process and capable of determining the DNE limits with and without TC.

4. The proposed solution method is tested on two different test systems: the IEEE-118 bus test system and the Tennessee Valley Authority (TVA) system.

5. The TC solution determined using the zonal approach is tested for the AC feasibility. The zonal DNE limit is based on DCOPF formulation. Therefore, the TC solution obtained from the DNE limit algorithm needed to be tested AC feasibility.

The chapter is structured as follows: the zonal DNE limits approach is described in Section 8.2. The clustering method, used in this chapter, to determine system zones is

presented in Section 8.3. The mathematical model for the zonal DNE limit approach is presented in Section 8.4. The solution method for the zonal DNE limit problem is presented in Section 8.5. The associated simulation results for the zonal DNE limit algorithm, on IEEE-118 bus test system is presented in Section 8.6. In Section 8.7, simulation results related to TVA test system are presented. Section 8.8 provides the conclusions and discusses potential future work.

8.2 Zonal DNE Limits

In [103], a procedure to determine real-time DNE limits without TC is presented. At ISONE, the DNE limits are determined, for the real-time application, considering the real-time (5 minutes ahead) dispatch instructions to conventional generators. The real-time DNE limits demands fast solution time, which necessitates to simplify the DNE limit problem and restricts the problem modeling details. In [103], the DNE limit formulation, used at ISONE, is presented, which consists of energy balance constraints, line flow constraints, and generator capacity constraints. However, in actual implementation, to reduce the computational time, only a handful of transmission lines and subsequent nodes are considered. This reduction in the modeling detail reduces the solution time but degrades the solution quality. Furthermore, the transmission lines considered under this formulation are determined based on operators' past knowledge or historical data.

To address the issue of systematically scaling down the system model, from including each node to only a critical node representation, the zonal approach is proposed in this chapter. The benefit of the zonal model is that it helps to reduce the model to few number of zones and associated branches. With this reduced system model, the DNE limits can be determined quickly without degrading the solution quality. In this chapter, to determine the zones, previously investigated clustering method is used [108].

In the zonal approach, the critical buses are represented with the associated zones; each

zone may have multiple buses. After identifying all the zones and their respected nodes, the aggregated level of conventional generation, renewable generation, and system demand at each zone is determined. Only the transmission lines connecting different zones are used in zonal analysis. Therefore, if the number of zones is equal to the number of buses, the resultant zonal structure will be the same as the detailed nodal structure.

8.3 Zonal Approach: Clustering Methods

Traditionally, clustering methods are used to sort big data. In electrical power systems, clustering methods are used to determine reserve zones [108], congestion zones [109], consumer classifications [110], and for additional applications. In [110], different clustering methods used in electrical power systems are studied and evaluated for electricity consumer classifications.

In this chapter, the k-means clustering algorithm is used to determine the zones. The k-means method is a simple clustering method, which attempts to partitions N observations (i.e., buses in this case) into Z clusters (i.e., zones in this case). In [108], power transfer distribution factor (PTDF) differences are used to determine reserve clusters. In this paper, also PTDF difference ($PTDFD$) is used to determine different zones from the nodal information. The PTDF difference between bus i and bus j is represented by (8.1), where K represents the number of transmission lines. The $PTDFD$ represents the difference between the flow on branch k due to a MW injection at bus i and the flow on branch k due to a MW injection at bus j. The PTDF difference provides a metric to group buses together based on their impact on the overall system.

$$PTDFD_{i,j} = \frac{\sum_{k=1}^{K} |PTDF_{k,i}^{R} - PTDF_{k,j}^{R}|}{K} \tag{8.1}$$

Note that the objective of this chapter is to study the effect of the zonal approach over

the nodal DNE limit approach; however, this chapter does not investigate the best clustering procedure to determine different zones. Future work may involve investigating better clustering method to determine zones; for instance, in [108], weighted PTDF difference method is proposed over the PTDF difference method.

8.4 Zonal DNE Limits Model

The basic DNE limit problem is a three stage optimization problem, as shown in (8.2)-(8.16). The objective function for the DNE limit problem is presented in (8.2). The first minimization part of the DNE limit problem is a mixed integer programing (MIP) problem, which determines the system topology and the uncertainty set. The second part of the DNE limit problem choses the worst-case realization of renewable generation from the uncertainty set, determined in the first part of the problem. The last part of the DNE limit problem is an optimal power flow (OPF) problem, which determines the feasibility of the worst-case realization of renewable generation, determined in the second part of the DNE limit problem, with the TC action determined in the first part of the DNE limit problem. The max-min part of formulation forms a robust counterpart (RC) of the DNE limit problem. The co-optimization of the first minimization part of the DNE problem along with the RC determines the maximum range of renewable generation (i.e., the DNE limit), and associated system topology, for a given security constraint unit commitment (SCUC) solution. The formulation for the DNE limit problem is as follows. The node balance constraint is represented by (8.3), the line capacity constraints are represented by (8.4) and (8.5), the TC actions for transmission elements are modeled as shown in (8.6) and (8.7), the generator ramp rate constraints are represented by (8.8) and (8.9), and the generator capacity constraints are represented by constraints (8.10) and (8.11). The deviation in renewable generation is determined using constraint (8.12). The uncertainty set, W, is defined by (8.13). In this formulation, the node balance constraint and line capacity constraints are

relaxed to achieve the feasibility of RC problem and the relaxation is penalized in the RC objective using parameter δ. Furthermore, the objective of this research is not to determine true value of δ; for simplicity, in this research, value of δ is set 1. Determining the true value of δ can be included in potential future work.

$$\min \left((P_w^{LP} - P_w^{UP}) + \max_{P_w \in \mathcal{W}} \ \min \delta [\sum_{\forall n} (L_n^+ + L_n^-) + \sum_{\forall k} (\gamma_k^+ + \gamma_k^-)] \right) \tag{8.2}$$

$$\text{s.t.} \sum_{k \in \delta(n)^+} P_k - \sum_{k \in \delta(n)^-} P_k + \sum_{\forall g(n)} P_g + \sum_{\forall w(n)} P_w \tag{8.3}$$

$$+ L_n^+ - L_n^- = d_n, \ \forall n$$

$$- \gamma_k^+ + P_k \leq P_k^{max} Z_k, \ \forall k \tag{8.4}$$

$$- \gamma_k^- - P_k \leq P_k^{max} Z_k, \ \forall k \tag{8.5}$$

$$P_k - B_k(\theta_n - \theta_m) + (1 - Z_k) M_k \geq 0, \ \forall k \tag{8.6}$$

$$P_k - B_k(\theta_n - \theta_m) - (1 - Z_k) M_k \leq 0, \ \forall k \tag{8.7}$$

$$P_g \leq R_g^{+c} + P_g^*, \ \forall g \tag{8.8}$$

$$- P_g \leq R_g^{-c} - P_g^*, \ \forall g \tag{8.9}$$

$$P_g \leq P_g^{max} u_g, \ \forall g \tag{8.10}$$

$$- P_g \leq -P_g^{min} u_g, \ \forall g \tag{8.11}$$

$$P_w^{min} \leq P_w^{LB} \leq P_w^* \leq P_w^{UB} \leq P_w^{max}, \ \forall w \tag{8.12}$$

$$P_w^{LB} \leq P_w \leq P_w^{UB}, \ \forall w \tag{8.13}$$

$$L_n^+, L_n^- \geq 0, \ \forall n \tag{8.14}$$

$$\gamma_k^+ \gamma_k^- \geq 0, \ \forall k \tag{8.15}$$

$$Z_k \in \{0, 1\} \tag{8.16}$$

The DNE limit problem, presented in (8.2)-(8.16), is for a zonal representation; however, the same formulation can be used for a nodal representation, considering each zone as a single node. Furthermore, the formulation presented in (8.2)-(8.16) can be represented in a generic form as shown in (8.17) and (8.18). In (8.17), c represents the cost associated with the first stage decision variable and b represents the cost associated with the second stage decision variable. System data is represented by parameters $A, B, C, D, E, F, H, J, L, P$.

$$\min_{x \in X} \left(c^T x + \max_{w \in W} \min_{y \in Y} b^T y \right) \tag{8.17}$$

$$\text{s.t.} Ax \leq B, Cy \leq D, Ex + Fy \leq H, Jy + Lw = P. \tag{8.18}$$

A systematic procedure to transform a three stage robust optimization problem into a two stage problem is presented in [97]. The RC part of the DNE limit formulation, i.e., max-min part of (8.17), consists of two linear programming (LP) problems. These two LP problems can be transformed into an optimization single problem by formulating the dual of OPF problem (i.e., minimization part of RC) and combining with the maximization part of RC. The resultant two stage robust formulation, for the DNE limit problem, is presented in (8.19) and (8.21), where minimization part of problem is known as a master problem and the maximization part of problem is known as a sub-problem. The master problem determines the range of renewable generation, i.e., the DNE limits, and associated TC action. The sub-problem is a RC of DNE limit formulation, which determines the worst-case violation associated with the renewable generation range and the TC action chosen in master problem. By co-optimizing the master and the sub-problem together the robust DNE limits can be found. The detail formulation of the master problem and the sub-problem is presented in Section 8.5. Note that, in (8.19), the term $\zeta^T Lw$ makes the objective function nonlinear; therefore, to overcome this nonlinearity, different methods have been proposed in prior literature. In [70], the outer approximation based approach is used to overcome

nonlinearity in the robust optimization problem; in [97], a big-M method is suggested to overcome the nonlinearity. This thesis also, for a zonal DNE limit formulation, a big-M method is used to overcome the nonlinearities in the sub-problem.

$$\min_{x \in X} c^T x + \max_{w,\mu,\lambda,\zeta} \lambda^T (Ex - H) - \mu^T D + \zeta^T (P - Lw) \tag{8.19}$$

$$\text{s.t.} Ax \leq B, -\mu^T C - \lambda^T F + \zeta^T J = b \tag{8.20}$$

$$\mu \geq 0,\ \lambda \geq 0,\ w \in W. \tag{8.21}$$

8.5 Zonal DNE Limits: Solution Method

In section 8.4, a generic robust optimization based DNE limit problem is presented, where the master problem is a mixed integer programming (MIP) problem and the sub-problem is a nonlinear problem. Furthermore, using a big-M formulation technique, the nonlinearity in the sub-problem is removed by reformulating the sub-problem into a MIP problem.

Initialization: It is assumed that the SCUC problem is solved prior to solving the DNE limit problem. The solution of SCUC problem, such as generator status and associated dispatch, is used as an input parameter to the DNE limit algorithm.

Stage-1 (master problem): The master problem is a MIP problem, which determines the range of renewable generation (i.e., the DNE limits) and its associated system topology (i.e., the TC action). The master problem, presented in (8.22)-(8.44), consists of four sections. The DNE section determines the deviation in renewable generation, the O^{lb} section considers the power flow under the lowest renewable generation realization, the O^{ub} section considers the power flow under the highest renewable generation realization, and the topology control actions are controlled by section TC. The DNE section determines the maximum range of renewable generation and is represented by (8.23). The O^{lb} section

consists of generator ramping constraints (8.25) and (8.26), generator capacity constraints (8.27) and (8.28), line flow constraints (8.29) and (8.30), line capacity constraints (8.31) and (8.32), and node balance constraint (8.33). Similarly, the O^{ub} section consists of constraints (8.34)-(8.42). In section TC, in constraint (8.43), the number of simultaneous TC actions are controlled by parameter M. In this chapter only one simultaneous TC action is considered for the analysis; therefore, M is set to 1. Note that the master problem can be formulated excluding the O^{lb} and O^{ub} sections. However, in that case, the number of iterations between the master problem and the sub-problem may increase. Furthermore, the master problem is an optimality problem which determines the renege of renewable generation and the associated TC action. The solution of master problem, i.e., P_w^{lb}, P_w^{ub} and Z_k are passed on to the sub-problem.

$$\min_{P_w^{lb},P_w^{ub},\phi,Z_k} \sum_{\forall w}(P_w^{LP} - P_w^{UP}) + \phi \tag{8.22}$$

s.t.

$$DNE: P_w^{min} \leq P_w^{lb} \leq P_w^* \leq P_w^{ub} \leq P_w^{max},\ \forall w \tag{8.23}$$

$$\phi \geq \sum_{\forall k} Z_k P_k^{max}(F_{k,l}^+ + F_{k,l}^-) + \sum_{\forall k}(1 - Z_k)M_k(S_{k,l}^+ + S_{k,l}^-) \tag{8.24}$$
$$+ \sum_{\forall n}(d_n - \sum_{\forall w(n)}(\zeta_{n,l}P_w^{uB} + (1-\zeta_{n,l})P_w^{lB}))\lambda_{n,l} + \sum_{\forall g}(P_g^* + R_g^{+c})\Omega_{g,l}^+$$
$$+ \sum_{\forall g}(R_g^{-c} - P_g^*)\Omega_{g,l}^- + \sum_{\forall g} u_g(P_g^{max}\alpha_{g,l}^+ - P_g^{min}\alpha_{g,l}^-),\ \forall l \in cut$$
$$\phi \geq 0$$

$$O^{lb}: P_g^{lb} \leq R_g^{+c} + P_g^*,\ \forall g \tag{8.25}$$

$$-P_g^{lb} \leq R_g^{-c} - P_g^*,\ \forall g \tag{8.26}$$

$$P_g^{lb} \leq P_g^{max} u_g,\ \forall g \tag{8.27}$$

$$-P_g^{lb} \leq -P_g^{min} u_g,\ \forall g \tag{8.28}$$

$$P_k^{lb} - B_k(\theta_n^{lb} - \theta_m^{lb}) + (1 - Z_k)M_k \geq 0,\ \forall k \tag{8.29}$$

$$P_k^{lb} - B_k(\theta_n^{lb} - \theta_m^{lb}) - (1 - Z_k)M_k \leq 0,\ \forall k \tag{8.30}$$

$$P_k^{lb} \leq P_k^{max} Z_k,\ \forall k \tag{8.31}$$

$$-P_k^{lb} \leq -P_k^{max} Z_k,\ \forall k \tag{8.32}$$

$$\sum_{k \in \delta(n)^+} P_k^{lb} - \sum_{k \in \delta(n)^-} P_k^{lb} + \sum_{\forall g(n)} P_g^{lb} + \sum_{\forall w(n)} P_w^{lb} = d_n,\ \forall n \tag{8.33}$$

$$O^{ub}: P_g^{ub} \leq R_g^{+c} + P_g^*,\ \forall g \tag{8.34}$$

$$-P_g^{ub} \leq R_g^{-c} - P_g^*,\ \forall g \tag{8.35}$$

$$P_g^{ub} \leq P_g^{max} u_g,\ \forall g \tag{8.36}$$

$$-P_g^{ub} \leq -P_g^{min} u_g,\ \forall g \tag{8.37}$$

$$P_k^{ub} - B_k(\theta_n^{ub} - \theta_m^{ub}) + (1 - Z_k)M_k \geq 0,\ \forall k \tag{8.38}$$

$$P_k^{ub} - B_k(\theta_n^{ub} - \theta_m^{ub}) - (1 - Z_k)M_k \leq 0,\ \forall k \tag{8.39}$$

$$P_k^{ub} \leq P_k^{max} Z_k,\ \forall k \tag{8.40}$$

$$-P_k^{ub} \leq -P_k^{max} Z_k,\ \forall k \tag{8.41}$$

$$\sum_{k \in \delta(n)^+} P_k^{ub} - \sum_{k \in \delta(n)^-} P_k^{ub} + \sum_{\forall g(n)} P_g^{ub} + \sum_{\forall w(n)} P_w^{ub} = d_n,\ \forall n \tag{8.42}$$

$$TC: \sum_{\forall k} (1 - Z_k) \leq M \tag{8.43}$$

$$Z_k \in \{0, 1\} \tag{8.44}$$

Stage-2 (sub-problem): The sub-problem is a RC of zonal DNE limit problem and it is presented in (8.45)-(8.56), where, $\lambda_n, F_k^+, F_k^-, S_k^+, S_k^-, \Omega_g^+, \Omega_g^-, \alpha_g^+, \alpha_g^-$ are dual variables

of (8.3)-(8.11). The sub-problem is a nonlinear optimization problem, with a nonlinear (bilinear) term in the objective function, as shown in (8.19). This nonlinearity in the (8.19) is removed, by using big-M formulation [97], as shown in (8.45), (8.49)-(8.52). Note that the sub-problem is an optimality problem and the solution is always feasible due to relaxation of the OPF problem.

$$\max \sum_{\forall n} \eta_n + \sum_{\forall k} Z_k P_k^{max}(F_k^+ + F_k^-) + \sum_{\forall g}(P_g^* + R_g^{+c})\Omega_g^+ \tag{8.45}$$
$$+ \sum_{\forall g}(R_g^{-c} - P_g^*)\Omega_g^- + \sum_{\forall k}(1 - Z_k)M_k(S_k^+ + S_k^-)$$
$$+ \sum_{\forall g} u_g(P_g^{max}\alpha_g^+ - P_g^{min}\alpha_g^-)$$

$$\text{s.t. } -S_k^+ + S_k^- + F_k^+ - F_k^- + \lambda_n - \lambda_m = 0,\ \forall k \tag{8.46}$$

$$\Omega_g^+ - \Omega_g^- + \lambda_n + \alpha_g^+ - \alpha_g^- = 0,\ \forall g \tag{8.47}$$

$$\sum_{\delta(n)^+} B_k(S_k^+ - S_k^-) + \sum_{\delta(n)^-} B_k(S_k^- - S_k^+) = 0, \forall n \tag{8.48}$$

$$\eta_n - (d_n - \sum_{\forall w(n)} P_w^{ub})\lambda_n + (1 - \zeta_n)M_n \geq 0\ \forall n \tag{8.49}$$

$$\eta_n - (d_n - \sum_{\forall w(n)} P_w^{ub})\lambda_n - (1 - \zeta_n)M_n \leq 0\ \forall n \tag{8.50}$$

$$\eta_n - (d_n - \sum_{\forall w(n)} P_w^{lb})\lambda_n + \zeta_n M_n \geq 0\ \forall n \tag{8.51}$$

$$\eta_n - (d_n - \sum_{\forall w(n)} P_w^{lb})\lambda_n - \zeta_n M_n \leq 0\ \forall n \tag{8.52}$$

$$\lambda_n \leq \delta,\ \forall n \tag{8.53}$$

$$-\lambda_n \leq \delta,\ \forall n \tag{8.54}$$

$$-F_k^+ \leq \delta,\ \forall k \tag{8.55}$$

$$-F_k^- \leq \delta,\ \forall k \tag{8.56}$$

$$F_k^+, F_k^-, S_k^+, S_k^- \leq 0, \ \forall k \tag{8.57}$$

$$\Omega_g^+, \Omega_g^-, \alpha_g^+, \alpha_g^- \leq 0, \ \forall g \tag{8.58}$$

$$\zeta_n \in \{0, 1\} \tag{8.59}$$

A detailed solution method for the zonal DNE limits problem is presented in Fig. 8.1. The threshold value for the termination condition is set to zero. The solution of the master problem, determined based on the day-ahead SCUC solution, is passed on to the sub-problem. The sub-problem determines the worst-case violation associated with the renewable generation range and the TC action, chosen in the master problem. If the worst-case violation is within the threshold value, which indicates that there is no realization within the renewable generation range with TC that will cause power flow violations, the solution method will terminate as the robust DNE limits with TC have been obtained. If the worst-case violation is more than the threshold value, an optimality cut in form of (8.24) will be added into the master problem and resolved. This case indicates that there is a renewable generation realization, within the chosen renewable generation operating range with TC, which will cause infeasibility in the OPF problem and may result in power flow violations. Thus, the resultant DNE limits are not robust and the master problem is resolved with the added optimality cut in form of (8.24). This two stage solution method is similar to Benders' decomposition algorithm.

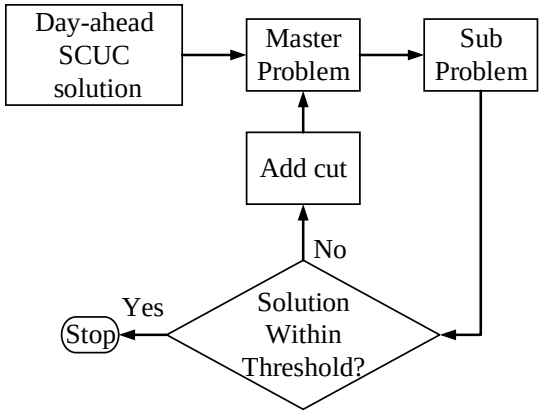

Figure 8.1: Algorithm to Solve the Zonal DNE Limit Problem.

The benefit of this solution method is that the master problem is simplified by using O^{lb} and O^{ub} structure, which results in less number of iterations and an improved solution time.

8.6 Numerical Results: IEEE-118 Bus Test Case

The IEEE-118 bus test case, consists of 186 branches, 71 conventional generators, and 9 wind injection locations with a peak demand of 4004MW. The branch data is given [87]; however, the conventional generation information for the IEEE-118 bus test system is not available. Hence, the generator mix of reliability test system 1996 is used to create conventional generator data for the IEEE-118 bus test case [87]. The load profile and wind forecast is obtained from California Independent System Operator (CAISO) duck chart [99].

The SCUC solution is used as a starting point for all the simulations presented in this chapter. A 24 hour SCUC problem is solved; the basic SCUC model and the fuel costs, given in [14], are used to calculate generator operating costs. The reserve requirements for the SCUC are modeled as sum of 5% of demand supplied by conventional generators and 10% of demand supplied by wind units or the single largest contingency, whichever is greater. On top of that, at least 50% of total required reserves will be supplied by spinning

reserves and the rest will be supplied by non-spinning reserves. A similar assumption is cited in CAISO's guidelines for spinning reserve and non-spinning reserve [59].

To determine zones from the k-mean clustering method, for zonal DNE limits, different clustering strategies are evaluated. On the IEEE-118 bus test case, zones are determined using different zoning strategies and evaluated, against the quality of the DNE limits obtained, with respect to accurate nodal DNE limits. In this chapter, different zoning strategies such as zones based on load centers, renewable injection locations, fossil-fuel based generation injection location, and combinations of these are evaluated. It is observed that the zonal DNE limits, based on renewable injection location along with fossil-fuel based injection location providing spinning reserve produces better quality zonal DNE limits. This observation can be justified as the uncertainty in renewable generation is addressed by changing DDPs of fossil-fuel based generators. Therefore, considering location of uncertainty and location of responding uncertainty together may give better results than considering each of them independently. Hence, in this chapter, all the zonal DNE limits are calculated based on zones determined using renewable injection location along with fossil-fuel based injection location.

Furthermore, the benefit of having maximum one wind injection location per zone, due to adopted clustering strategy, simplifies the problem of the DNE limit sharing within the zone. Multiple wind injection locations per zone imposes question of determining true DNE limits of each wind injection location for the zonal DNE limit solution. By allowing only one wind injection location per zone, this DNE limit sharing problem can be eliminated.

8.6.1 DNE limits without TC

The DNE limits obtained without TC using the nodal and the zonal approach are presented in Fig. 8.2. The zonal DNE limits are determined with 21 zones. In this case,

the upper bound of DNE limits obtained from the zonal approach is always greater than or equal to the upper bound of DNE limits obtained from the nodal DNE limits approach. This is an anticipated result as the zonal approach is an approximation of the nodal approach; therefore, the solution obtained from the zonal approach will not be better off than the solution obtained from the nodal approach. Furthermore, the lower bound obtained from the zonal approach is close to the lower bound obtained from the nodal approach.

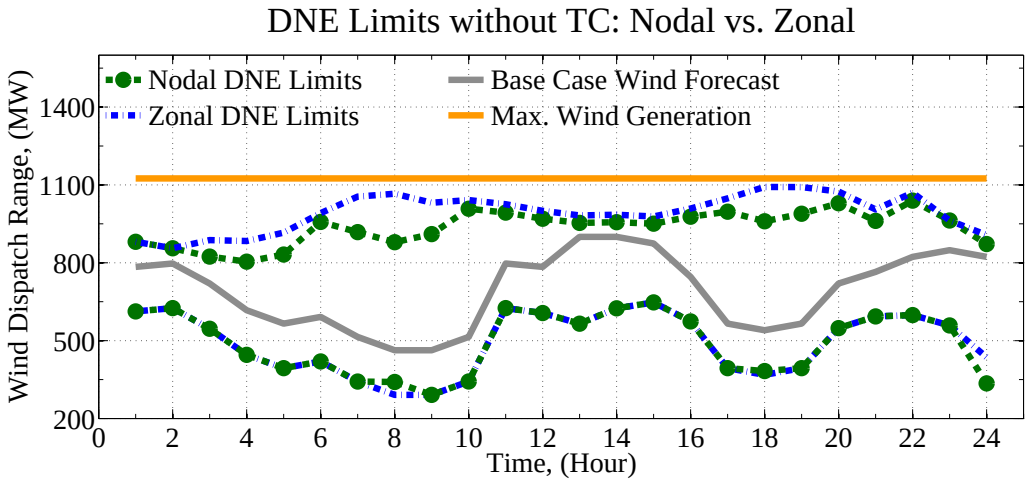

Figure 8.2: Comparison of DNE Limits on IEEE-118 Bus Test Case Without Topology Control.

Fig. 8.3 shows the average error, over 24 hours, between solutions obtained from the zonal approach and the nodal approach, for different number of zones. With an increase in number of zones the average error in the zonal DNE limit calculations (compared with nodal DNE limit solution) decreases. However, the decrease in the average error in DNE limit calculation is not monotonic in nature; for instance, the average error increases by 2% from DNE limits determined with 18 zones over 19 zones. Furthermore, the maximum error in the zonal DNE limit calculation decreases with increase number of zones; the maximum error in DNE limit calculation decreases from $\sim$320 MW to $\sim$130 MW with

increase in number of zones from 10 to 21. This decrease in maximum error is due to the increase in modeling details with higher number of zones. Furthermore, in this particular test case, the maximum error occurs in hour 8 of DNE limit calculation. Note that in this analysis, the first 9 zones are based on renewable injection locations; the consecutive zones are determined considering the maximum spinning reserve supplied by the fossil-fueled generators.

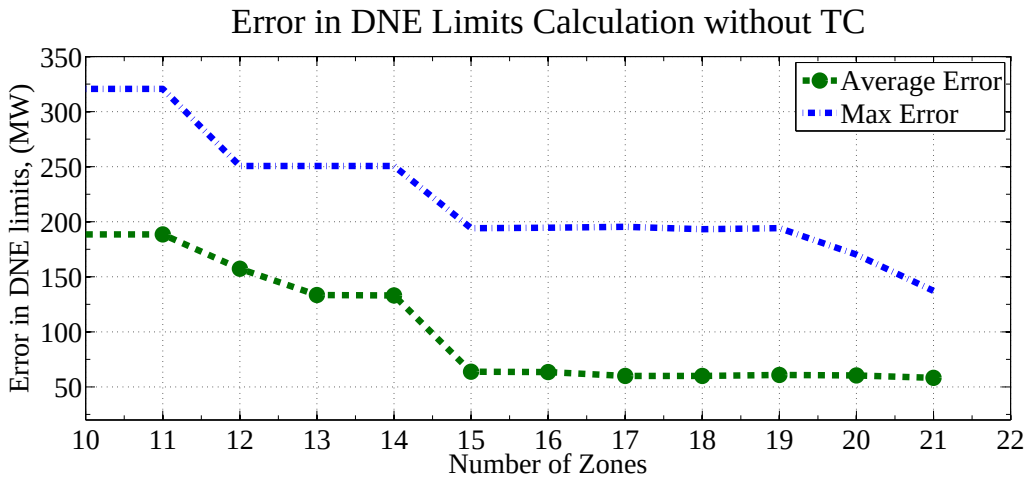

Figure 8.3: Error in DNE Limits on IEEE-118 Bus Test Case Without Topology Control.

8.6.2 DNE limits with TC

The DNE limits obtained with TC using the nodal and the zonal approach is presented in Fig. 8.4. The zonal DNE limits are determined with 21 zones. For the zonal approach, the DNE limits obtained with TC are greater or at least equals to the DNE limits determined without TC action. Furthermore, due to limited modeling details, in hours 1, 2, and 12-16, the upper bound of DNE limits determined with the zonal approach is lower than the upper bound of DNE limits determined with the nodal approach. In the zonal approach, only branches connecting different zones are considered; therefore, in the zonal DNE limit approach, the possible TC actions are also limited, which subsequently restricts the DNE

limits. Furthermore, the lower bound of DNE limits obtained with the zonal approach is close to the lower bound of DNE limits obtained with the nodal approach. Note that the zonal DNE limits, presented in Fig. 8.4, are determined with the same 21 zones used to determine the zonal DNE limits in Fig. 8.2.

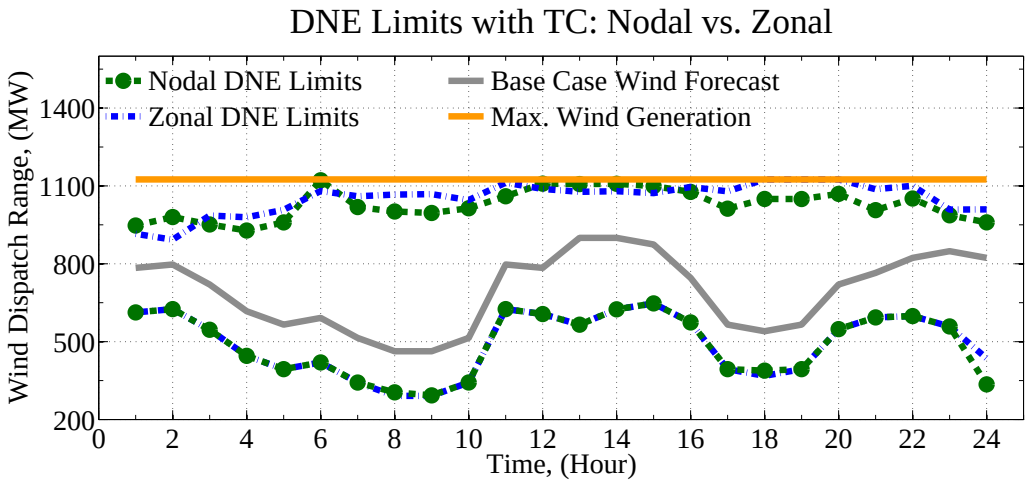

Figure 8.4: Comparison of DNE Limits on IEEE-118 Bus Test Case With Topology Control.

Fig. 8.5 shows the average error with TC, over 24 hours, between solutions obtained from the zonal approach and the nodal approach, for different number of zones. Over 24 hours, with increase in number of zones, the average error in the zonal DNE limit with TC decreases from 197MW per hour to 112MW per hour. Furthermore, the average error in the zonal DNE limits calculation with TC is lower than the average error in the zonal DNE limits calculation without TC. With TC the average error in zonal DNE limits is between 100-50 MW per hour; however, the average error in zonal DNE limits without TC is between 180-55 MW per hour.

The total difference between the DNE limits determined with the zonal approach (21 zones) and the nodal approach is $\sim$4-12%, as shown in Table 8.1. The computational time

needed to solve the DNE limits problem, for entire 24 hours, with the zonal approach is ∼75-93% lower than the computational time required for the nodal approach. With the zonal approach, the equivalent system size can be reduced by ∼65-82% as compared with detailed nodal representation of the system.

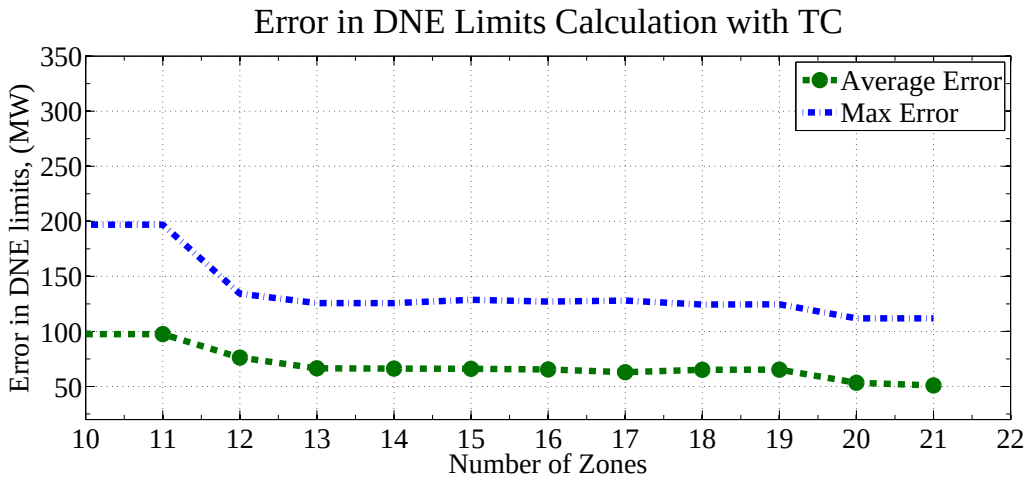

Figure 8.5: Error in DNE Limits on IEEE-118 Bus Test Case With Topology Control.

Table 8.1: Comparison of DNE Limits Obtained with the Zonal and the Nodal Approaches on the IEEE-118 Bus Test Case

	Nodal DNE Limits	Zonal DNE Limits	Difference
DNE Limits without TC (MW)	10674	11998	12.4%
DNE Limits with TC (MW)	13444	12883	4.17%
Computational time without TC (sec.)	33	8	75.75%
Computational time with TC (sec.)	200	13	93.5%
Number of buses	118	21	82.2%
Number of branches	186	64	65.6%

The TC solutions, determined with the zonal approach, are tested for the AC feasibility on the detail nodal model to observe the capability of the zonal approach to produce AC feasible solution at base case. For the IEEE-118 bus test case, $\sim 80\%$ zonal TC solution have produced AC feasible solution. These results are critical from operational point of view, as it fills the gap between DCOPF based optimization framework solutions to the real AC operating state. For example, in practice solutions obtained from optimization algorithms based on DCOPF formulation, which could not produce AC feasible solutions are discarded. However, the zonal DNE limit algorithm is capable of producing AC feasible TC solutions.

8.7 Numerical Results: TVA Test System

The TVA test system consists of 1779 buses, 1708 transmission lines, 321 traditional generators, 299 two-winding transformers, 98 three-winding transformers, and 178 switchable shunts. The TVA test system data does not have wind generation information; therefore, for analysis purposes, 10 different wind injection locations are considered. The wind forecast is obtained from the NERL western wind resource database, profile case$\#12514$ for 20^{th} December 2005 [105]. A 24-hour SCUC model is solved to provide a starting solution for the DNE limit problem. The SCUC model uses the same reserve rules as what was used within the IEEE-118 bus test case. For the TVA test system, the DNE limits with TC using the zonal approach (with 72 zones) and the nodal approach are presented in Fig. 8.6. For this analysis the same zoning strategy, used for the IEEE-118 bus test system, is utilized. Table 8.2 presents a comparison between the zonal and the nodal DNE limit approaches. The zonal-based DNE limits determined are approximately equals to the nodal-based DNE limits; the difference between the zonal and the nodal DNE limits approaches is $\sim 1.64\%$. The computational time for the zonal approach is significantly lower than the computational time required for the nodal approach; the zonal method requires only 0.81%

of computational time compared with the nodal method. With the zonal approach, the equivalent system can be reduced to $\sim$5-10% of its original nodal representation.

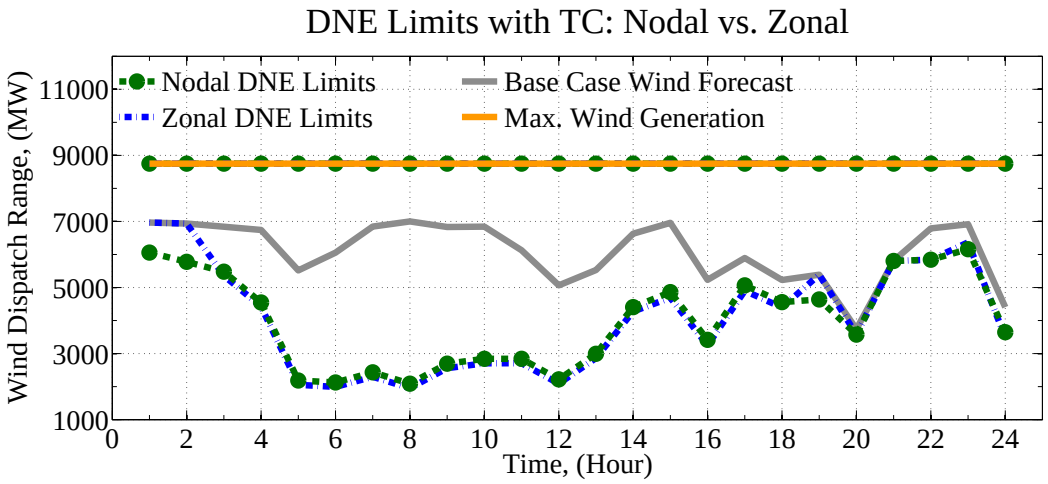

Figure 8.6: Comparison of DNE Limits on TVA Test System With Topology Control.

Table 8.2: Comparison of DNE Limits Obtained with the Zonal and the Nodal Approaches on the TVA Test System

	Nodal DNE Limits	Zonal DNE Limits	Difference
DNE Limits without TC (MW)	90538	96892	7.02%
DNE Limits with TC (MW)	113742	111882	1.64%
Computational time without TC (sec.)	735	25	96.60%
Computational time with TC (sec.)	4685	38	99.19%
Number of buses	1779	72	95.95%
Number of branches	2301	210	90.87%

The average error with TC between solutions obtained from the zonal approach and the nodal approach, with reference to different number of zones, for the TVA test system

is shown in Fig. 8.7. From Fig. 8.7, over 24 hours, with increase in number of zones, the average error in the zonal DNE limit decreases from 658MW per hour to 202MW per hour. Subsequently, the maximum error in the zonal DNE limit solution and the nodal DNE limit solution also decreases from 2195MW to 907MW. Furthermore, the decrease in the average error and the maximum error in the DNE limit calculation is not monotonic in nature with the increase in number of zones as shown in Fig. 8.7. Similar average error analysis without TC, between solutions obtained from the zonal approach and the nodal approach, is performed on the TVA test system. Over 24 hours, with increase in number of zones, the average error in the zonal DNE limit without TC decreases from 562MW per hour to 287MW per hour. Subsequently, the maximum error in the zonal DNE limit solution without TC and the nodal DNE limit solution without TC also decreases from 3832MW to 1633MW. This analysis shows that TC helps to reduce the error in the zonal DNE limits calculation.

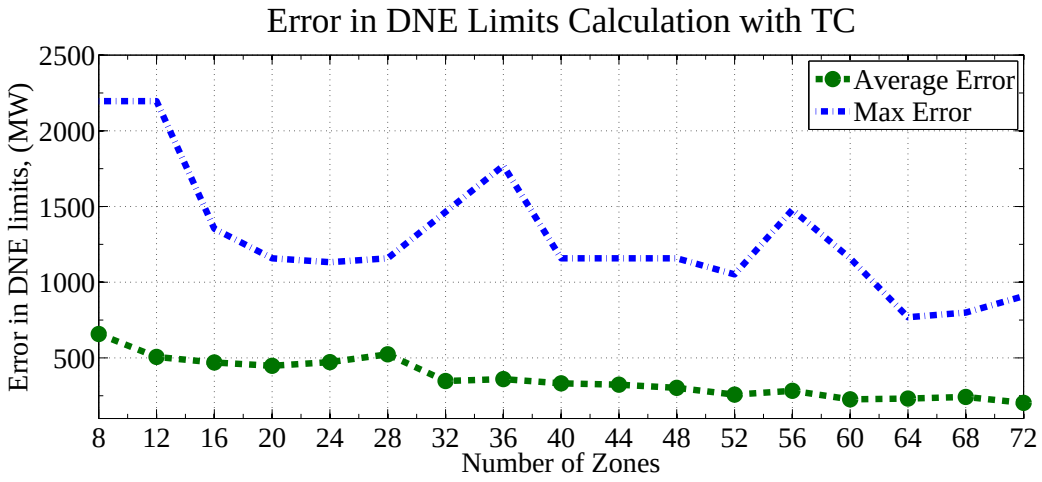

Figure 8.7: Error in DNE Limits on TVA Test System With Topology Control.

The TC solutions, determined with the zonal approach, are tested for the AC feasibility on the detail nodal model to observe the capability of the zonal approach to produce AC

feasible solution. For the TVA test system, $\sim 85\%$ zonal TC solution have produced AC feasible solution. These results demonstrate the critical operational benefits of the zonal DNE limits approach.

8.8 Conclusion

The increased levels of intermittent renewable resources adds complexities to power system operations. Unlike fossil-fuel generators, renewable generators are not dispatchable to DDPs; therefore, intermittent renewable generators are dispatched based on an operating range, known as a DNE limit. Accurate DNE limits are critical for power system operations. The DNE limit procedure, proposed by ISONE, determines DNE limits for real-time application using AGCs; however, same procedure may not be used to determine DNE limits in day-ahead time frame. This chapter provides a systematic approach to determine DNE limits in day-ahead time frame.

In this chapter, the zonal DNE limit methodology is presented, which systematically reduces the system size and determines the DNE limits. The error in DNE limits obtained from the zonal method and the nodal method is $\sim$2-12%. Furthermore, the computational time reduces by $\sim$75-99% with the zonal DNE limit formulation. This chapter also addresses the scalability issue of the DNE limit problem, which is critical for real life applications and fast solution time. The DNE limit results, on TVA system, shows that with 5-10% of modeling information $\sim$98% accurate solutions can obtained with less than 1% computation time. This result shows the benefit of the zonal formulation. The tread off between the computational and the accuracy shows the potential of the zonal formulation and application in determining DNE limits. Furthermore, the TC solution, obtained from the zonal DNE limit algorithm, is capable of producing AC feasible operating state. $\sim$80-85% of TC solutions obtained from the zonal DNE limit algorithm can produce AC feasible solution.

The zonal methodology, presented in this chapter, is not limited only to the DNE limit calculation. The zonal methodology can be used to address scalability of other power system operational problems. For instance, potential future work may involve developing the zonal methodology for planning studies and SCUC problem. The future work may also involve investigating the locational aspect of the renewable injection location and developing a methodology to address the correlation between different renewable generation locations.

Chapter 9

SCALABILITY OF TOPOLOGY CONTROL ALGORITHMS: HEURISTICS APPROACH

9.1 Motivation

Robust topology control methodology, presented in Chapter 4, is tested on an IEEE-118 bus test case, which consists of 54 generators, 118 buses, and 186 transmission lines. This test system is much smaller than any realistic test case, for example, the PJM system is consists of 1375 generators, $62,556$ miles long transmission network and peak demand of $183,604$ megawatts [111]. Therefore, for any practical implementation, the robust topology control methodology must scale from IEEE-118 bus test case to much larger test system.

The master problem, presented in Chapter 6, Section 6.5, is a MIP problem with a combinatorial cut to determine the system topology. However, combinatorial cut is computationally inefficient, may lead to many iterations between the master problem and the sub-problem, which will increase the computational time and/or the master problem will become so big that it will be even infeasible to solve. To overcome this issue, topology control heuristic, presented in [19], is proposed to replace the master problem. The topology control heuristics is based on a sensitivity analysis and provides the topology control solutions in terms of a ranking list. This ranking list will be further used as a chosen topology control action and will be evaluated for its robustness properties in a sub-problem. The detail analysis of topology control heuristic is presented in Section 9.2, where accuracy and effectiveness of heuristic to identify correct topology control action is tested on 2383 bus Polish test system.

9.2 Performance of AC and DC Based Topology Control Heuristics

Traditionally, the transmission network is considered as a passive system and generation was optimized assuming a fixed transmission topology. The concept of dispatchable transmission was introduced in [20], which proposed a paradigm shift in the way the transmission topology is viewed. As a result, optimal topology control (OTC) was developed to harness the benefits of co-optimizing generation with transmission topology [91, 21]. Previous research shows that OTS would result in significant cost savings even under reliability constraints [18, 14]. Transmission switching has other applications, such as reliability improvement via corrective switching [97].

Binary variables representing the status of transmission lines make OTC a mixed-integer program problem. Real world power systems have thousands of transmission lines making the resulting OTC MIP a computationally expensive problem. Since the available computational time is limited, an MIP based implementation of OTC in day-ahead and real-time procedures is not practical. An alternative to solving the full MIP is the use of switching heuristics to obtain a good, suboptimal solution significantly faster. The MIP-heuristic introduced in [23] allows only one switching at a time, reducing the number of binary variables to one per iteration. This would significantly reduce the complexity of the problem. However, the formulation still requires mixed integer programming, which may still be too computationally challenging for certain applications that require fast solutions. There are other heuristics proposed in the literature, which only need the results of the original OPF. A DC-based heuristic is introduced in [81, 80], which ranks the lines based on their economic value. The lines value, or the congestion rent of a single line, is the price difference at the two ends of the line multiplied by the flow it carries [112]. The calculations are based on the results of a DCOPF. This will be referred to as the 'DC heuristic'. A similar heuristic is derived based on an ACOPF [113], which will be referred to as the

'AC heuristic'. In addition to the real power value of the line, the AC heuristic takes into account the reactive power and losses. The results obtained from the heuristics in small scale test cases show that they perform relatively well [112].

In this section, these heuristics are tested to see if they perform well for a large-scale test case, the Polish system. The mathematical representations of the heuristics are presented briefly in the next section. The results suggest that the heuristics are not very different and the inclusion of losses and reactive power does not have a significant impact. This finding is in line with the conclusions made in [113], stating that the heuristics would be significantly different if the system was voltage constrained. The results also show that the best solutions are among the top twenty candidates identified by the heuristics. However, the correlation between the estimated and actual benefits from switching is not very strong.

9.2.1 Methodology

In this section, MATPOWER, a MATLAB based open sources power system simulation package, is used to solve the OPF problems [114, 115]. The detailed formulation and solution method for ACOPF and DCOPF problem is provided in [115]. Here, brief descriptions of AC as well as DCOPF formulations are presented. The ACOPF problem can be represented as shown in (9.1)-(9.10), with an objective function presented in (9.1). The upper bound on AC line flow equations are provided in (9.2), The real and reactive power flow across the transmission line k is represented by (9.3) and (9.4) respectively, the node balance constraints for real and reactive power are represented by (9.5) and (9.6). Note that the dual variables for node balance constraints, λ_{Pn} and λ_{Qn}, represent the active and reactive power locational marginal prices (LMP). Constraints (9.7)-(9.10) represent the lower and upper bounds on variables.

$$\min \sum_{\forall g} c_g P_g \tag{9.1}$$

$$\text{s.t. } P_k^2 + Q_k^2 \leq S_k^2, \forall k \tag{9.2}$$

$$P_k = V_m^2 G_k - V_m V_n (G_k \cos(\theta_m - \theta_n) + B_k \sin(\theta_m - \theta_n)), \forall k \tag{9.3}$$

$$Q_k = -V_m^2 B_k - V_m V_n (G_k \sin(\theta_m - \theta_n) - B_k \cos(\theta_m - \theta_n)), \forall k \tag{9.4}$$

$$\sum_{\forall k \in \delta(n)^+} P_k - \sum_{\forall k \in \delta(n)^-} P_k + \sum_{\forall g(n)} P_g = d_n, \forall n \tag{9.5}$$

$$\sum_{\forall k \in \delta(n)^+} P_k - \sum_{\forall k \in \delta(n)^-} P_k + \sum_{\forall g(n)} P_g = d_n, \forall n \tag{9.6}$$

$$P_g^{min} \leq P_g \leq P_k^{max}, \forall g \tag{9.7}$$

$$Q_g^{min} \leq Q_g \leq Q_k^{max}, \forall g \tag{9.8}$$

$$V_n^{min} \leq V_n \leq V_n^{max}, \forall g \tag{9.9}$$

$$\theta^{min} \leq \theta_n - \theta_m \leq \theta^{max}, \forall k \tag{9.10}$$

Using the ACOPF formulation presented, the sensitivity of the objective function to a marginal change in the status of a transmission line is calculated in [113]. This metric is used as a heuristic to estimate the benefits of switching the line. The heuristic is shown in (9.11),

$$LV_{AC} \quad = \quad P_{km}\lambda_{Pm} - P_{kn}\lambda_{Pn} + Q_{km}\lambda_{Qm} - Q_{kn}\lambda_{Qn}, \forall k \tag{9.11}$$

In this research, we refer to the method that ranks lines based on (9.11) as the AC Heuristic. The metric represents the economic value of the line, which equals the revenue collected from the sale of power at the importing end minus the cost of buying power at the exporting end, considering losses and reactive power. AC heuristic considers the negative of the line value, suggesting that a line with a larger negative economic value is a potential

switching candidate. It is not expected that the heuristic estimates match the actual benefits accurately, because the change in the status of the line is not marginal.

With the well-known assumptions of DC power flow, the ACOPF formulated in (9.1)-(9.10) can be simplified to a DCOPF, in which there is no reactive power or network losses. Moreover, the power flow constraint can be approximated by a linear equation presented in (9.12). Under this set of assumptions, and with linear cost functions, the DCOPF becomes a linear program (LP). Because of the special properties of LP, LP-based DCOPF can be solved much faster than the original ACOPF.

$$P_k = B_k(\theta_n - \theta_m), \forall k \tag{9.12}$$

The same sensitivity is calculated with the DC set of assumptions in [81, 80]. The metric estimating the DC benefits of the line is presented in (9.13). We refer to the method ranking lines based on this metric as the DC heuristic. The DC estimation of the lines value is the same as the AC estimation, ignoring the reactive power and losses. It is concluded in [113] that the two heuristics may produce significantly different results if the system is voltage constrained.

$$LV_{DC} = P_k(\lambda_{Pm} - \lambda_{Pn}), \forall k \tag{9.13}$$

9.2.2 Simulation Studies

We test the two heuristics on the Polish test case provided by MATPOWER. The system has 2383 nodes, 327 generators, and 2896 transmission lines. We assume that all of the generators are on. The cost functions included in the dataset are linear, which matches the formulation presented in the previous section. In order to study the performance of the heuristics, we compare the actual benefit from the proposed switching action with the estimated benefit calculated by the heuristics. The actual switching benefit is the total cost

difference between the case in which the transmission line is in the system, and the case in which it is taken out. We simulate the performance of the heuristics under three different settings:

1. DC Heuristic with DCOPF: a DCOPF is performed and all the primal and dual variables are taken from the DCOPF solution. The actual benefits are calculated through the total cost comparison of the two DCOPFs. The switching benefits are also estimated through the DC heuristic introduced in (9.13). A comparison between the actual and estimated benefits provides information on the performance of the DC heuristic with a DCOPF. Note that the solution to a DCOPF may or may not be AC feasible.

2. DC Heuristic with ACOPF: the dual and primal variables as well as the actual benefits are calculated through an ACOPF. The estimated switching benefits are obtained from the DC heuristic, which does not include losses or reactive power. Note that under this setting, despite using the DC heuristic, the power flow and active power LMP come from an ACOPF. A comparison between the actual and estimated benefits provides information on the performance of the DC heuristic with an ACOPF.

3. AC Heuristic with ACOPF: the dual and primal variables are specified through an ACOPF algorithm. The actual switching benefits are also calculated by comparing the total cost obtained from the two ACOPFs. Under this setting, the benefits are estimated through the AC heuristic presented in (9.11). A comparison between the actual and estimated benefits provides information on the performance of the AC heuristic with an ACOPF.

Fig. 9.1 compares the benefits obtained by a single switching action with the estimated benefits calculated by the DC heuristic under setting 1. Fig. 9.2 shows the performance

of an algorithm based on the DC heuristic using a DCOPF for the first twenty switching candidates. The dashed line specifies the maximum possible benefit from the switching identified by an ACOPF while the dotted line shows the maximum possible benefits of switching using a DCOPF. The results show that the algorithm is not able to find the best switching action in the first twenty candidates it proposes. Five out of twenty proposed candidates are beneficial actions when tested with a DCOPF. However, there exist only two candidates that provide ACOPF beneficial switching actions. In electricity markets today, all the procedures are based on DCOPF due to the computational complexity of ACOPF. However, operators need to make sure that the solution is AC feasible. This is often done via out of market correction (OMC) mechanisms [116]. Our results suggest that switching candidates identified by the solution of a DCOPF may not be AC feasible or may not be beneficial even though DCOPF identifies them to be beneficial.

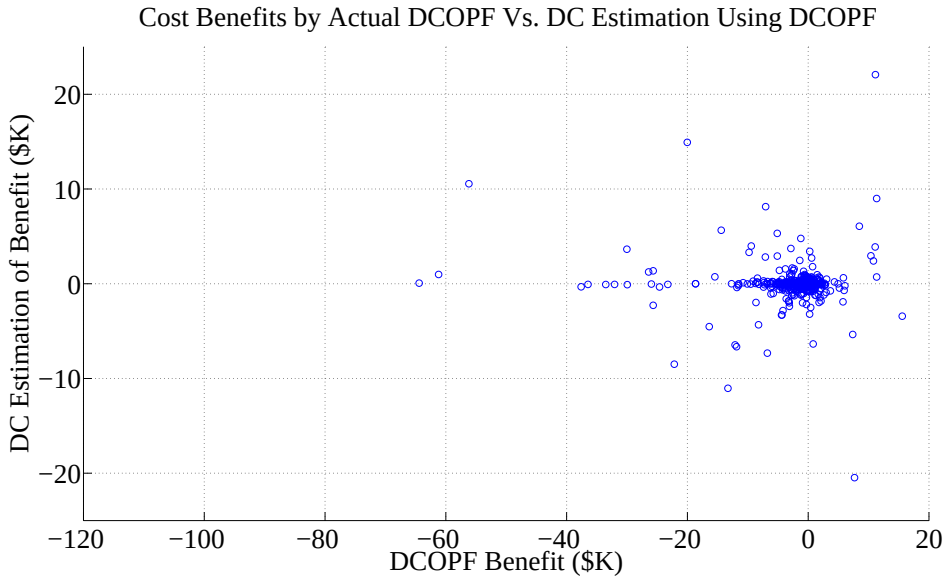

Figure 9.1: The Benefits Identified by DCOPF Versus the DC Heuristic Estimation of the Benefits Using DCOPF.

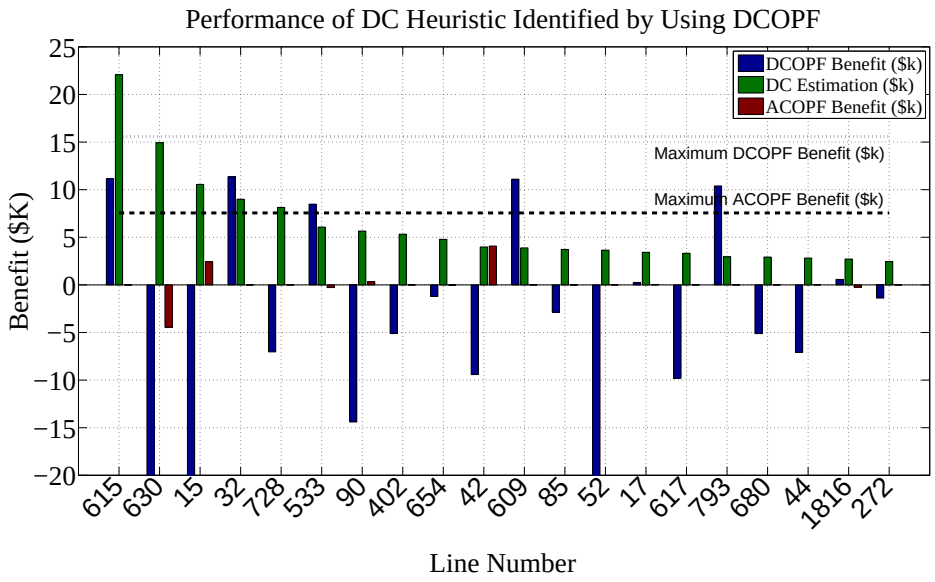

Figure 9.2: Performance of the DC Heuristic for the First Twenty Lines Identified by the Heuristic Using DCOPF.

Fig. 9.3 and 9.4 show the same results under setting 2 where ACOPF is used instead of DCOPF. The results suggest that the algorithm is able to identify the best switching action among its first twenty proposed candidates. Six out of twenty proposed actions are beneficial. Note that the only difference between settings 1 and 2 is the fact that ACOPF solution is used under setting 2 for both actual and estimated benefit calculation. However, under both settings the DC heuristic presented in (9.13) is employed. The difference between the results comes from the fact that the dispatch and prices are different when AC power flow constraints are taken into account in the optimal power flow problem.

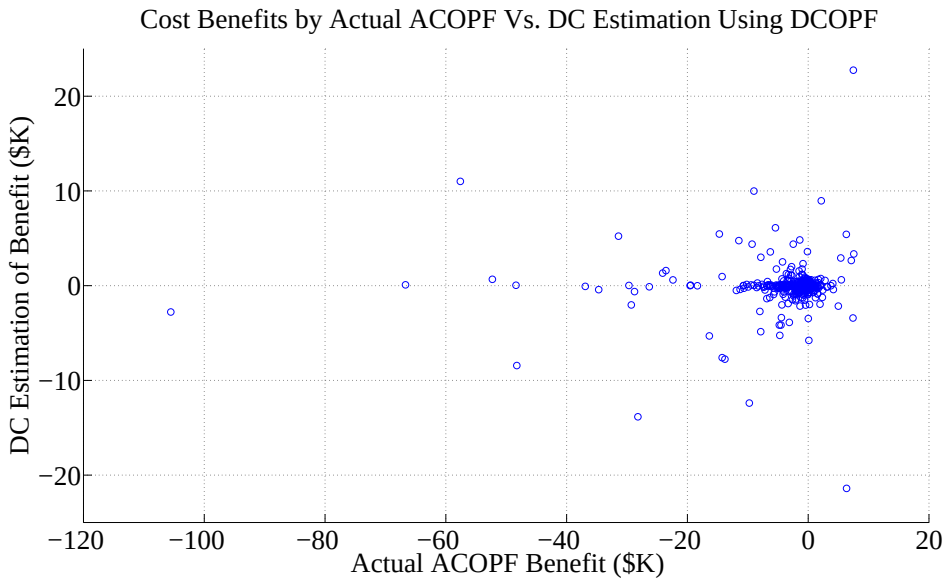

Figure 9.3: The Actual Benefits Obtained by ACOPF Versus the DC Heuristic Estimation of the Benefits Using ACOPF.

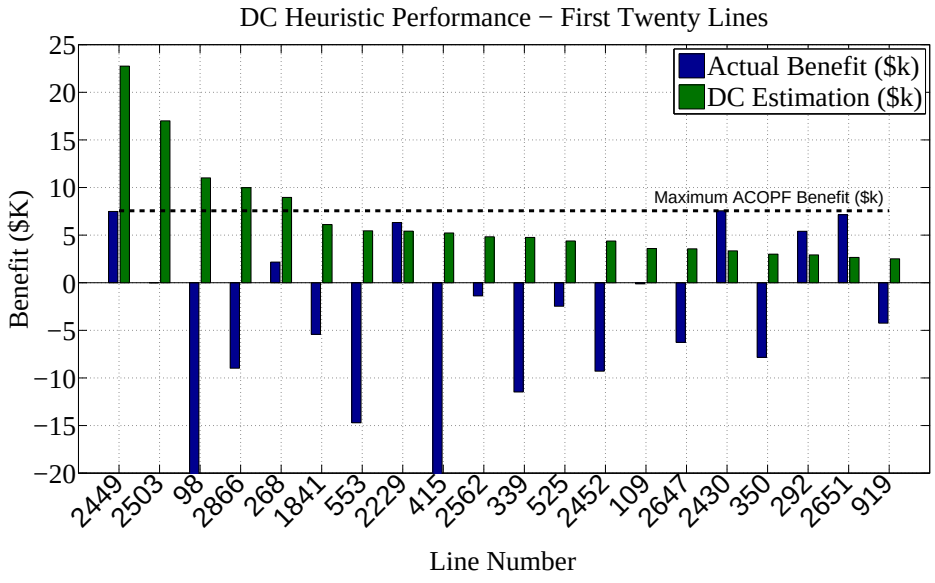

Figure 9.4: Performance of the DC Heuristic for the First Twenty Lines Identified by the Heuristic Using ACOPF.

Fig. 9.5 and 9.6 show the results under setting 3 where the AC heuristic is used with ACOPF solution. The results are very similar to those of setting 2 with six beneficial solutions among the first twenty proposed actions.

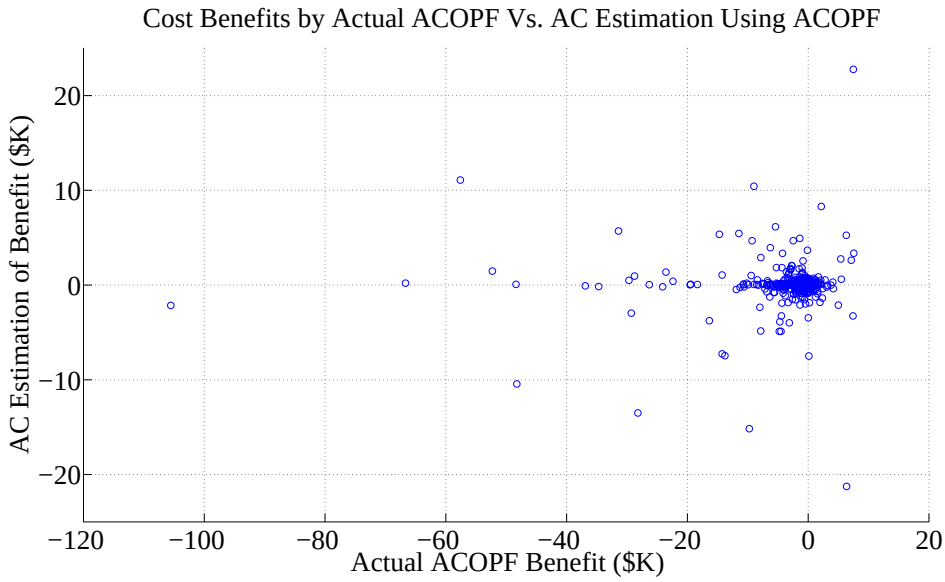

Figure 9.5: The Actual Benefits Obtained by ACOPF Versus the AC Heuristic Estimation of the Benefits Using ACOPF.

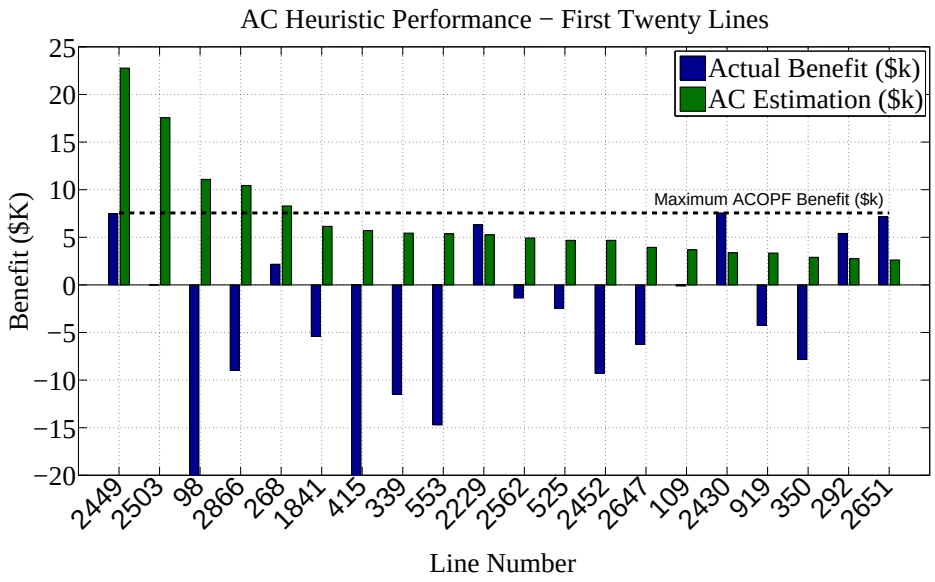

Figure 9.6: Performance of the AC Heuristic for the First Twenty Lines Identified by the Heuristic Using ACOPF.

The results obtained under settings 2 and 3 show that AC and DC heuristics produce very similar results when the ACOPF solution is used. Under both settings, six out of twenty proposed actions were beneficial and the algorithm was able to identify the best switching action. The only difference was a slight change in the candidates order. Such results were expected and are in line with the conclusions of [113], which suggests the results to be similar when the system is not heavily voltage constrained. Nevertheless, the results obtained under setting 1, where the DCOPF solution is used for heuristic calculations, are substantially different from those of settings 2 or 3. The difference appears both in the suggested switching candidates and the benefits.

As was stated before, in electricity markets today, ACOPF solutions are not generally available similar to setting 1. Our results show that the studied heuristics do not provide consistent results when they are based on the DCOPF solution compared to a more real-

istic ACOPF. The more realistic benefits, ACOPF based benefits, as well as the proposed candidates are different than those based on a DCOPF.

9.2.3 Conclusion

Due to the computational complexity of the OTC problem, different heuristics are used to obtain fast sub-optimal solutions. The heuristics are often tested on small scale systems and the scalability of their application is not well understood. We studied the performance of two such fast heuristics on the Polish system. The heuristics were studied under three different settings: DC heuristic with DCOPF, DC heuristic with ACOPF, and AC heuristic with ACOPF. Our results suggest that the AC and DC heuristics are not very different when they are based on the solution to ACOPF. However, the heuristics do produce different results if they are based on DCOPF solutions. Our results suggest that DCOPF based solutions obtained for OTC may not perform well under realistic system conditions modeled by an ACOPF. Since the market procedures are based on DCOPF, not ACOPF, and AC feasibility is achieved via OMC routines, implementation of ACOPF based heuristics would not be straightforward.

Chapter 10

CONCLUSION

10.1 Conclusion

Topology control is an integral part of power system operations. Today, most of the topology control actions are determined based on operators' past knowledge about the system or other ad-hoc methods. Relying on only prior observations to determine potential corrective topology control action limits the capability to harness the existing flexibility in the transmission network. Systematic procedures that are capable of capturing such complexities should be preferred over these limited methods. Furthermore, the hardware requirements to implement topology control (circuit breakers) already exist, leaving only the need to develop the appropriate decision support tools, which are low in cost, to obtain such benefits.

In this research, three different corrective topology control methodologies are presented: real-time, deterministic planning based, and robust corrective topology control. Real-time corrective topology control is very difficult to implement with existing technologies due to a lack of computational power and the practical barriers of needing to ensure AC feasibility, voltage stability, and transient stability. Deterministic planning based corrective topology control can be solved offline, but such an approach relies on predicting the operating state. Furthermore, the deterministic planning based methods cannot guarantee solution feasibility over a wide range of system states. The proposed method of robust corrective topology control fills the technology gap between the real-time and the deterministic planning based corrective topology control methodologies. The offline mechanism of robust corrective topology control algorithm generates solutions, which can be implemented

in real-time with the help of a real-time dynamic security assessment tool. As a result, the proposed robust corrective topology control model provides a mathematical decision support tool that integrates topology control into every day operations by being able to guarantee the robustness of solutions.

While deterministic corrective topology control frameworks may suggest many potential switching solutions, the empirical results presented in this research show that many of these solutions will be infeasible for minor changes in the operating state. In contrast, the robust corrective switching scheme guarantees solution feasibility for a wide range of system states, given a DCOPF formulation. In addition, the robust corrective topology control formulation demonstrates the ability of generating multiple corrective switching actions for a particular contingency. Moreover, a single resulting corrective switching solution is capable of mitigating multiple contingencies.

Day-ahead unit commitment problems, with proxy reserve requirements, do not guarantee N-1 feasibility. Contingency analysis is used to determine whether there are contingencies that cannot be satisfied by the unit commitment solution. When this happens, unit commitment must be resolved or the operator will employ out-of-market corrections to obtain a feasible N-1 solution. The results have shown that robust corrective topology control can be used to reduce the occurrence of contingencies that are not satisfied by the re-dispatch capabilities of the unit commitment solution alone. Furthermore, the numerical results proved that the topology control does not necessarily degrade system reliability; on the contrary, it can help the system to achieve N-1 feasibility even with uncertainty.

The penetration of renewable resources in electric power systems has increased in recent years. This increase in intermittent renewable resources forces changes in the operational paradigm of the bulk electric power systems. This research shows the usefulness of topology control actions for integration of renewable resources, in terms of determining DNE limits. For renewable resource integration, the determination of DNE limits is crit-

ical; in this research, a systematic procedure to determine DNE limit is presented. With corrective topology control actions, the DNE limits can be increased by 30-100%, as compared with no topology control actions. At the same time, topology control actions can lower the operational cost by at least 6%. The robust topology control algorithm is based on a DCOPF; therefore, the topology control solutions obtained from the robust optimization problem must be checked for AC feasibility. On the IEEE-118 bus test case, ∼85-90% of topology control solutions obtained from the robust topology control algorithm are AC feasible.

The stability studies, presented in this research, demonstrated that the solution obtained from the robust topology control algorithm can pass AC feasibility and stability tests. Furthermore, 30 topology control solutions, obtained from robust topology control algorithm, are tested for stability and ∼66% of the topology control solutions pass the stability check.

This research also address the scalability of the DNE limit problem; for a realistic system the DNE limit formulation, presented in Chapter 7, is cumbersome and may result in longer computational time. Therefore, in this research, the zonal DNE limit methodology is presented, which systematically reduces the system size and determines the DNE limits. The error in DNE limits obtained from the zonal method and the nodal method is ∼2-12%. Furthermore, the computational time reduces by ∼75-99% with the zonal DNE limit formulation. This chapter also addresses the scalability issue of the DNE limit problem, which is critical for real life applications and fast solution time. The DNE limit results, on the TVA system, show that with 5-10% of modeling information, the accuracy of the solutions is ∼98% while, at the same time, the computational time is ∼1% of what it would otherwise take to solve a nodal model for the DNE limit problem. This result shows the benefit of the zonal DNE limit formulation. The tradeoff between the computational time and the accuracy shows the potential of the zonal DNE limit formulation. Furthermore, numerical results demonstrated that a DC optimal power flow based zonal approach can produce

topology control solutions, which can pass AC feasibility test. Based on the empirical studies conducted, $\sim 80\%$ of TC solutions obtained from the zonal DNE limit algorithm produced AC feasible solution.

10.2 Proposed Future Research

10.2.1 Probabilistic Do-not-exceed Limits

In Chapters 7 and 8, the DNE limits are determined without considering the locational aspect of at each renewable injection location. In Chapter 7, it is assumed that all the renewable generation deviates uniformly over all renewable injection nodes. This modeling approach is a conservative approach as it is assumes that renewable generation varies uniformly, from its forecasted value, at the same time. The benefit of this method is that it simplifies the uncertainty set definition and reduces the number of variables. However, past research has shown that forecasting renewable generation and predicting the renewable uncertainty is difficult. From a DNE limit point of view, this approximation is most conservative in nature and results in narrower DNE limits. In Chapter 8, it is assumed that the renewable generation, at each node, is allowed to deviate independently with respect to each other. This approach is more practical and close to realistic behavior of renewable generating units, as the variability of one wind farm is not directly related output of other wind farms. However, this modeling approach complicates the robust DNE limit formulation with TC; in this approach, there are more variables and subsequently requires more complex solution method. The future work may involve extending the concept of DNE limit considering the locational aspect of renewable generation. In this modeling approach, each renewable injection location can be weighted based on the expected probabilistic value of deviation and the DNE limits can be determined based on a probabilistic function. In this case, the weights for each renewable injection node would be determined based on his-

torical data and improved scenario selection techniques. This approach can be combined with a stochastic model that captures the correlation of the wind farms and quantifies the spatial-temporal correlation in wind generation. This approach is complex and may prove to be beneficial for future power system operations.

10.2.2 Non-uniqueness of Do-not-exceed Limits

In Chapter 8 and [117], for a fixed topology, it is observed that the lower limit of the DNE limits are bounded by the amount of available spinning reserves in the system. However, in some cases, the DNE limits are not unique in nature; for instance, identical DNE limits, in terms of total MW, can be obtained with different injections of renewable generation. This problem exists when the DNE limits are determined assuming the deviation in renewable generation is independent of each other. In power system operations, locational aspects of renewable injection is critical; future work may involve understanding the non-unique nature of the DNE limits and establishing the methodology to analyze this nature of the DNE limit problem.

10.2.3 Co-optimization of Do-not-exceed Limits

In an ideal situation, the DNE limits should be determined within the SCUC problem. Co-optimizing the DNE limit with the SCUC problem may provide better results in terms of addressing uncertainty in renewable generation. In recent years, multiple research initiatives has investigated the benefits of robust optimization for solving unit commitment problem and addressing uncertainties in renewable generation. The DNE limits can extend this robust unit commitment problem to address uncertainties in renewable generation and power system operations.

10.2.4 Effect of Clustering Methods on Do-not-exceed Limits

In Chapter 7, PTDF difference with k-means clustering method is used to determine the clusters for the zonal DNE limit problem. In this research, the effect of different clustering method on the solution quality of this problem is not addressed. Future work may involve understating effects of different clustering methods on the solution quality of the zonal DNE limit problem and improving the zonal DNE limit formulation.

10.2.5 Co-optimization of Robust Corrective Topology Control for System Reliability

In this thesis, the robust corrective topology control methodologies are presented to achieve N-1 reliability. However, these methodologies are outside the SCUC problem formulation. Co-optimizing the SCUC with the robust corrective topology control methodologies can help in improving the system reliability. In this case, including all N-1 contingencies in the robust corrective topology control formulation with the SCUC may lead to an insolvable problem. However, only including critical contingencies, with the robust corrective topology control methodologies in SCUC may lead to a more secured SCUC solution and improved system reliability.

10.2.6 Robust Corrective Topology Control Heuristics

The future work may also involve investigating new methods of modeling TC problem and developing better topology control heuristics. The TC problem is complex problem and solving it in its genetic form is computationally cumbersome for large scale realistic systems. TC heuristics may help to reduce the computational time but does not guarantees AC feasibility and its effects on system stability. Understating these critical operational issues and addressing them in a optimization framework is essential.

10.2.7 AC feasibility and Stability of Robust Corrective Topology Control

From TC point of view, AC feasibility and system stability is critical. At present, there are not many reliable methods to address the AC feasibility and the system reliability of the TC solution in a optimization framework, which can scale to realistic test systems. Future work may involve investigating these issues.

REFERENCES

[1] P. Kundur, J. Paserba, V. Ajjarapu, G. Andersson, A. Bose, C. Canizares, N. Hatziargyriou, D. Hill, A. Stankovic, C. Taylor, T. V. Cutsem, and V. Vittal, "Definition and classification of power system stability IEEE/CIGRE joint task force on stability terms and definitions," *IEEE Trans. Power Syst.*, vol. 19, no. 2, pp. 1387 – 1401, May 2004.

[2] G. Granelli, M. Montagna, F. Zanellini, P. Bresesti, R. Vailati, and M. Innorta, "Optimal network reconfiguration for congestion management by deterministic and genetic algorithms," *Elect. Power Syst. Res*, vol. 76, no. 6-7, pp. 549–556, Apr. 2006.

[3] A. A. Mazi, B. F. Wollenberg, and M. H. Hesse, "Corrective control of power system flows by line and bus-bar switching," *IEEE Trans. Power Syst.*, vol. 1, no. 3, pp. 258–264, Aug. 1986.

[4] W. Shao and V. Vittal, "Bip-based opf for line and bus-bar switching to relieve overloads and voltage violations," in *Proc. 2006 IEEE Power Syst. Conf. and Expo.*, Nov. 2006.

[5] A. G. Bakirtzis and A. P. S. Meliopoulos, "Incorporation of switching operations in power system corrective control computations," *IEEE Trans. Power Syst.*, vol. 2, no. 3, pp. 669–675, Aug. 1987.

[6] R. Bacher and H. Glavitsch, "Loss reduction by network switching," *IEEE Trans. Power Syst.*, vol. 3, no. 2, pp. 447–454, May 1988.

[7] S. Fliscounakis, F. Zaoui, G. Simeant, and R. Gonzalez, "Topology influence on loss reduction as a mixed integer linear programming problem," *IEEE Power Tech. 2007*, pp. 1987–1990, Jul. 2007.

[8] G. Schnyder and H. Glavitsch, "Security enhancement using an optimal switching power flow," *IEEE Trans. Power Syst.*, vol. 5, no. 2, pp. 674–681, May 1990.

[9] ——, "Integrated security control using an optimal power flow and switching concepts," *IEEE Trans. Power Syst.*, vol. 3, no. 2, pp. 782–790, May 1988.

[10] R. Bacher and H. Glavitsch, "Network topology optimization with security constraints," *IEEE Trans. Power Syst.*, vol. 1, no. 4, pp. 103–111, Nov. 1986.

[11] W. Shao and V. Vittal, "Corrective switching algorithm for relieving overloads and voltage violations," *IEEE Trans. Power Syst.*, vol. 20, no. 4, pp. 1877–1885, Nov. 2005.

[12] F. Kuntz, "Congestion management in germany the impact of renewable generation on congestion management costs," 2011. [Online]. Available: http://idei.fr/doc/conf/eem/papers_2011/kunz.pdf

[13] T. Potluri and K. W. Hedman, "Network topology optimization with ACOPF," *IEEE PES General Meeting*, pp. 1–7, Jul. 22-26 2012.

[14] K. W. Hedman, M. C. Ferris, R. P. O'Neill, E. B. Fisher, and S. S. Oren, "Co-optimization of generation unit commitment and transmission switching with N-1 reliability," *IEEE Trans. Power Syst.*, vol. 25, pp. 1052 – 1063, May 2010.

[15] H. Glavitsch, "State of the art review: switching as means of control in the power system," *INTL. JNL. Elect. Power Energy Syst.*, vol. 7, no. 2, pp. 92–100, Apr. 1985.

[16] B. G. Gorenstin, L. A. Terry, M. F. Pereira, and L. M. V. G. Pinto, "Integrated network topology optimization and generation rescheduling for power system security applications," *in IASTED International Symposium: High Tech. in the Power Industry, Bozeman, MT*, pp. 110–114, Aug. 1986.

[17] J. G. Rolim and L. J. B. Machado, "A study of the use of corrective switching in transmission systems," *IEEE Trans. Power Syst.*, vol. 14, pp. 336–341, 1999.

[18] K. W. Hedman, R. P. O'Neill, E. B. Fisher, and S. S. Oren, "Optimal transmission switching with contingency analysis," *IEEE Trans. Power Syst.*, vol. 24, no. 3, pp. 1577–1586, Aug. 2009.

[19] P. Balasubramanian and K. W. Hedman, "Real-time corrective switching in response to simultaneous contingencies," *JNL of Energy Engineering*, vol. 141, no. 1, pp. 1–10, 2014.

[20] R. P. O'Neill, R. Baldick, U. Helman, M. H. Rothkopf, and W. S. Jr., "Dispatchable transmission in RTO markets," *IEEE Trans. Power Syst.*, vol. 20, no. 1, pp. 171 – 179, Feb. 2005.

[21] K. W. Hedman, R. P. O'Neill, E. B. Fisher, and S. S. Oren, "Optimal transmission switching - sensitivity analysis and extensions," *IEEE Trans. Power Syst.*, vol. 23, pp. 1469–1479, Aug. 2008.

[22] R. P. O'Neill, K. W. Hedman, E. A. Krall, A. Papavasiliou, and S. S. Oren, "Economic analysis of the isos multi-period N-1 reliable unit commitment and transmission switching problem using duality concepts," *Energy Systems Journal*, vol. 1, no. 2, pp. 165–195, 2010.

[23] K. W. Hedman, R. P. O'Neill, E. B. Fisher, and S. S. Oren, "Smart flexible just-in-time transmission and flowgate bidding," *IEEE Trans. Power Syst.*, vol. 26, no. 1, pp. 93–102, Feb. 2011.

[24] K. W. Hedman, S. S. Oren, and R. P. O'Neill, "A review of transmission switching and network topology optimization," in *IEEE Power and Energy Society General Meeting*, Jul. 2011.

[25] ISO-NE, *ISO New England Outlook:Smart Grid is About Consumers*, Apr. 2010. [Online]. Available: http://www.isone.com/nwsiss/nwltrs/outlook/2009/outlook_may_2009_final.pdf

[26] J.C.Villumsen, G. Bronmo, and A. B. Philpott, "Line capacity expansion and transmission switching in power systems with large-scale wind power," *IEEE Trans. Power Syst.*, vol. 28, no. 2, pp. 731–739, May 2013.

[27] A. Khodaei, M. Shahidehpour, and S. Kamalinia, "Transmission switching in expansion planning," *IEEE Trans. Power Syst.*, vol. 25, no. 3, pp. 1722–1733, Aug. 2010.

[28] PJM, *Manual 3: Transmission Operations, Revision: 40*, 2012. [Online]. Available: http://www.pjm.com/~/media/documents/manuals/m03.ashx

[29] ——, *Manual 3: Transmission Operations, Revision: 44*, Nov. 2013. [Online]. Available: http://www.pjm.com/markets-andoperations/compliance/nercstandards/

~/media/documents/manuals/m03.ashx

[30] A. Ott, VP, PJM, Norristown, PA, private communication, Nov. 2012.

[31] Energy Policy Act (EPACT) of 2005, Aug. 2005. [Online]. Available: http://energy.gov/eere/femp/downloads/energy-policy-act-epact-2005

[32] A. J. Wood and B. F. Wollenberg, *Power generation, operation, and control*, 2nd ed. Wiley-Interscience, 1996.

[33] J. Carpentier, "Contribution l'tude du dispatching conomique," *Bull. Soc. Franc. Electriciens*, vol. 3, pp. 431–447, 1962.

[34] A. R. Bergen. and V. Vitta, *Power Systems Analysis*, 2, Ed. Prentice Hall, Aug. 16, 1999.

[35] M. Huneault and F. D. Galiana, "A survey of the optimal power flow literature," *IEEE Trans. Power Syst.*, vol. 6, no. 2, pp. 762–770, 1991.

[36] O. W. Akinbode and K. W. Hedman, "Fictitious losses in the dcopf with a piecewise linear approximation of losses," *IEEE PES General Meeting, Vancouver, BC*, pp. 1–5, 21-25 Jul. 2013 2013.

[37] M. B. Cain, M. B. Cain, and R. P. O'Neill, "History of optimal power flow and formulations," *FERC staff technical paper*, Dec. 2012. [Online]. Available: http://www.ferc.gov/industries/electric/indus-act/market-planning/opf-papers/acopf-1-history-formulation-testing.pdf

[38] R. P. O'Neill, A. Castillo, and M. Cain, "The IV formulation and linearizations of the AC optimal power flow problem," *FERC staff technical paper*, Dec. 2012. [Online]. Available: http://www.ferc.gov/industries/electric/indus-act/market-planning/opf-papers/acopf-2-iv-linearization.pdf

[39] ——, "The computational testing of AC optimal power flow using the current voltage (IV) formulations," *FERC staff technical paper*, Dec. 2012. [Online]. Available: http://www.ferc.gov/industries/electric/indus-act/market-planning/opf-papers/

acopf-3-iv-linearization-testing.pdf

[40] A. Castillo and R. P. O'Neill, "Survey of approaches to solving the ACOPF," *FERC staff technical paper*, Mar. 2013. [Online]. Available: http://www.ferc.gov/industries/electric/indus-act/market-planning/opf-papers/acopf-4-solution-techniques-survey.pdf

[41] ——, "Computational performance of solution techniques applied to the ACOPF," *FERC staff technical paper*, Jan. 2013. [Online]. Available: http://www.ferc.gov/industries/electric/indus-act/market-planning/opf-papers/acopf-5-computational-testing.pdf

[42] A. Schecter and R. P. O'Neill, "Exploration of the ACOPF feasible region for the standard IEEE test set optimal power flow," *FERC staff technical paper*, Feb. 2013. [Online]. Available: http://www.ferc.gov/industries/electric/indus-act/market-planning/opf-papers/acopf-6-test-problem-properties.pdf

[43] P. A. Lipka, R. P. O'Neill, and S. Oren, "Developing line current magnitude constraints for IEEE test problems," *FERC staff technical paper*, Apr. 2013. [Online]. Available: http://www.ferc.gov/industries/electric/indus-act/market-planning/opf-papers/acopf-7-line-constraints.pdf

[44] M. Pirnia, R. O'Neill, P. Lipka, and C. Campaigne, "A computational study of linear approximations to the convex constraints in the iterative linear IV-ACOPF," *FERC staff technical paper*, Jun. 2013. [Online]. Available: http://www.ferc.gov/industries/electric/indus-act/market-planning/opf-papers/acopf-8-preprocessed-constraints-iliv-acopf.pdf

[45] C. Campaigne, P. A. Lipka, M. Pirnia, R. P. ONeill, and S. Oren, "Testing step-size limits for solving the linearized current voltage AC optimal power flow," *FERC staff technical paper*, Jun. 2013. [Online]. Available: http://www.ferc.gov/industries/electric/indus-act/market-planning/opf-papers/acopf-9-stepsizelimits-iliv-acopf.pdf

[46] P. A. Lipka, R. P. O'Neill, S. S. Oren, A. Castillo, M. Pirnia, and C. Campaigne, "Optimal transmission switching using the IV-ACOPF linearization," *FERC staff technical paper*, Nov. 2013. [Online]. Available: http://www.ferc.gov/industries/electric/indus-act/market-planning/opf-papers/acopf-10.pdf

[47] R. P. O'Neill, A. Castillo, and M. Cain, "A note on the computational testing of AC optimal power flow using the current voltage formulations," *FERC staff technical paper*, Sep. 2013. [Online]. Available: http://www.ferc.gov/industries/electric/indus-act/market-planning/opf-papers/acopf-11.pdf

[48] B. Stott, J. Jardim, and O. Alsac, "DC power flow revisited," *IEEE Trans. Power Syst.*, vol. 24, no. 3, pp. 1290–1300, Aug. 2009.

[49] R. P. O'Neill, T. Dautel, and E. Krall, "ISO software enhancements of the last decade and future software and modeling plans," *FERC staff report*, Nov. 2011. [Online]. Available: http://www.ferc.gov/industries/electric/indus-act/rto/rto-iso-soft-2011.pdf

[50] A. J. Ardakani and F. Bouffard, "Identification of umbrella constraints in DC-based security-constrained optimal power flow," *IEEE Trans. Power S*, vol. 28, no. 4, pp. 3924–3934, Nov. 2013.

[51] P. A. Ruiz, A. Rudkevich, M. C. Caramanis, E. Goldis, E. Ntakou, and C. R. Philbrick, "Reduced mip formulation for transmission topology control," in *50th Annual Allerton Conference on Communication, Control, and Computing*, 2012.

[52] T. Guler, G. Gross, and M. Liu, "Generalized line outage distribution factors," *IEEE Trans. Power Syst.*, vol. 22, no. 2, pp. 879–881, May 2007.

[53] G. B. Sheble and G. N. Fahd, "Unit commitment literature synopsis," *IEEE Trans. Power Syst.*, vol. 9, no. 1, pp. 128–135, Feb. 1994.

[54] N. P. Padhy, "Unit commitment-a bibliographical survey," *IEEE Trans. Power Syst.*, vol. 19, no. 2, pp. 1196 – 1205, May 2004.

[55] H. Yamin, "Review on methods of generation scheduling in electric power systems," *Electric Power Systems Research*, vol. 69, no. 2-3, p. 227248, May 2004.

[56] D. Streiffert, R. Philbrick, and A. Ott, "A mixed integer programming solution for market clearing and reliability analysis," *IEEE PES General Meeting*, vol. 3, pp. 2724 – 2731, 12-16 Jun. 2005.

[57] A. Ott, "Mip-based unit commitment implementation in PJM markets," in *HEPG Forty-Ninth Plenary Session*, Dec. 2007. [Online]. Available: http://www.hks.harvard.edu/hepg/Andrew_Ott.pdf

[58] D. Rajan and S. Takriti, "Minimum up/down polytopes of the unit commitment problem with start-up costs," *IBM Research Report*, Jun. 2005.

[59] California ISO, *Spinning Reserve and Non-Spinning Reserve*, 2006. [Online]. Available: http://www.caiso.com/docs/2003/09/08/2003090815135425649.pdf

[60] A. Casto, "Overview of MISO day-ahead markets," *Midwest ISO*. [Online]. Available: http://www.atcllc.com/oasis/Customer_Notices/NCM_MISO_DayAhead111507.pdf

[61] A. Wald, *Statistical decision functions*. John Wiley, 1950.

[62] A. L. Soyster, "Convex programming with set-inclusive constraints and applications to inexact linear programming," *Oper. Res.*, vol. 21, no. 5, pp. 1154–1157, Sep.-Oct. 1973.

[63] P. Kouvelis and G. Yu, *Robust discrete optimization and its applications (nonconvex optimization and its applications)*. Springer, 1996.

[64] D. Bertsimas and S. Melvyn, "The price of robustness," *Oper. Res.*, vol. 52, no. 1, pp. 35–53, Jan.-Feb. 2004.

[65] P. Khargonekar, I. R. Petersen, and K. Zhou, "Robust stabilization of uncertain linear systems: quadratic stabilizability and H^∞ control theory," *IEEE Tras. Auto. Ctrl.*, vol. 35, no. 3, pp. 356–361, Mar. 1990.

[66] C. S. Yu and H. L. Li, "A robust optimization model for stochastic logistic problems," *Inter. JNL Prod. Eco.*, vol. 64, no. 1-3, pp. 385 – 397, Mar. 2000. [Online]. Available: http://www.sciencedirect.com/science/article/pii/S0925527399000742

[67] F. J. Fabozzi, P. N. Kolm, D. Pachamanova, and S. M. Focardi, *Robust portfolio*

optimization and management. Wiley, 2007.

[68] M. Chu, Y. Zinchenko, S. G. Henderson, and M. B. Sharpe, "Robust optimization for intensity modulated radiation therapy treatment planning under uncertainty," *Phys. Med. Biol.*, vol. 50, no. 23, pp. 54–63, 2005.

[69] F. P. Bernardo and P. M. Saraiva, "A robust optimization framework for process parameter and tolerance design," *AIChE JNL*, vol. 44, no. 9, pp. 2007–2017, 1998.

[70] D. Bertsimas, E. Litvinov, X. Sun, J. Zhao, and T. Zheng, "Adaptive robust optimization for the security constrained unit commitment problem," *IEEE Trans. Power Syst.*, vol. 28, no. 1, pp. 52 – 63, Feb. 2013.

[71] R. Jiang, M. Zhang, G. Li, and Y. Guan, "Two-stage robust power grid optimization problem," *JNL Operations Research*, submitted, 2010. [Online]. Available: http://www.optimization-online.org/DB_FILE/2010/10/2769.pdf

[72] L. El Ghaoui, F. Oustry, and H. Lebret, "Robust solutions to uncertain semidefinite programs," *SIAM JNL Optimization*, vol. 9, no. 1, pp. 33–52, 1998.

[73] A. Ben-tal and A. Nemirovski, "Robust solutions of linear programming problems contaminated with uncertain data," *Mathematical Programming*, vol. 88, pp. 411–424, 2000.

[74] A. Ben-Tal, L. E. Ghaoui, and A. Nemirovski, *Robust optimization*. Princeton Univ. Press, 2009.

[75] P. C. Gupta, "A stochastic approach to peak power-demand forecasting in electric utility systems," *IEEE Trans. Power Apparatus Syst.*, vol. PAS-90, no. 2, pp. 824–832, Mar. 1971.

[76] A. Ben-Tal and A. Nemirovski, "Robust convex optimization," *Math. Oper. Res.*, vol. 23, no. 4, pp. 769–805, Nov. 1998.

[77] D. Bertsimas and M. Sim, "Robust discrete optimization and network flows," *Math.*

Prog., vol. 98, no. 1-3, pp. 49–71, Sep. 2003.

[78] D. Mejia-Giraldo and J. McCalley, "Adjustable decisions for reducing the price of robustness of capacity expansion planning," *IEEE Trans. Power Syst.*, 2014.

[79] C. P. Steinmetz, "Power control and stability of electric generating stations," *AIEE Trans.*, vol. XXXIX, pp. 1215–1287, Jul. 1920.

[80] J. D. Fuller, R. Ramasra, and A. Cha, "Fast heuristics for transmission-line switching," *IEEE Trans. Power Syst.*, vol. 27, no. 3, pp. 1377–1386, Aug. 2012.

[81] P. A. Ruiz, J. M. Foster, A. Rudkevich, and M. C. Caramanis, "Tractable transmission topology control using sensitivity analysis," *IEEE Trans. Power Syst.*, vol. 27, no. 3, pp. 1550–1559, Aug. 2012.

[82] ——, "On fast transmission topology control heuristics," *IEEE PES General Meeting*, Jul. 2011.

[83] L. Chen, O. Sangyo, Y. Tada, H. Okamoto, R. Tanabe, and H. Mitsuma, "Optimal reconfiguration of transmission systems with transient stability constraints," *International Conference on Power System Technology*, pp. 1346–1350, Aug. 1998.

[84] B. Perunicic, M. Ilic, and A. Stankovic, "Short time stabilization of power systems via line switching," *IEEE International Symposium on Circuits and Systems*, pp. 917 – 921, Jun. 1988.

[85] P. Kundur, *Power system stability and control*. New York: McGraw Hill, 1994.

[86] P. M. Anderson and A. A. Fouad, *Power system control and stability*, 2nd ed. Wiley-IEEE Press, 2002.

[87] Power System Test Case Archive, Univ. of Washington, Dept. of Elect. Eng., 2007. [Online]. Available: http://www.ee.washington.edu/research/pstca/

[88] GE Energy, *PSLF Version User's Manual Ver. 18.1*, 2013.

[89] P. Pourbeik, "Proposed changes to the WECC WT4 generic model for Type-4 wind turbine generators," *EPRI*, 23 Jan. 2013.

[90] K. Clark, N. W. Miller, and J. J. Sanchez-Gasca, "Modeling of GE wind turbine-generators for grid studies," *GE Energy, Ver. 4.5*, 16 Apr. 2010.

[91] E. B. Fisher, R. P. O'Neill, and M. C. Ferris, "Optimal transmission switching," *IEEE Trans. Power Syst.*, vol. 23, no. 3, pp. 1346–1355, Aug. 2008.

[92] ISO-NE, *ISO New England Operating Procedure no. 19: Transmission Operations, Revision 5*, Jun. 1, 2010. [Online]. Available: http://www.iso-ne.com/rules_proceds/operating/isone/op19/op19_rto_final.pdf

[93] California ISO, *Minimum Effective Threshold Report*, March 1, 2010. [Online]. Available: http://www.caiso.com/274c/274ce77df630.pdf

[94] J. M. Foster, P. A. Ruiz, A. Rudkevich, and M. C. Caramanis, "Economic and corrective applications of tractable transmission topology control," *in Proc. 49th Allerton Conference on Communications, Control and Computing, Monticello, IL,*, Sep. 2011.

[95] M. Li, P. Luh, L. Michel, Q. Zhao, and X. Luo, "Corrective line switching with security constraints for the base and contingency cases," *IEEE Trans. Power Syst.*, vol. 27, no. 1, pp. 125–133, Feb. 2012.

[96] PJM, Switching Solutions. [Online]. Available: http://www.pjm.com/markets-and-operations/etools/oasis/system-information/switching-solutions.aspx

[97] A. S. Korad and K. W. Hedman, "Robust corrective topology control for system reliability," *IEEE Trans. Power Syst.*, vol. 28, no. 4, pp. 4042 – 4051, Nov. 2013.

[98] M. Sahraei-Ardakani, A. S. Korad, K. W. Hedman, P. A. Lipka, and S. Oren, "Performance of AC and DC based transmission switching heuristics on a large-scale

polish system," in *IEEE Power and Energy Society General Meeting*, Jul. 2014.

[99] K. Meeusen, "Flexible resource adequacy criteria and must-offer obligation," Dec. 2012. [Online]. Available: http://www.caiso.com/informed/Pages/StakeholderProcesses/Default.aspx

[100] R. H. Byrd, J. Nocedal, and R. A. Waltz, "KNITRO: An integrated package for nonlinear optimization," *Nonconvex Optimization and Its Applications*, vol. 83, pp. 35–59, 2006.

[101] L. Bu, W. Xu, L. Wang, F. Howell, and P. Kundur, "A PSS tuning toolbox and its applications," *IEEE PES General Meeting*, pp. 2090–2095, 13-17 Jul. 2003.

[102] N. W. Miller, M. Shao, and S. Venkataraman, "Report California ISO (CAISO) frequency response study," *GE Energy*, 9 Nov. 2011. [Online]. Available: http://www.caiso.com/Documents/Report-FrequencyResponseStudy.pdf

[103] J. Zhao, T. Zheng, and E. Litvinov, "Variable resource dispatch through do-not-exceed limit," *IEEE Trans. Power Syst.*, vol. 30, no. 2, pp. 820–828, Feb. 2014.

[104] R. Jiang, J. Wang, M. Zhang, and Y. Guan, "Two-stage minimax regret robust unit commitment," *IEEE Trans. Power Syst.*, vol. 28, no. 3, pp. 2271–2282, Aug. 2013.

[105] NREL Western Wind Resources Dataset. [Online]. Available: http://wind.nrel.gov/Web_nrel/

[106] D. Bertsimas and J. Tsitsiklis, *Introduction to Linear Optimization*. Athena Scientific, 1997.

[107] E. Nicholson, "Staff analysis of operator-initiated commitments in RTO and ISO markets," *Federal Energy Regulatory Commission*, Dec. 2014. [Online]. Available: http://www.ferc.gov/legal/staff-reports/2014/AD14-14-operator-actions.pdf

[108] F. Wang and K. W. Hedman, "Dynamic reserve zones for day-ahead unit commitment with renewable resources," *IEEE Trans. Power Syst.*, vol. 99, no. 99, pp. 1–9,

2014.

[109] A. Kumar, S. C. Srivastava, and S. N. Singh, "A zonal congestion management approach using real and reactive power rescheduling," *IEEE Trans. Power Syst.*, vol. 19, no. 1, pp. 554–562, Feb. 2004.

[110] G. Chicco, R. Napoli, and F. Piglione, "Comparisons among clustering techniques for electricity customer classification," *IEEE Trans. Power Sys*, vol. 21, no. 2, pp. 933 – 940, May 2006.

[111] PJM, *PJM Statistics*, 26 Mar. 2014. [Online]. Available: http://www.pjm.com/~/media/about-pjm/newsroom/fact-sheets/pjm-statistics.ashx

[112] R. Baldick, "Border flow rights and contracts for differences of differences: models for electric transmission property rights," *IEEE Trans. Power Syst.*, vol. 22, no. 4, pp. 1495–1506, Nov. 2007.

[113] M. Soroush and J. D. Fuller, "Accuracies of optimal transmission switching heuristics based on dcopf and acopf," *IEEE Trans. Power Syst.*, vol. 29, no. 2, pp. 924–932, Mar. 2014.

[114] R. D. Zimmerman, C. E. Murillo-Sanchez, and R. J. Thomas, "MATPOWER's extensible optimal power flow architecture," *IEEE PES General Meeting*, pp. 1–7, Jul. 26-30 2009.

[115] ——, "MATPOWER: steady-state operations, planning, and analysis tools for power systems research and education," *IEEE Trans. Power Syst.*, vol. 26, no. 1, pp. 12–19, Feb. 2011.

[116] Y. Al-Abdullah, M. A. Khorsand, and K. W. Hedman, "Analyzing the impacts of out-of-market corrections," *2013 IREP Symposium IX -Bulk Power System Dynamics and Control, Rethymnon, Greece*, pp. 1–10, 2013.

[117] S. Zhang, N. G. Singhal, K. W. Hedman, V. Vittal, and J. Zhang, "An evaluation of algorithms to solve for do-not-exceed limits for renewable resources," 48^{th} *Hawaii International Conference on System Sciences*, 2015.